UNIVERSIDAD DE CÓRDOBA

Departamento de biología celular, fisiología e inmunología

Programa de doctorado en Biomedicina

TESIS DOCTORAL

Determination of new DYRK2 functions in response to genotoxic stress

---

Determinación de nuevas funciones de la quinasa DYRK2 en respuesta a estrés genotóxico

Memoria presentada para optar al grado de Doctora en Biomedicina por

Rosario Morrugares Carmona

Directores

Marco Antonio Calzado Canale

Eduardo Muñoz Blanco

Córdoba, febrero de 2022

TITULO: *Determination of new DYRK2 functions in response to genotoxic stress*

AUTOR: *Rosario Morrugares Carmona*

TÍTULO DE LA TESIS: Determinación de nuevas funciones de la quinasa DYRK2 en respuesta a estrés genotóxico

DOCTORANDO/A: Rosario Morrugares Carmona

INFORME RAZONADO DEL/DE LOS DIRECTOR/ES DE LA TESIS

El documento presentado por la doctoranda Rosario Morrugares Carmona, con título "Determinación de nuevas funciones de la quinasa DYRK2 en respuesta a estrés genotóxico", corresponde a su trabajo de tesis doctoral realizado en el periodo comprendido entre Febrero de 2017 y Diciembre de 2020. En este trabajo se han cumplido los objetivos establecidos al comienzo del proyecto, haciendo posible el aprendizaje de técnicas experimentales de gran relevancia y utilidad en el campo de la investigación en biología molecular. Este trabajo ha permitido la obtención de resultados acerca de nuevas funcionalidades de la quinasa DYRK2. Específicamente, se ha definido a la proteína NOTCH1 como un nuevo sustrato de esta quinasa. Además, ha permitido el análisis del perfil proteómico y de expresión génica de fibroblastos primarios a diferentes dosis de radiación. Esto con la finalidad de describir nuevos marcadores para el tratamiento de la radiodermatitis. La finalidad del estudio ha sido compensada con la publicación de un artículo científico en una revista indexada dentro del primer cuartil de su área. De manera conjunta a la elaboración de este proyecto, se han realizado trabajos en apoyo a otros miembros del grupo los cuales también han contribuido al avance y finalización de este trabajo dando lugar a otras publicaciones. Además, se ha dado difusión a los resultados obtenidos de todos los trabajos mediante la presentación de estos a jornadas y congresos siendo expuestos a través mediante comunicaciones orales.

PUBLICACIONES Y TRABAJOS DERIVADOS DE LA TESIS DOCTORAL

Publicaciones derivadas de la tesis doctoral

- **Morrugares R**, Correa-Sáez A, Moreno R, Garrido-Rodríguez M, Muñoz E, de la Vega L, Calzado MA. Phosphorylation-dependent regulation of the NOTCH1 intracellular domain by dual-specificity tyrosine-regulated kinase 2. Cell Mol Life Sci. 2020 Jul;77(13):2621-2639. doi: 10.1007/s00018-019-03309-9. Epub 2019 Oct 11. PMID: 31605148; PMCID: PMC7320039.

Publicaciones en colaboración durante el desarrollo de la tesis doctoral

- Correa-Sáez A, Jiménez-Izquierdo R, Garrido-Rodríguez M, **Morrugares R**, Muñoz E, Calzado MA. Updating dual-specificity tyrosine-phosphorylation-regulated kinase 2 (DYRK2): molecular basis, functions and role in diseases. Cell Mol Life Sci. 2020 Dec;77(23):4747-4763. doi: 10.1007/s00018-020-03556-1. Epub 2020 May 27. PMID: 32462403; PMCID: PMC7658070.

- Lara-Chica M, Correa-Sáez A, Jiménez-Izquierdo R, Garrido-Rodríguez M, Ponce FJ, Moreno R, Morrison K, Di Vona C, Arató K, Jiménez-Jiménez C, **Morrugares R**, Schmitz ML, de la Luna S, de la Vega L, Calzado MA. A novel CDC25A/DYRK2 regulatory switch modulates cell cycle and survival. Cell Death Differ. 2022 Jan;29(1):105-117. doi: 10.1038/s41418-021-00845-5. Epub 2021 Aug 6. PMID: 34363019; PMCID: PMC8738746.

- Alvarez Fallas ME, Pedraza-Arevalo S, Cujba AM, Manea T, Lambert C, **Morrugares R**, Sancho R. Stem/progenitor cells in normal physiology and disease of the pancreas. Mol Cell Endocrinol. 2021 Dec 1;538:111459. doi: 10.1016/j.mce.2021.111459. Epub 2021 Sep 20. PMID: 34543699; PMCID: PMC8573583.

- Palomares B, Ruiz-Pino F, Garrido-Rodriguez M, Eugenia Prados M, Sánchez- Garrido MA, Velasco I, Vazquez MJ, Nadal X, Ferreiro-Vera C, **Morrugares R**, Appendino G, Calzado MA, Tena-Sempere M, Muñoz E. Tetrahydrocannabinolic acid A (THCA-A) reduces adiposity and prevents metabolic disease caused by diet-induced obesity. Biochem Pharmacol. 2020 Jan;171:113693. doi: 10.1016/j.bcp.2019.113693. Epub 2019 Nov 9. PMID: 31706843.

Comunicaciones presentadas a congresos internacionales

- Maribel Lara-Chica; **Rosario Morrugares Carmona**; Carla Jiménez-Jiménez; Eduardo Muñoz Blanco; Marco A. Calzado Canale. "Identification of new DYRK2 substrates and their implications in carcinogenesis". Talk. DYRK1A, related kinases and human disease International Conference (ManROS Therapeutics), Saint Malo, Bretagne, France, March 28 – April 1st, 2017.

<u>Comunicaciones presentadas a congresos o jornadas nacionales</u>

- **Morrugares R**, Correa-Sáez A, Prados-González ME, Muñoz E & Calzado MA. (November 2019). *VCE-005.1 induces dephosphorylation of prolyl hydroxilase 2 (PHD2) and activates the HIF pathway.* II Reunión de la Red Temática de Excelencia de Investigación en Hipoxia (RedHYPOX) y V Reunión del Grupo Español de Hipoxia. Bilbao, Spain. Poster.
- Alejandro Correa Sáez, **Rosario Morrugares**, Rafael Jiménez Izquierdo, Martín Garrido Rodríguez, Francisco J. Ponce, Eduardo Muñoz, Laureano de la Vega, Marco A. Calzado. (November 2020*). Identificación e implicaciones de un nuevo mecanismo de regulación de DYRK2 basado en eventos de autofosforilación*. IV Congreso Nacional de Jóvenes Investigadores en Biomedicina, Universidad de Córdoba, Córdoba, Spain. Talk.
- Alejandro Correa-Sáez, **Rosario Morrugares**, Rafael Jiménez-Izquierdo, Martín Garrido-Rodríguez, Eduardo Muñoz and Marco A. Calzado. (October 2020). *Characterization of a new signalling pathway regulating the tumour suppressor FBXW7 in cancer*. Presented at: XI Young Investigators Meeting. IMIBIC – Instituto Maimónides de Investigación Biomédica de Córdoba, Córdoba, Spain. Talk..
- **Rosario Morrugares**, Alejandro Correa-Sáez, Rita Moreno, Martín Garrido-Rodríguez, Eduardo Muñoz, Laureano de la Vega and Marco A. Calzado. (May 2019). *Phosphorylation-dependent regulation of the NOTCH1 intracellular domain by dual-specificity tyrosine-regulated kinase 2*. Presented at: X Young Investigators Meeting. IMIBIC – Instituto Maimónides de Investigación Biomédica de Córdoba, Córdoba, Spain. Talk.
- Martín Garrido-Rodríguez, **Rosario Morrugares**, María Peña-Chilet, Eduardo Muñoz, Marco A Calzado and Joaquin Dopazo. *Using multi-omics to depict the response of human fibroblasts to X-ray radiation*. Disease Maps Community Meeting. Seville, Spain. 2019. Poster.
- Palomares B, Ruiz-Pino F, Garrido-Rodriguez M, **Morrugares R**, Velasco I, Sánchez-Garrido MA, Vázquez MJ, Gómez-Cañas M, Gonzalo C, Fernández-Ruiz J, Nadal X, Ferreiro-Vera C, Calzado MA, Tena-Sempere M, Muñoz E. *Target characterization of Δ9-Tetrahydrocannabinolic acid*. Implications in metabolic syndrome. 19th Annual SEIC Symposium on the Cannabinoids. Madrid, Spain. Talk.
- **Rosario Morrugares**, Maribel Lara Chica, Carla Jiménez Jiménez, Eduardo Muñoz and Marco A. Calzado. *Regulation of Notch1 expression and activity by DYRK2: New Insights of Carcinogenesis Signalling Pathways.* Presented at: 8th Young Investigators Meeting. IMIBIC – Instituto Maimónides de Investigación Biomédica de Córdoba, Córdoba, Spain. Talk.
- Carla Jiménez-Jiménez, Maribel Lara-Chica, **Rosario Morrugares**, Eduardo Muñoz, Marco A Calzado. (May 2017). *Hypoxia-Inducible Factor (HIF)-1 Regulatory Pathway and its Potential for Therapeutic*

Intervention in Metabolic Disease. Presented at: 8th Young Investigators Meeting. IMIBIC – Instituto Maimónides de Investigación Biomédica de Córdoba, Córdoba, España. Poster.

- Maribel Lara-Chica, **Rosario Morrugares**, Carla Jiménez-Jiménez, Eduardo Muñoz, Marco A. Calzado Canale. (April 2017). *Identification of new DYRK2 substrates and their implications in carcinogenesis.* Presented at: DYRK1A, related kinases & human disease. Saint Malo, France. Talk.

- **Morrugares-Carmona, R**., Waldron, K.W. & Azeredo, H. M. C. (November 2014). *Influence of pomegranate juice and citric acid on the physical properties of pectin films*. Presented at: Total Food 2014. IFR - Institute of Food Research, Norwich, Norfolk, England. Poster.

Por todo ello, se autoriza la presentación de la tesis doctoral.

Córdoba, 26 de Enero de 2022

Firma de los directores

CALZADO CANALE MARCO ANTONIO - 30808211X

Firmado digitalmente por CALZADO CANALE MARCO ANTONIO - 30808211X Fecha: 2022.02.01 20:43:38 +01'00'

MUÑOZ BLANCO EDUARDO - 30448749S

Firmado digitalmente por MUÑOZ BLANCO EDUARDO - 30448749S Fecha: 2022.02.01 20:44:08 +01'00'

Fdo.: Marco Antonio Calzado Canale   Fdo.: Eduardo Muñoz Blanco

A mi madre, a mis parejas, a mis amigas y a mi psicóloga.

Gracias por ayudarme a sobrevivir.

_____

To my mother, my partners, my friends, and my psychologist.

Thank you for keeping me alive.

"I am not young enough to know everything"

- *Oscar Wilde*

Table of contents

Abstract

Cancer is a complex disease enhanced by alterations in signaling pathways. In fact, DNA damage response (DDR) pathways play a key role in cancer development when they are deregulated. DDR pathways induce a cellular response that includes principally DNA repair pathways activation, cell cycle arrest, and cell death. Although there is a great knowledge of the signaling pathways that take place in DDR, further research is required to assess new molecular mechanisms for fully comprehend this complex scheme. In this sense, kinases like DYRK2, with an important role in DDR, are key to better understand and control DNA genomic damage situations. Thus, identification of new substrates for this kinase, as well as to elucidate novel pathways implicated in DDR would open a road to the development of new therapeutic strategies against cancer.

In the present work we show NOTCH1 as a novel substrate for DYRK2. We describe for the first time a new regulation mechanism of the NOTCH1 signaling pathway mediated by this kinase. We demonstrate that DYRK2 phosphorylates Notch1-IC in response to DNA damage and facilitates its proteasomal degradation by FBXW7 ubiquitin ligase through a Thr2512 phosphorylation-dependent mechanism. We show that DNA damage-dependently triggered DYRK2 has a relevant effect on the viability, motility and invasion capacity of cancer cells expressing NOTCH1. In summary, we reveal a novel DRYK2-dependent mechanism of regulation for NOTCH1 which might help us to better understand its role in cancer biology. Besides, we attempted to overview of cellular circuits that are involved in ionizing radiation triggered DNA damage response in human dermal fibroblasts. To allow this, we employed three different approaches: RNA-seq and proteomic and phosphoproteomic analysis based on SILAC labelling. This is, to our knowledge, the first work that compare these 3 different functional approaches to this aim.

The description of NOTCH1 as a new DYRK2 substrate, as well as the acquisition of solid data compilation that would permit a deeper understanding of the pathways that take place in response to ionizing radiation. This will provide new therapeutic opportunities for radiodermatitis prevention and treatment. Taken together, these data contribute to better understand the network of signaling pathways activation-deactivation under DNA damage conditions, opening a road to the development of new therapeutic strategies against cancer.

Resumen

El cáncer es una enfermedad compleja que se ve impulsada por alteraciones en rutas de señalización. De hecho, las rutas de respuesta al daño al ADN juegan un papel esencial en el desarrollo de cáncer cuando se encuentran desreguladas. Estas rutas inducen una respuesta celular que incluye principalmente la reparación del ADN, el arresto del ciclo celular y la muerte celular. A pesar de que existe un amplio conocimiento de las rutas de señalización de respuesta al daño al ADN, una mayor investigación es necesaria para detectar nuevos mecanismos moleculares que nos permitan comprender este complejo entramado de señales. En este sentido, proteínas como DYRK2 son esenciales para entender y controlar situaciones de daño al ADN. Por tanto, la identificación de nuevos sustratos para esta quinasa, así como de nuevas rutas de señalización implicadas en la respuesta al daño al ADN podrían ser herramientas muy útiles en el desarrollo de estrategias contra esta enfermedad.

En este trabajo mostramos cómo NOTCH1 es un nuevo sustrato de DYRK2. Describimos por primera vez un nuevo mecanismo regulatorio de la ruta de señalización de Notch por medio de esta quinasa. Demostramos que DYRK2 fosforila a NOTCH1-IC en la Thr2512 en respuesta a daño al ADN y promueve su degradación proteosomal gracias a la ubiquitinación por parte de la ubiquitín-ligasa FBXW7. Además, mostramos que el efecto de DYRK2 en respuesta a estrés genotóxico tiene un efecto relevante en la viabilidad, motilidad y capacidad de invasión de células tumorales que expresan NOTCH1. En resumen, mostramos un nuevo mecanismo de regulación de NOTCH1 por parte de DYRK2 que podría ayudarnos a comprender mejor su papel en la biología del cáncer. Además, hemos tratado de obtener una visión general de los circuitos celulares implicados en la respuesta al daño al ADN generado por radiación ionizante en fibroblastos. Para ello hemos analizado 3 niveles ómicos distintos: transcriptómico (por RNA-seq), proteómico y fosfoproteómico (empleando SILAC). Este sería hasta ahora el primer trabajo que emplea estas 3 aproximaciones diferentes para este fin.

En resumen, en este trabajo se describe NOTCH1 como un nuevo sustrato de DYRK2, así como la adquisición de datos sólidos que permiten una comprensión más profunda de las rutas que se activan en respuesta al daño al ADN. En conjunto, estos data contribuyen a una mejor comprensión de las redes de señalización que se activan y desactivan en respuesta al daño al ADN, abriendo una puerta al desarrollo de nuevas estrategias terapéuticas frente al cáncer.

Abbreviations

- **ADR:** Adriamycin
- **ALL:** Acute lymphoblastic leukemia
- **ANK:** Ankyrin-like repeat
- **ATM:** Ataxia telangiectasia mutated
- **ATR:** Ataxia telangiectasia and Rad3 related
- **BER:** Base-excision repair
- **BMI:** Body mass index
- **BPDE:** Benzo(a)pyrene diolepoxide
- **Cep78:** Centrosomal protein 78
- **CHKs:** Checkpoint kinases
- **CHX:** Cicloheximide
- **CLL:** Chronic lymphocytic leukemia
- **CMGC:** CDKs, GSKs, MAP kinases and CDK-like kinases
- **CoA:** Co-activator
- **CoR:** Co-repressor
- **CTGF:** Connective tissue growth factor
- **DDR:** DNA damage response
- **DH box:** DYRK homology box
- **DNMT1:** DNA (cytosine-5)-methyltransferase 1
- **DS:** Down syndrome
- **DSB:** Double-strand break
- **DSBR:** Double-strand break repair
- **DSCR:** Down syndrome critical region
- **DYRK2:** Dual-specificity tyrosine-(Y)-phosphorylation regulated kinase 2
- **DYRKs:** Dual-specificity tyrosine regulated kinases
- **EDVP:** EDD-DDB1-VprBP
- **EGF:** Epidermal growth factor
- **EMS:** Ethyl methanesulfonate
- **EMT:** epithelial to mesenchymal transition
- **ER:** Endoplasmic reticulum
- **ETP:** Etoposide
- **FBXW7:** F-Box and WD repeat domain containing 7
- **FIH:** Factor inhibiting HIF

- **GSK3β:** Glycogen synthase kinase 3 β
- **HD:** Heterodimerization domain
- **HIF:** Hypoxia inducible factor
- **HIPK2:** Homeodomain-interacting protein kinase 2
- **HR:** homolgous recombination
- **ICL:** Insterstrans crosslink
- **IP:** Immunoprecipitation
- **IR:** Ionizing radiation
- **KD:** Kinase dead
- **KM:** Kinase mutant
- **KO:** Knock-out
- **LDN:** LDN19296
- **LET:** Linear energy transfer
- **MAO-A:** Monoamine oxidase A
- **MMR:** Mismatch repair
- **MMS:** Methyl methanesulfonate
- **MNU:** Methylnitrosourea
- **NAPA:** N-terminal autophosphorylation accessory region
- **NECD:** Notch extracellular domain
- **NER:** Nucleotide-excision repair
- **NEXT:** Notch external truncation
- **NHEJ:** Non-homologous end-joining
- **NICD:** Notch intracellular domain
- **Ni-NTA:** Nickel-nitrilotriacetic acid
- **NLS:** nuclear localization signal
- **NSCLC:** Non-small cell lung cancer
- **PAH:** Polycyclic aromatic hydrocarbons
- **PEST:** Proline (P), glutamic acid (E), serine (S), and threonine (T) enriched sequence
- **PKC:** Protein kinase C
- **PRKDC:** Protein kinase, DNA-activated, catalytic subunit
- **PTMs:** Post-translational modifications
- **qPCR:** Quantitative real time polymerase chain reaction

- **RAM:** RBPJ-associated molecule
- **ROS:** Reactive oxygen species
- **RT:** Radiotherapy
- **SILAC:** Stable isotope labeling by amino acids in cell culture
- **SSB:** Single-strand break
- **SSBR:** Single-strand break repair
- **TAD:** Transactivation domain
- **T-ALL:** T cell acute lymphoblastic leukemia
- **TAM:** Tumor-associated macrophages
- **TERT:** Telomerase reverse transcriptase
- **TLS:** Translesion DNA synthesis
- **TMD:** Transmembrane domain
- **TNBC:** Triple-negative breast cancer
- **TOP:** Topoisomerase
- **UV:** Ultraviolet
- **VEGF:** Vascular endothelial growth factor
- **WT:** Wild type

Introduction

4.1. DYRK2

4.1.1. DYRK family

Dual-specificity tyrosine regulated kinases (DYRKs) constitute a highly evolutionarily conserved family which belongs to the CMGC group of kinases. This CMGC group also includes other families of kinases like CDK-like kinases (CLKs), cyclin-dependent kinases (CDKs), mitogen-activated protein kinases (MAPKs) and glycogen synthase kinases (GSKs) (1). DYRK family proteins are distributed on three different subfamilies concerning their homology within their kinase domain: pre-mRNA processing protein 4 kinases (PRP4s), homeodomain-interacting protein kinases (HIPKs) and DYRK kinases (1-3). DYRK members are present in all eukaryote organisms and share common properties like structure or function (3). In mammals, DYRK members can be at the same time classified in 2 classes: DYRK1A and DYRK1B belong to the class I and DYRK2, DYRK3 and DYRK4 are allocated in class II (1). Regarding their domains, all of them present a common kinase region and a homology box (DYRK-homology or DH box) in the N-terminal part. Despite this, there exist differences between the two classes concerning substrate specificity, tissue distribution or subcellular localization. Class I DYRKs are mainly localized in the nucleus while class II DYRKs are generally cytoplasmatic (1).

DYRK1A is the most deeply studied member of all 5 DYRK subfamily members. It is encoded in the DSCR (Down Syndrome Critical Region) of chromosome 21, and its overexpression is responsible for most cognitive deficits in DS patients (4). Besides, DYRK1A is also implicated in Alzheimer's Disease by phosphorylating Tau (5), diabetes (6, 7) and is a risk factor for Parkinson's Disease (8). Some works have reported a link between DYRK1A and pancreatic, brain or Acute Lymphoblastic Leukemia (ALL) cancers among others (4). In addition to its clear neurodevelopment implications, DYRK1A is involved in Ca^{2+} signaling by phosphorylating NFAT (9), as well as diverse signaling pathways due to the phosphorylation of eIF2B, Tau (10) and STAT3 (11) among other substrates. On the other hand, DYRK1B has been described to mediate cell survival and differentiation, and its levels are increased in muscle tissues (12-14). Additionally, it has been also reported that DYRK1B mutations are related to metabolic syndrome conditions (15). With respect to class II DYRKs, DYRK3 is specially elevated in testis and hematopoietic cells, where contributes to a decrease in apoptosis in response to cytokine

starvation (16). Besides, Guo and collaborators registered that DYRK3 phosphorylates SIRT1 (17). Finally, DYRK4 is the less studied DYRK family member. DYRK4 expression is limited to testis, where collaborates to the spermiogenesis process (18).

4.1.2.   Expression and structure of DYRK2

DYRK2 is probably the most relevant member in class II DYRK subfamily (2, 3, 19, 20). The gene encoding this protein (*Dyrk2*) is located in chromosome 12q15, with a length of 17069 bp (21). To date, 6 different splice variants of DYRK2 have been described, from which only 2 have been isolated. One of them correspond to a 528 aminoacids (aa) protein, encoded by DYRK2-203 transcript (22). This isoform is widely known as isoform 1 and is considered the most prevalent DYRK2 isoform. On the other hand, isoform 2 would derive from DYRK2-202 transcript. This second isoform is a 601 aa sequence, with a 73 aa longer N terminus. It is important to remark that despite isoform 1 is the most prevalent, most databases and some works employ DYRK2 isoform. In fact, this thesis is centered in the use of this longer isoform of DYRK2 (Figure 1).
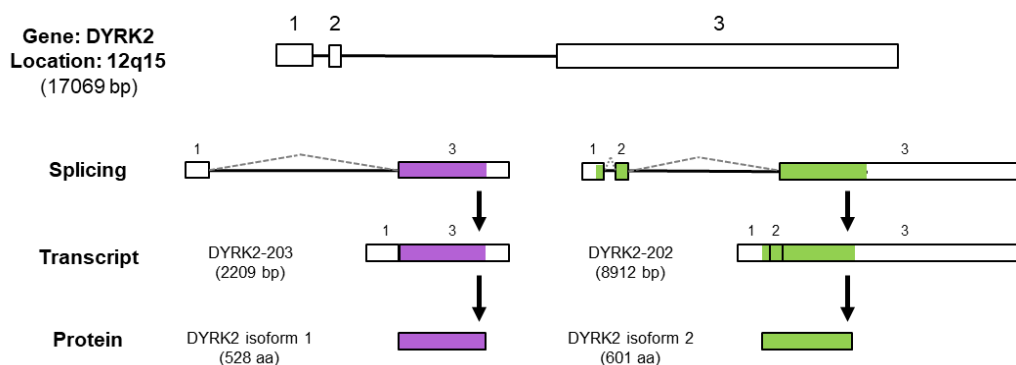
Figure 1. DYRK2 processing, from gene to protein. Schematic illustration of DYRK2 human expression processing. Rectangles represent exons and lines represent introns. Purple and green rectangles depict translated exons of isoforms 1 or 2, respectively (**23**).

According to data collected from The Human Protein Atlas by Correa and colleagues, expression of DYRK2 varies depending on tissue and the measured biological level. For example, small intestine or heart muscle present high mRNA and protein levels of DYRK2. Despite this, elevated levels of DYRK2 mRNA are detected, negatively correlating to protein levels of the kinase (23). Additionally, DYRK2 expression is modulated in certain diseases, especially in tumors. In fact, most works suggest a

down-regulation of DYRK2 expression in cancer. It has been reported a repression of DYRK2 by KLF4 in leukemic stem/progenitor cells (24), as well as in colorectal cancer cells by DNMT1-dependent methylation (25). Besides, DYRK2 expression is also downregulated by miRNAs 662, 208a, 338-3p, 499 and 187-3p in colorectal, intestinal, and liver cancer cells, among others (26-29).

Regarding its structure, DYRK2 comprises various functional domains (Figure 2). There are two regions shared with the rest of the family: a) DYRK-homology box (DH box, aa 200-210), and b) the kinase domain (aa 222-535) (1). Another common sequence among all DYRKs (except for DYRK3) is the NLS (Nuclear Localization Signal, aa 189-191) motif, in charge of protein translocation to the nucleus (30, 31). The "activation loop" sequence (aa 380-382) is key, since autophosphorylation in Tyr382 during protein translation is essential for DYRK2 activity. Besides, there are two NAPA (N-terminal autophosphorylation accessory region) domains, NAPA1 and NAPA2 (aa 167-185 and 162-220, respectively), that provide chaperone functions permitting self-phosphorylation of the kinase during the activation loop. These NAPA regions are also present in the rest of class II DYRKs. Finally, at the most C-terminal region, DYRK2 presents its kinase domain, including the active site (residues 344-356) and the ATP binding site (Lys251), located in the ATP binding pocket (aa 228-251) (1, 3, 19, 20, 31, 32).

4.1.3.   Regulation of DYRK2

Not much information has been reported about DYRK2 regulation at a transcriptional level. Nevertheless, it was described that *DYRK2* gene expression is repressed by KLF4 in stem and progenitor cells (24), and by DNMT1 in human colorectal cancer cells (25). Likewise, several miRNAs have been reported to modulate DYRK2 gene expression in different human cell lines: miR-187-3p, miR-208a, miR338-3p, miR449 and miR-662 (26-29, 33).

As reported by Lochhead and collaborators, autophosphorylation of an essential Tyr residue in the activation loop of DYRKs is required for a proper kinase functionality (20). This self-phosphorylation is common to all DYRKs, being Tyr382 the affected aminoacid for DYRK2 (34). This phosphorylation event occurs during protein translation by a transitional intermediate version of the kinase. After this initial Tyr phosphorylation,

DYRK2 kinase activity is restricted to Ser and Thr residues (3, 20, 35). In fact, no phosphorylated Tyr residues have been found in any DYRK2 substrate nowadays. Previous works have demonstrated that autophosphorylation events play important roles in DYRK1A, DYRK1B and DYRK3 proteins, like modulating their stability, intracellular location or activity (19, 36-39). In the case of DYRK2, up to 10 new autophosphorylation residues within the activation loop (Thr32, Thr33, Thr82, Ser483, Thr484, Thr488, Ser489 and Ser498/499/501) have been detected (40). Regarding other post-translational modifications (PTMs), there have been reported different proteins that modulate DYRK2 protein levels and activity. On the one hand, it has been described that MDM2 normally ubiquitinates nuclear DYRK2. After DNA damage, ATM phosphorylates DYRK2 promoting DYRK2 avoidance of MDM2-dependent ubiquitination and then enabling its nuclear stabilization (31). Additionally, our group previously described that ubiquitin ligase SIAH2 interacts and ubiquitinates DYRK2 under hypoxic conditions (41). Besides, MAP3K10 has been described to double phosphorylate DYRK2 by a high throughput screening altering Hedgehog signaling pathway by modulating GLI regulation by DYRK2 (42). Cep78 (Centrosomal protein 78) modulates DYRK2 scaffolding function by inhibiting the EDD-DYRK2-DDB1^VprBP complex, affecting CP110 ubiquitination and then centriole length and cilia assembly (22). Also, LPS has been reported to induce DYRK2 translocation to the nucleus altering its levels (43).
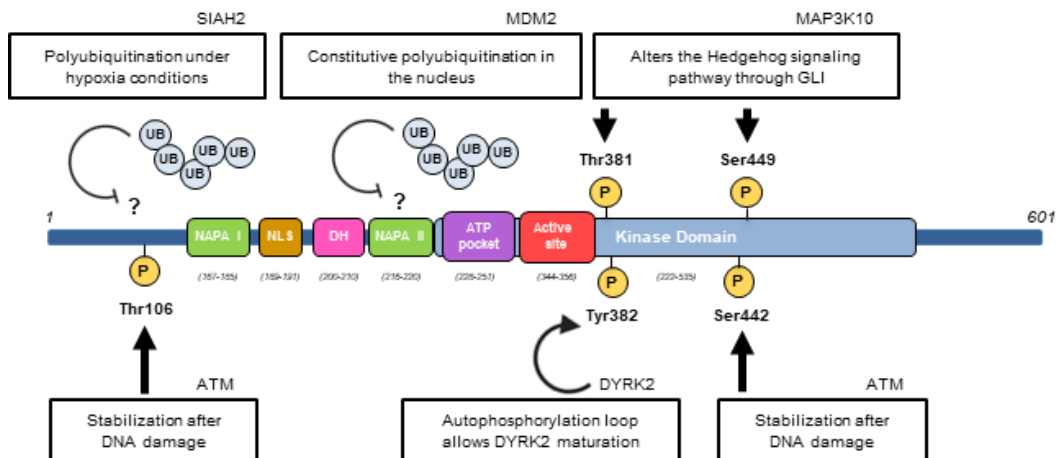
Figure 2. Schematic overview of DYRK2 isoform 2 with PTMs. NAPA I and NAPA II domains, nuclear localization signal (NLS), DYRK-homology box (DH), the ATP binding pocket, the kinase domain, and the active site are represented, as well as their residues. DYRK2 is regulated by phosphorylation and ubiquitination events. These modifications alter DYRK2 stability, function, and subcellular localization among others. Residues affected by these phosphorylations and ubiquitinations are represented (**23**).

4.1.4. DYRK2 mechanism of action

DYRK2 activity is based principally on the phosphorylation of Ser/Thr residues of its substrates. Despite at first DYRK2 was reported as a Pro-directed kinase, later works demonstrated that there exists a wide diversity of motifs phosphorylated by DYRK2 (19). The existence of an Arg residue at -2 position and Pro at +1 is essential (44), although it has been described a certain degree of variability. In example, on occasion the Arg residue is located at -1 position (45). Taking all data together result in a consensus sequence which would represent a potential target for DYRK2 phosphorylation: 'Rx(x)S/TP' (19). Anyway, it is important to remark that not all DYRK2 phosphorylation sites present this pattern. In addition, DYRK2 has been described as a priming kinase for GSK3β (Glycogen synthase kinase 3 β) (10, 46-50). GSK3β is a Ser/Thr kinase with a vast number of functions and substrates (51, 52) and sometimes requires the previous phosphorylation of those substrates to correctly carry out its activity (53, 54). Regarding this, some DYRK2 substrates like c-Myc, c-Jun, SNAIL, eIF2Bε or CRMP4 are subsequently recognized by GSK3β (10, 46, 47). These consecutive phosphorylations result in substrates proteasomal degradation in a ubiquitination dependent way.

It has also been shown that DYRK2 presents a role as scaffold protein. It has been reported that DYRK2 acts as an intermediate support protein for EDD and DDB1 components of the EDVP (EDD-DDB1-VprBP) E3 ligase complex. This happens in the G2/M phase of the cell cycle. In the same study it was demonstrated that DYRK2 phosphorylates katanin p60 leading to its proteasomal degradation after ubiquitination (55). A similar function has been described for telomerase reverse transcriptase (TERT). TERT is also an EDVP substrate and presents a key function in genomic stability by maintaining telomeres (56). CP110 (Centrosomal Protein of 110 kDa) is also regulated by the axis DYRK2-EDVP E3 ligase through phosphorylation and proteasomal degradation (22).

4.1.5. DYRK2 biological function and cancer

DYRK2 is implicated in several essential events related to diverse biological functions like cell proliferation, cell differentiation, apoptosis, or cell survival, among others (Figure 3). Nevertheless and in spite of its apparent key role in those pathways,

barely more than 20 substrates of DYRK2 have been reported: H3F3A (57), eIF2Bε, Tau (10), STAT3 (11), eIF4EBP1 (58), Glycogen synthase 1 (59), CARHSP1 (60), NFAT (9), p53 (61), Gli2 (42), Katanin p60 (55), CRMP4 (50), DCX (62), c-Jun, c-Myc (47), SIAH2 (41), Snail (46), TERT (56), TBK1 (63), Rpt3 (64), NDEL1 (65), HSF1 (66) and CDC25A (40).

Some of the biological functions of DYRK2 are related to cell proliferation, apoptosis, cell growth or cell migration, among others. This variety of functions are essential for the proper function of the organism, but also turn DYRK2 into a key protein in tumorigenesis. Regarding apoptosis, several works reported that this kinase modulates apoptosis in response to DNA damage by phosphorylating p53 (47, 61). In addition, DYRK2 protein levels increase after DNA damage when ATM phosphorylates residues Thr33 and Ser369. This supports the concept of the proapoptotic role of DYRK2 (31, 61). In the same vein, apoptosis is reduced in leukemic stem and progenitor cells when DYRK2 is inhibited by KLF4 (24). On the other hand, some other works reported that DYRK2 is an antiapoptotic protein. It has been described that DYRK2 interacts with RNF8 for DNA repair after double strand break (DSB) (67), and modulates proteotoxic response via HSF1, showing higher apoptotic rates for DYRK2 knock out breast cancer cell lines comparing to the wild type ones (66). Antiapoptotic role for DYRK2 has been also described in human intestinal cancer cells (HICs), in which miR3883-3p targets DYRK2 after ionizing radiation (33). Regarding patient survival rates to DYRK2, there has been shown a positive correlation of patient survival and DYRK2 expression in NSCLC, lung adenocarcinoma, hepatocellular, non-Hodgkin's lymphoma and bladder and colorectal cancers (68-74). On the opposite, DYRK2 levels are negatively correlated to patient survival in neuroblastoma (75). Controversial results have been reported for breast cancer (46, 64, 76).

In addition to these apoptosis-related roles, DYRK2 can also modulate cell cycle. EDPV-DYRK2 complex phosphorylates and degrades katanin-p60 and TERT at G2/M transition (55, 56). Also, DYRK2 regulates G1/S transition in different manners: by phosphorylating c-Jun and c-Myc, thus reducing breast cancer invasiveness (47), and by phosphorylating Rpt3 26S proteasome subunit (64). Nonetheless, in the second case, loss of DYRK2 reduced cell growth rather than promoting it. It has been also reported that DYRK2 inhibition reduces cell proliferation and induces apoptosis, and so

jeopardizing triple negative breast cancer and multiple myeloma progression (30, 77). Recently, Lara-Chica and collaborators have described a novel role of DYRK2 in cell cycle progression via CDC25A modulation through the ubiquitin-proteasome pathway (40).

Finally, and concerning metastasis and epithelial to mesenchymal transition (EMT), it must be mention SNAIL phosphorylation by DYRK2, which induces its degradation thus reducing EMT and metastatic potential in breast and ovarian cancer (46, 78, 79). Besides, DYRK2 results important for glioma EMT and metastatic processes, since EMT is suppressed by vimentin, SNAIL and E-cadherin levels modulation in a DYRK2-dependent manner and DYRK2 levels negatively correlate to glioma invasiveness (80, 81). Metastatic potential of cancer cells is modulated by DYRK2 in breast cancer via CDK14 modulation (82) or colorectal cancer, where DYRK2 is targeted by miR-622 (27). Taken together, these data support an antitumoral role for DYRK2, but there exist some works in which DYRK2 is reported as a protumoral protein since its inhibition reduces aggressiveness of TNBC cells (30, 77).
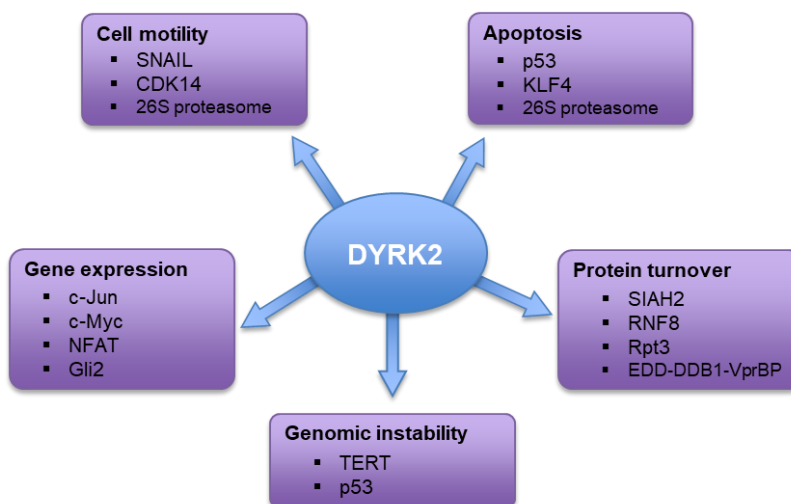
Figure 3. DYRK2 in cancer. Schematic summary of the main functions of DYRK2 in cancer development and the substrates responsible of them.

4.1.6.   Pharmacological modulation of DYRK2

In addition to the previously described endogenous regulations of DYRK2 levels and activity, several drugs have been reported to modulate this kinase (83). Among them, it is worth to mention 3 main molecules that have been employed during the experimental phase of this thesis: harmine, curcumin and LDN19296 (LDN).

The most widely used DYRK2 inhibitor to date is harmine, a derivative of β-carboline isolated from *Peganum harmala L.* This drug is a high-affinity inhibitor of MAO-A (Monoamine oxidase A) and is commonly employed to study all DYRK family. Harmine is an ATP-competitive inhibitor with a strong activity against DYRK1A. Its IC_{50} for DYRK2 is 0.8 mM (84, 85). Harmine treatments induce a reduction of cell proliferation, as well as invasion and migration when tested in different human cancer cell lines (75, 86). Curcumin is a well-known drug obtained from *Curcuma longa* with multiple biological activities (87) that inhibits *in vitro* and *in vivo* DYRK2 activity in a dose-dependent manner (77). DYRK2 inhibition occurs when curcumin occupies the ATP-binding pocket of the kinase. This action happens in vitro with an IC_{50} of 5 nM, and in HEK293T cells inhibits DYRK2-dependent RPT3 phosphorylation of Thr25 with a maximum effect at 10 μM. Besides, curcumin inhibits other DYRK family members and some works have reported its ability to sensitise multiple myeloma TNBC and triple-negative breast cancer cells by reducing their proteasome activity (77). Finally, the most recently described inhibitor of DYRK2, as well as the most efficient to date, is LDN (30). This compound was firstly developed as a Haspin inhibitor (88, 89) and inhibits DYRK2 in vitro activity with an IC_{50} of 13 nM, occupying the ATP-binding pocket through stablishing multiple hydrogen bonds. Besides, Banerjee and collaborators have described LDN-dependent inhibition of pThr25 RPT3 in a dose-dependent manner, with maximum effects at 1-10 μM. Like curcumin, it has been reported that LDN modulates cancerous progression in different cell lines by affecting DYRK2-dependent phosphorylation of the proteasome (30).

4.2. NOTCH1

4.2.1. NOTCH proteins

Notch gene was first found more than 100 years ago when Morgan and collaborators were studying *Drosophila melanogaster* development. They reported a partial loss of function in notches at the win margin (90). Few decades after, Notch was described as a neurogenic gene, since loss of function approaches induced change of fate of epidermal cells to neural cells (91). In mammals, there have been described up to 4 different Notch proteins (NOTCH1-4). NOTCH receptors are normally transduced as single-chain precursors and transported to the endoplasmic reticulum. There, the extracellular region (NECD) is glycosylated, which will modulate their affinity for ligands. These NOTCH precursors are then transferred to the Golgi and cleaved by furin-like proteases, resulting in NOTCH extracellular-transmembrane subunits heterodimers that will finally reach the plasma membrane (92, 93).

NOTCH ligands comprehend 2 jagged (Jag1/2) and 3 delta-like (DLL1, DLL3, and DLL4) transmembrane proteins (94). NOTCH receptors share a modular structure that can be summarized into different functional regions (Figure 4): an extracellular domain (at the N-terminal domain), an intracellular tail (NOTCH-IC, at the C-terminal domain), and a connector between the two. NOTCH extracellular domain exhibits two main different regions: on the one hand a cluster of EGF (epidermal growth factor) repeats (36 repeats in NOTCH1/2 and 34 in NOTCH3/4) and on the other hand, various Lin-12/Notch repeats (LNR) (3 in the case of NOTCH1/2 and 29 when talking about Notch3/4) (95). Moving to the C-terminal of the NECD the heterodimerization domain (HD) can be found, linking NECD and NOTCH intracellular domain (NOTCH-IC). NOTCH-IC presents, from N-terminal to C-terminal, a RBPJ-associated molecule (RAM) region, 7 ankyrin-like repeats (ANK) (96, 97), and the nuclear localization sequences (NLS, within the transactivation domain (TAD). Finally, it is important to mention the PEST (proline, glutamic acid, serine, threonine) sequence, which is a region enriched in these residues. This PEST sequence is found in other proteins in which it acts as a signal peptide for protein degradation (98).
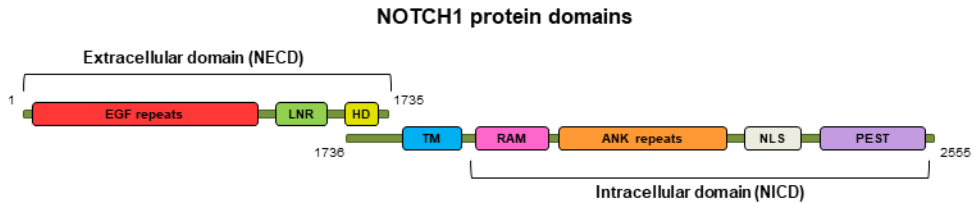
Figure 4. NOTCH1 protein structure. Schematic representation of mature NOTCH1 protein structure showing its domains. EGF repeats: 36 x epidermal growth factor repeats. LNR: 3 x Lin12/Notch units. HD: heterodimerization domain. TM: transmembrane domain. RAM: RBPJ-associated molecule region. ANK: 7 x ankyrin-like repeats. NLS: Nuclear localization sequences. PEST: Proline, glutamic acid, serine, and threonine enriched domain.

4.2.2.   Notch signaling pathway

Regarding canonical Notch signaling, the first step of the pathway is the interaction of the NECD with a canonical NOTCH transmembrane ligand (DLL1/3/4 or Jagged1/2) from an adjacent cell. This interplay promotes a cascade of 3 main cleavages of the receptor (S1, S2 and S3) and concludes in the intracellular region of NOTCH (NOTCH-IC) being cleaved by γ-secretase (99-101) (Figure 5).

- S1 cleavage has been described as the first proteolytic process Notch is subjected to. It takes places during maturation of the receptor in the Golgi. At first Notch is expressed as a 300 kDa protein, but after S1 cleavage by furin protease it is separated into 120 and 200 kDa peptides. These two pieces associate in a non-covalent way before being exposed on the cell surface (102).

- S2 cleavage is the second NOTCH proteolysis, and it is irreversible and ligand dependent. When NECD interacts with the ligand, an ADAM protein (ADAM10 in mammals) (103) induce S2 cleavage in the negative regulatory region of Notch, right C-terminal to the S1 cleavage. This leads to a separate extracellular domain of Notch that stay linked to the ligand and is endocytosed into that adjacent cell. Anchored to the membrane remains an intermediate called NOTCH external truncation (NEXT), in which we can found NOTCH-IC. (104-106).

- Finally, S3 cleavage takes place. NEXT transient molecule quickly undergoes this proteolysis in the transmembrane domain, because of the activity of the γ-secretase complex. This final step may happen either at the cell membrane or in the endosomes (107) but either way Notch intracellular domain (NOTCH-IC) is released, as well as a residual transmembrane domain (TMD). NOTCH-IC translocates to the nucleus and interacts with CSL/RBP-JK, a DNA-binding protein (108), to exert its function as transcriptional factor. TMD fate and function remain unclear, but a recent study has described its role regulating F-actin organization in response to shear stress in the vascular endothelial barrier (109).
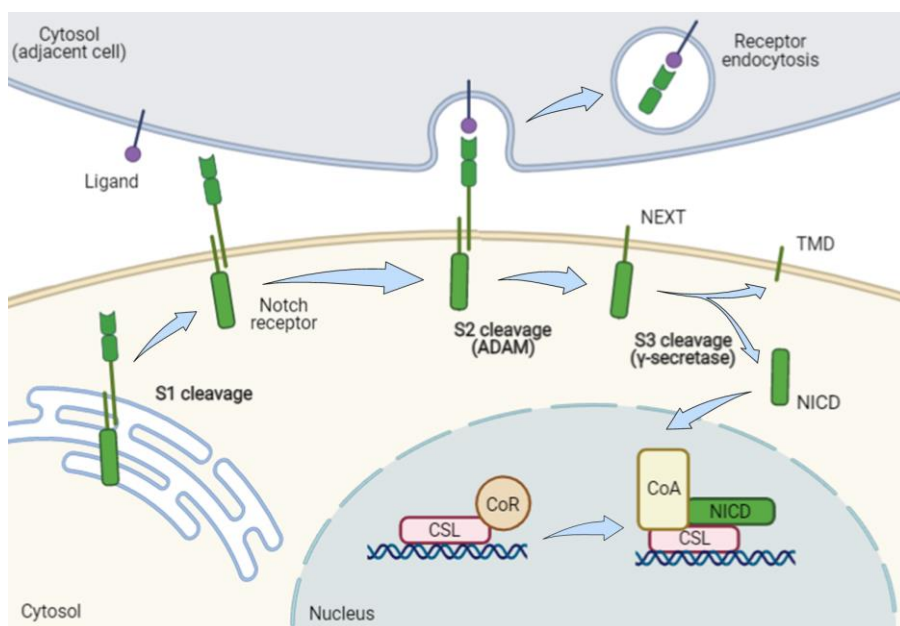
Figure 5. NOTCH signaling pathway. Schematic overview of NOTCH signaling pathway, from the first cleavage at the Golgi to the activation of the transcriptional machinery in the nucleus.

CLS has been reported to be habitually repressing transcription together with a co-repressor complex what includes SMRT, histone deacetylases and SHARP/MINT, among other proteins (110). NOTCH-IC union to CSL induces the recruitment of a co-activator complex along with MAML1-3, SKIP and/or CREB-binding protein/p300 proteins (111-113). Then, NOTCH pathway leads to the transcriptional activation of CSL-dependent elements. Traditionally, it has been considered that CSL is bound to a co-repressor (CoR) complex but in presence of NOTCH-IC that CoR complex is substituted by a co-activator (CoA) one. Nevertheless, this paradigm has been questioned since

works in *Drosophila* suggest that CSL-containing repressor complexes may bind chromatin in a highly dynamic, transient way (114). According to this, NOTCH-IC would be promoting chromatin opening and enhancing CSL complexes recruitment. Whichever the sequence of molecular events is, the synergic activity of NOTCH-CSL leads to the expression of numerous NOTCH response genes essential for cellular survival, fate, and proper function, including HES1, HES2 and HES5, MYC, CCND1, and VEGF (115). Among NOTCH targeted genes, is important to mention Hairy enhancer of split genes 1-7 (Hes 1-7), Hey (Hey1, 2 and L) and Nrarp. These target genes likewise modulate expression of secondary targets such as c-Myc, Cyclin D1, CDKN1A or Deltex.

4.2.3.   NOTCH1 regulation

NOTCH receptors are extensively regulated by post-translational modifications (PTMs) along the multiple steps of the signaling pathway. Among these PTMs, phosphorylation and ubiquitination are the most remarkable ones when talking about activated NOTCH1 regulation. NOTCH is modified at different moments since its translation, besides the previously explained cleavages S1, S2 and S3. These PTMs are modifiers of signaling that transform an activated signal to a specific output. There can be recognized different types of PTMs: glycosylation, hydroxylation, acetylation, methylation, sumoylation, phosphorylation and ubiquitination.

Glycosylation: It is the first PTMs that occur regarding NOTCH signaling, since NECD domain is affected during its synthesis and processing in the ER (116, 117). This modification consists in the link of glycans on the oxygen of a hydroxy group of Ser or Thr, altering NOTCH structure and specificity for its ligands. All of them occurs in the EGF region of NOTCH. Three different O-glycosylations of NOTCH can be distinguished: O-glucosylation, O-fucosylation and O-GlcNAcylation (118). This O-fucosylation is carried out by Manic, Lunatic and Radical Fringe proteins (MFNG, LNFG, RFNG), that tune NOTCH receptor-ligand interactions (119). Besides, O-GalNAc glycan alteration has been described to modify NOTCH outside the EGF-repeats, near the S2 cleavage site (120). There exist studies that report N-glycosylations of NOTCH in mammals, but they do not seem indispensable for NOTCH signaling (121, 122).

Hydroxylation: It has been described that FIH (the asparaginyl hydroxylase Factor Inhibiting HIF) promotes NOTCH-IC hydroxylation of Asn residues within the ANK domain of NOTCH1, inducing NOTCH signaling downregulation (123-125). Additionally, NOTCH-IC has been shown to act as a HIF-1α competitor for FIH, since it has higher affinity for NOTCH-IC (125, 126).

Acetylation: Several acetyltransferases have been studied as regulators of NOTCH-IC: p300, PCAF and GCN5 (127, 128). These acetylations block NOTCH-IC ubiquitination and posterior proteasomal degradation, thus promoting NOTCH-IC stabilization. In the other hand, some deacetylases like SIRT1 or HDAC1 have been showed to reverse that effect in a variety of models and systems like neural stem and progenitor cells, neonatal rat cardiomyocytes, macrophages and T-reg cells (33, 129-131).

Methylation: This process consists in the transference of a methyl group to Lys or Arg residues and normally collaborate to the establishment of epigenetic control by affecting histones, as well as modulate other proteins expression and stability. To date, little is known about NOTCH-IC methylation. Nevertheless, CARM1 has been described to methylate NOTCH-IC on 5 different conserved Arg residues within NOTCH-IC TAD region (132). This methylation stimulates NOTCH transcriptional activity, but also induces proteasomal degradation of NOTCH-IC through ubiquitination.

Phosphorylation: Numerous protein kinases have been reported to affect NOTCH proteins at different domains thus producing different effects. To date, both NEXT and NOTCH-IC have been demonstrated to be phosphorylated (133, 134). Cyclin C enhances CDK1-3, CDK8 or CDK19 inducing NOTCH1 phosphorylation at several residues of the PEST domain. These phosphorylations generally induce NOTCH-IC proteasomal degradation in a FBXW7/Sel10 dependent manner (135-138). Other kinases like CDK2, ILK, SRCs or NLK modulate NOTCH-IC transcriptional activity. In the case of CDK2, it phosphorylates NOTCH-IC at two different residues (Ser1900 and Thr1897), reducing NOTCH-IC interaction with Mastermind-CSL complex thus compromising transcriptional activity (139). In the other hand, ILK regulates NOTCH-IC by phosphorylating it. This event inhibits NOTCH-IC transcriptional activity and conduces it to proteasomal degradation via FBXW7 (140). SRC kinases also have a role in regulating NOTCH-IC transcriptional activity. They act downstream of integrins and

phosphorylates ANK domain of NOTCH-IC, promoting a decreased MAML recruitment and NOTCH-IC half-life (141). NLK (Nemo-like kinase) also phosphorylates NOTCH1 protein, at both membrane-tethered and intracellular domain forms. This phosphorylation does not modulate NOTCH-IC stability, but interferes with the interaction of Mastermind, thus reducing the association of the transcription complex and reducing the transcriptional effects of the pathway (142). In addition to the previous kinases described, PIM-kinases have been described to phosphorylate NOTCH-IC at the second NLS sequence, promoting nuclear localization thus transcriptional activity (143). Conversely, AKT has the opposite effect, since NOTCH-IC phosphorylation by AKT inhibits proper nuclear localization and transcriptional activity. This occurs with NOTCH1 and 4 and it is mediated by 14-3-3 proteins interference (144, 145). Phosphorylation also impacts receptor recycling, as it was reported because of PKCz activity on NOTCH1 at both NEXT and full-length receptor. This phosphorylation has been described for Ser1719 in mouse (Ser1801 in human) and modulate NOTCH endocytosis either enhancing NOTCH-IC formation or NOTCH receptor recycling (146). The case of NOTCH-IC phosphorylation by GSK3β is conflictive regarding its effects. The complex GSK3β/Shaggy phosphorylates NOTCH1 preventing NOTCH-IC proteolysis by Itch at the same time as reinforces HES1 expression in different biological models (137, 147, 148). By contrast, it has been reported that GSK3β is a negative regulator of NOTCH1 by phosphorylating various Thr residues (147). DYRK1A, a member of DYRK family of kinases, can modulate NOTCH1 transactivation by phosphorylating it at up to 18 residues in the AKN domain, although this process does not affect NOTCH-IC protein stability (149). Nevertheless, is not the only member of DYRK family that can phosphorylate NOTCH1. In the later years, Homeodomain-interacting protein kinase 2 (HIPK2), also member of the same family, has been identified as a regulator of NOTCH-IC by phosphorylating it at Thr2512 and then promoting its proteasomal degradation via FBXW7 E3-ubiquitin ligase (150).

Ubiquitination: On the one hand, NOTCH ligands ubiquitination is necessary to activate NOTCH1 signaling pathway. This ubiquitination induces the ligand endocytosis, promoting the S2 cleavage of NOTCH1 and the subsequent activation of the pathway (151, 152). On the other hand, ubiquitination of NOTCH1 is crucial downregulating the resultant signal transduction. Even though NOTCH poly-ubiquitination not always induces reduced NOTCH levels, proteasomal degradation of NOTCH is critical to modulate NOTCH-IC lifespan. This process is so important that flaw in NOTCH

degradation normally leads to numerous diseases (153). A wide range of ubiquitin E3 ligases have been described to affect NOTCH-IC. The number of NOTCH receptors that are exposed at the cell membrane is constitutively regulated by endocytosis via NEDD4 ubiquitin ligase. From these endosomes, the receptor can be stored for later use, recycled, or degraded in the lysosomes (107). Numb protein is a negative regulator of NOTCH and prevents its recycling to the plasma membrane, promoting NOTCH ubiquitination by Itch and the subsequent targeting for lysosomal degradation (154, 155). This process is negatively regulated by Shootin1, which stabilizes NOTCH by interfering with Itch complex or ubiquitinating NUMB (156). USP12 has also been reported to be a NOTCH downregulator by targeting NOTCH thus promoting its lysosomal degradation (157). Nevertheless, it is remarkable give a special mention to PEST domain role in NOTCH-IC proteasomal degradation via ubiquitination. A being phosphorylated, this sequence is recognized by FBXW7 E3 ligase, which ubiquitinates NOTCH-IC leading to its proteasomal degradation (135, 136, 150, 158-160). Failure in this interaction is generally related to leukemia and many other cancers (161-163). It has also been described that RNF8 affects NOTCH-IC inducing its degradation, as well as a correlation of low levels of RNF8 with bad prognosis for breast cancer patients (164). Despite these data, ubiquitination not always reduces NOTCH-IC levels. NOTCH-IC ubiquitination by RNF4 or MDM2 support and reinforce NOTCH-IC transcriptional activity (165, 166). In addition, ubiquitination processes are compensated by deubiquitinases (DUBs), which remove ubiquitin molecules from ubiquitinated proteins. For example, loss of Usp5 promotes NOTCH upregulation during *Drosophila* eye development (167, 168).

4.2.4. NOTCH signaling and cancer

A wide range of biological functions are controlled by NOTCH signaling pathway (Figure 6). Among them, angiogenesis, vasculature development during embryogenesis, wound healing, tissue repair, stem cell maintenance, cell proliferation, differentiation, or cell death are remarkable (169-171). Although under physiological conditions these functions are crucial for the organism, NOTCH signaling roles in cancer are not surprising (172). Inhibition of apoptosis, induction of EMT, drug resistance, enhancement of a stem-lie phenotype and metastasis are some of NOTCH signaling oncogenic effects (173, 174). In spite of this, there are also some reports that point NOTCH out like a tumor

suppressor such as in case of cell cycle arrest and differentiation of epidermal keratinocytes (175, 176). This would suggest that these mechanisms may be context dependent.

Both hyper- or hypoactivation of NOTCH pathway can result in a cancerous situation depending on the genetic alterations, the specific tissue and the ligand-receptor interaction. In example, there has been identified NOTCH1 mutations related to hypoactivation of the pathway in squamous cell carcinoma of skin, head and neck, and esophagus (177). On the other hand, NOTCH1 hyperactivating mutations are normally linked to breast cancer, T-ALL, CLL, mantle cell lymphoma and adenoid cystic carcinoma (172, 178-180). For instance, T-ALL, breast cancer and adenoid cystic carcinoma have been described to be promoted by mutations, chromosomal rearrangement, or deletions in the NOTCH1 gene, which derives in higher levels of NOTCH-IC thus supporting tumor development (178, 180-182). Other types of mutations that induce NOTCH activation would consist in mutation on the regulatory portions of the receptor (either PEST or TAD). This would stabilize the protein and its activity, promoting an anomalous activation of the pathway in NSCLC (183). Besides, chromosomal aberrations related to NOTCH are generally related to the initiation of tumoral situations. The first time that NOTCH pathway was related to human cancer was by studying chromosome translocation in T-ALL. This translocation generates a permanently active form of NOTCH1 (184). Posterior research reported that >50% of patients with T-ALL present activating NOTCH1 mutations (172, 178, 185). Nevertheless, NOTCH pathway drive tumorigenesis in other ways. For instance, hyperactivation of the signal may be promoted by either increased expression or stabilization of NOTCH-IC, not to mention ligand-independent activation of the signaling pathway (178, 186, 187).

Expression levels of receptor and ligands may justify different results of tissue-specific carcinogenesis. In prostate, liver, and pancreatic cancer, as well as in brain tumors, NOTCH pathway changes are linked to altered protein expression. In example, in some astrocytomas DLL1 is upregulated, leading to higher activation of Hes6 (188), while Jag1 upregulation is linked to an advanced metastatic stage of prostate cancer (189, 190). In addition, the specific ligand that interacts with NOTCH receptor is determined not only by its abundance and/or distribution, but also by their affinity. As previously mentioned, Fringe proteins (LNFG, MNFG and RNFG) play a main part at this

point of NOTCH regulation. On the one hand, LNFG and MNFG promote NOTCH1 sensitivity to DLL and decrease it to JAG in breast and pancreatic cancer (191, 192) and intestinal cancer (193), respectively. RNFG enhances both interactions equally (191, 194). Regarding cis or trans ligand-receptor interactions, different outcomes may be observed. In the case of trans interaction, a lateral-inhibition or induction is triggered, which is clearly essential during embryonic development (195). Nevertheless, lateral inhibition has been described to happen in pancreatic carcinoma and glioblastoma models under hypoxic conditions, implying that these processes might have a role in development of tumor microenvironment (196).

Concerning NOTCH pathway implications in tumor microenvironment maintenance, it is important to mention is role in vascularization. This process is key for carrying nutrients to any tissue, specially a persistently overgrowing one like a tumor. In this sense, NOTCH pathway plays an important role since it controls angiogenesis and endothelial sprouting. Because of Wnt, MAPK and VEGF activation, DLL4 is highly expressed in endothelial tip cells, which is particularly important in the branching process. This promotes NOTCH higher activity, thus downregulating VEGFR2 expression in stalk in a negative regulation route (197-200). At the same time, JAG1 inhibit NOTCH in tip cells, facilitating the raise of DLL4 and VEGFR2, supporting the tip phenotype. This whole and delicate process might be a hallmark in cancer when is aberrantly regulated since NOTCH modulate V-cadherin in endothelial, thus regulating endothelial rearrangement and cellular motility, which could result in aberrant angiogenesis (201). In other ways, reduced vascularization compromises oxygen levels, which promotes a proper environment for the development of several tumors (202, 203). This diminished oxygen levels induce HIF1, promoting angiogenesis in physiological conditions, but also promotes a favored microenvironment for tumor growing. This hypoxic situation increases the release of oxygen radicals and cell migration due to the downregulation of anchoring molecules (204, 205). NOTCH pathway is modulated by hypoxic conditions, leading epithelial to mesenchymal transition (EMT) downregulating E-cadherin by stimulating their inhibitors expression, SNAIL and SLUG. This process permits epithelial cells to detach, which translates in increased cell migration and metastatic potential (181, 206, 207). Another element for tumor growth control is interaction with the surrounding stroma. It has been described that CSL ablation in mesenchyme downregulates p53 and

activates matrix-remodeling enzymes, leading to uncontrolled proliferation of keratinocytes (208, 209).

Finally, immune system is also related to tumor development via NOTCH pathway. NOTCH pathway is a main modulator of immune differentiation, specifically of lymphocytes and myelomonocytic by inhibiting Hes1 transcription (210). Besides, tumor-associated macrophages (TAMs) have been found in a wide range of tumors, like breast, ovarian or blather, among others (211). It has been demonstrated that levels of TAMs in head and neck cancer correlates with high expression of NOTCH1, as well as a correlation between NOTCH1 and TAM-anti-inflammatory phenotype, via JAG1 (212, 213). This anti-inflammatory phenotype for TAM activation is CSL-dependent since depletion of this protein in TAMs blocks the anti-inflammatory fate and induces a cytotoxic microenvironment (211, 214).
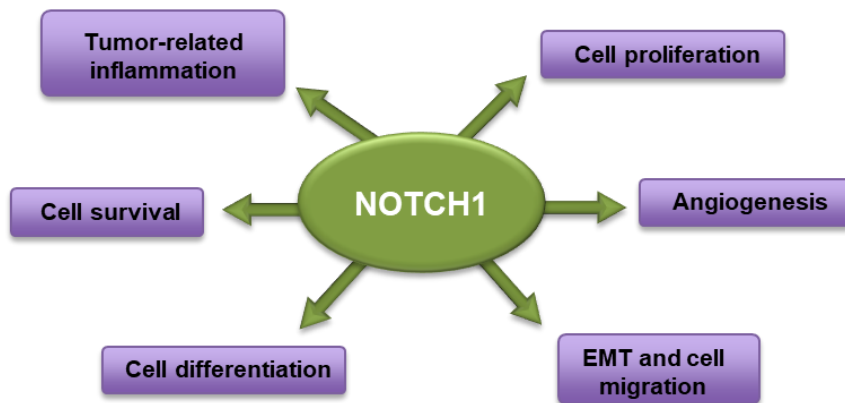
Figure 6. NOTCH1 and cancer. Summary of the main pro-tumoral functions of NOTCH1.

4.3. DNA damage: types, response and use in therapy

DNA is considered the basic unit of inheritance and is a highly reactive molecule susceptible to chemical modifications by either endogenous or exogenous agents. To respond to DNA damage, the DNA damage response (DDR) is activated. Several pathways comprise the DDR diminishing the deleterious consequences of the damage, including DNA repair pathways, damage tolerance, cell death pathways and cell cycle

checkpoints. Depending on the source, DNA damage can be endogenous or exogenous (215).

4.3.1. Endogenous DNA damage

Endogenous DNA damage is generated when DNA molecules are involved in hydrolytic and oxidative reactions with water and ROS (reactive oxygen species), both typically present in cells. This predisposition of DNA to react with other molecules promotes the emergence of a wide range of diseases like cancer or hereditary malignancies (216, 217).

High fidelity synthesis of DNA during replication or repair occurs thanks to structural and biochemical features of replicative DNA polymerases, guaranteeing the addition of proper complementary bases to the template ones. When an incorrect dNTP is inserted, a 3'-5' deoxynucleotide exonuclease removes it improving replication fidelity, which is the base of mismatch repair (MMR) pathway (218-220). Despite this, a frequency of up to 10^{-8} per cell per generation is observed single base insertions or deletions and base substitutions errors are accumulated (219). Replicative polymerases oftentimes incorporate the wrong base. For instance, they end up with a compromised fidelity or add U instead of T or C due to the alterations of the concentrations of NTPs in the cell (221, 222), constituting a main source of mutagenesis. Topoisomerase (TOP) enzymes activity during replication and transcription is centered in removing superhelical tension on DNA, but they can be an origin of endogenous DNA damage too (223).

Base deamination is another important cause of spontaneous mutagenesis in human cells. These errors happen more frequently in single- versus double-stranded DNA and are expectedly increased by in replication or transcription, when single strandedness situations emerge (224). Although this process is logically responsible of numerous hereditary diseases in humans (225), it has also an important role in the proper function of the immune system, since cytosine deamination is essential for somatic hypermutagenesis during antibody development (226-228). It has been also described that base deamination may be a relevant event for genetic diversity, from an evolutionary point of view (229). Furthermore, abasic sites are constantly created when the N-glycosyl bond hydrolyzes, either spontaneously or by cleavage, sometimes induced by extreme

pH or temperature conditions. In the human cell, around 104 abasic sites are generated every day. AP endonucleases remove most abasic sites in BER (base-excision repair) pathway, but sometimes these abasic sites are avoided by TLS polymerases (translesions DNA polymerases) and become SSBs due to their instability (230).

Another important endogenous source of DNA damage is radical oxygen species (ROS). At low levels they carry out essential roles in physiological conditions but when in excess, ROS can cause almost 100 different oxidative base lesions (231). ROS harmful effects are normally regulated by restricting respiration, protecting DNA with histones and antioxidant enzymes. Despite this, excess of ROS is associated with different diseases like diabetes, Parkinson's disease, Alzheimer's disease, or cancer (232-235). Besides, ROS compromise DNA backbone in mammalian cells leading to approximately 2300 SSBs (single strand breaks) per cell per hour (236). Different DNA damage repair pathways take place when correcting oxidation-derived errors: BER, SSBR (single-strand break repair) and DSBR (double-strand break repair). It is worth to mention that hydroxyl radicals, the most reactive and harmful, also affect DNA stability in an indirect manner through lipid peroxidation. This generates aldehyde products that react with A, G, and C forming mutagenic adducts, thus leading to the apparition of different diseases like hemochromatosis or Wilson's disease (237, 238).

4.3.2.   Exogenous DNA damage

Furthermore, DNA damage is classified as exogenous when the source is located outside from the organism. This means, when physical chemical or environmental agents damage DNA. Some examples of exogenous DNA damage would be alkylating agents, aromatic amines, PAH (polycyclic aromatic hydrocarbons) or UV and ionizing radiation, being the last one described in a specific paragraph.

UV (ultraviolet) radiation comes naturally from the sunlight and is catalogued into three different types depending on the wavelength: UV-C (190-290 nm), UV-B (290-320 nm) or UV-A (320-400 nm). DNA can absorb maximal UV radiation at 260 nm, for what UV-C rays represent the most hazardous ones. Despite this, UV radiation can affect DNA through an indirect pathway: nearby molecules called photosensitizers absorb energy from UV and affect DNA. UV-C induce DNA damage by enhancing pyrimidine dimers

formation depending on wavelength and dose of light (239, 240) and resulting in cytotoxicity when unrepaired. UV-B also causes pyrimidine dimers but with less efficiently than UV-C (241). Finally, UV-A damages DNA in and indirect way by photo-oxidating either endogenous or exogenous photosensitizers and resulting in DNA adduct formation (242). Additionally, UV radiation has been reported to induce protein crosslinks and DNA strand breaks in mammalian cells (243). UV lesions are repaired by NER nucleotide excision repair) or HR (homologous recombination) among other repairing pathways (244, 245).

Alkylating agents add an alkyl group to nucleophilic base ring nitrogens and are usually present in tobacco smoke, industrial processing, chemotherapeutic agents or even dietary components (246). The most common alkylating agents normally used in laboratories include MMS, EMS (methyl and ethyl methanesulfonate, respectively), and MNU (methylnitrosourea), among others. These molecules interact with DNA generating carcinogenic lesions (247, 248). Other examples of these agents are sulfur and nitrogen mustards, regrettably used in multiple conflicts, from Word War I to Syria nowadays. Mustards react with DNA in different ways, leading to intra and inter-strand crosslinking and blocking DNA metabolic activity (249). Despite their use in wars, deleterious characteristics of mustards are useful as chemotherapeutic agents (250, 251). Alkylated base damage are normally countered by BER and ICL (interstrand crosslink) repair (247). In addition, aromatic amines represent an important source of exogenous DNA damage. They are mainly generated by pesticides, cigarette smoke, fuel, industrial dyes and high temperature cooking (252). Aromatic amines are metabolized by P450 monooxygenase system, resulting in carcinogenic alkylating agents (253) that results in frameshift mutations and base substitutions (254). The most studied aromatic amines are aminofluorenes, originally used as insecticides until their carcinogenic effects were reported (255). The main repairing pathway activated in response to aromatic amines adducts is NER (256).

Polycyclic aromatic hydrocarbons (also known as PAHs) are carbon compounds that present various aromatic rings. PAHs are inert, nonpolar and widely distributed along the environment. These compounds mainly come from tobacco smoke and organic matter and fossil fuel incomplete combustion (257) and, like aromatic amines, are metabolized by P450 system resulting in molecules that react with DNA (258). Some

known examples of PAHs are naphthalene, pyrene or benzopyrene, which upon P450-dependen activation promotes BPDE (Benzo(a)pyrene diolepoxide) intermediates that intercalate into DNA forming adducts (259). NER and BER normally repair PAH-related DNA lesions (260). Besides the mentioned PAHs and aromatic amines, other electrophiles act as DNA damage agents. Among them, N-nitrosamines can be found. N-nitrosamines are strong carcinogens mainly present in tobacco smoke and are involved in the development of different respiratory and digestive tract tumors (261, 262). Finally, it is worth mentioning some environmental sources of genotoxic stress like extreme temperatures, hypoxia and oxidative stress, that have been described to promote DNA damage in human cells (263-265). They have been reported to be implicated in diverse neurodegenerative disorders due to their action in mutagenesis at trinucleotide repeats (266). Other daily use products have been related to DNA damage in sperm cells. An example of this could be butyl paraben or bisphenol A, found in cosmetics, food-products and beverage processing (267). This, together with the carcinogenic effects of some food additives of plant protection products, enhance the relevance of regulatory requirements on the use of potentially hazardous everyday compounds.

4.3.3.   Mechanisms of DNA repair

DNA Damage Response (DDR) is one of the most affected signaling pathways in cancer. DDR is normally activated when DNA is altered after exposition to genotoxic agents, but also because of DNA instability itself (268). When this occurs, a complex cellular mechanism is activated in an attempt of reduce general damage. To allow this, cellular processes such as DNA repair pathways, cell cycle arrest or cell death are activated (269). Nevertheless, sometimes these mechanisms are not enough to restrain and cell behavior is altered, either providing a selective advantage or leading to cancer development. In addition, DDR effectiveness may determine the response to therapy in tumors (270). As previously explained, DNA-damage agents promote several types of DNA lesions that include crosslinks, base modification, single strand breaks (SSBs) and double strand breaks (DSBs). Different types of DNA damage are detected and processed by specific proteins related to DNA damage response pathways. Under physiological conditions, there have been described 6 main mechanisms for damaged DNA repairing: mismatch repair (MMR), nucleotide excision repair (NER), base excision

repair (BER), homologous recombination (HR), non-homologous end-joining (NHEJ) and translesion DNA synthesis (TLS).

In this sense, replication errors lead to base mismatches, are normally repaired through the MMR pathway (271), in which MSH2 and MLH1 proteins are crucial. Other lesions like pyrimidine dimers induced by UV radiation are processed by the NER pathway (272). NER requires the activity of excision repair cross-complementing protein 1 (ERCC1) to be carried out. On the other hand, most of the DNA subtle changes, such as oxidative lesions, alkylation products and SSBs are repaired by BER proteins. Some examples of BER proteins are XRCC1, APE1, PARP1 or IIIa (273). Unlike SSBs, DSBs are mainly restored either by NHEJ or HR. HR normally requires the MRN (MRE11–RAD50–NBS1) complex, RPA, BRCA1-2, PALB2 and RAD51 (274, 275). For its part, NHEJ is based on the activity of, DNA-PKCs, XRCC4, XLF and the Ku70/Ku80 complex, among other proteins (276). Finally, translesion synthesis (TLS) allow DNA to continue to replicate despite the presence of DNA lesions. Even though mechanisms in charge telomeric DNA maintenance are not usually considered part of the DDR, they perform an essential role in genome instability (277). These DDR pathways interact with cell-cycle checkpoint proteins to facilitate DNA repair before mitosis, thus guaranteeing the proper genetic material is replicated and split up to daughter cells (278).

Among all DNA lesions, it is worth to mention DSBs, the main result of ionizing radiation, which promote cell death or genome instability that may lead to cancer when either unrepaired or repaired incorrectly. Regarding the HR response, the MRN complex is recruited to the damaged DNA sites. Once there, MRN phosphorylates H2A histone generating the γH2AX variant. (279, 280). The appearance of γH2AX enhances the signal, thus recruiting new molecules to the DSB lesion, where ATM kinase is activated by phosphorylation. Nevertheless, it has been reported that ATM can be straightly phosphorylated by the MRN complex itself (281, 282). Once phosphorylated, ATM trigger the activation of many downstream effectors (283). For instance, BRCA1 phosphorylation by ATM, as well as CtIP phosphorylation result in S phase arrest of the cell cycle, as well as DSB repair (284, 285). ATM also phosphorylates Ser15 of p53, leading to its activation and either apoptosis or cell cycle arrest in G1 phase.
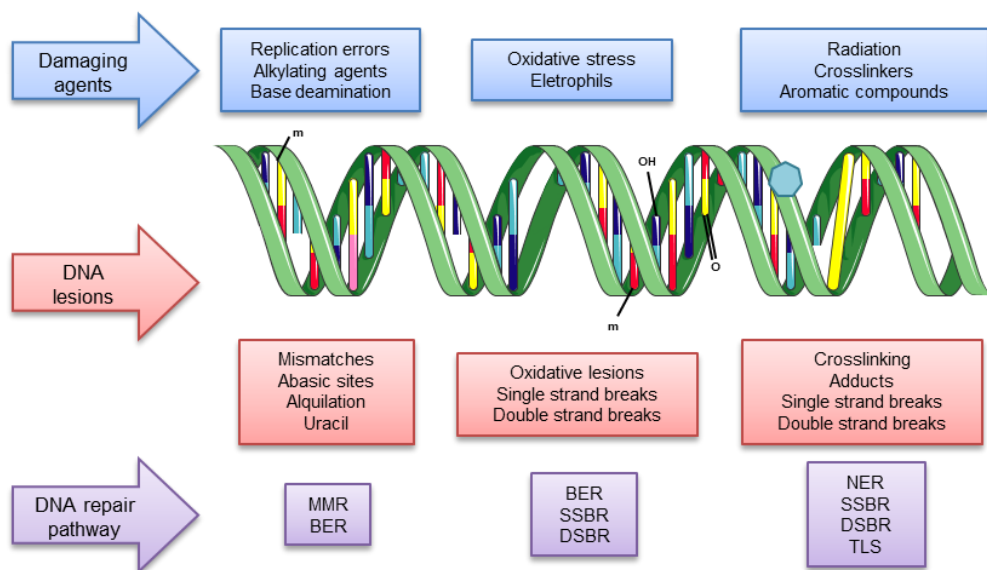
Figure 7. DNA damage, responsible agents and repair pathways. Schematic summary of the main damaging agents known, the type of DNA lesions that they promote and the most common DNA repair pathways that are activated in response to them.

4.3.4. Ionizing radiation: effects and applications

Ionizing radiation (IR) comprise alpha, beta and gamma, neutrons and X-rays. This type of radiation is abundant in the environment, coming from soil to medical devices. Every kind of radiation is classified depending on its direct or indirect effect and ionization density (LET, linear energy transfer). Regarding the energy transferred to matter, radiations are sorted as low LET (beta and gamma rays) or high LET (alpha rays). When IR is accumulated, it damages DNA in different ways, like affecting surrounding water by radiolysis thus generating highly reactive hydroxyl radicals (286). This indirect DNA damage by hydroxyl radicals excuses up to 65% of the radiation-derived DNA damage (287). Thus, ionizing radiation induces a range of base lesions like those generated by ROS, including 8-oxoguanine and formamidopyrimidines, among others. IR also leads to a very specific type of SSBs in which DNA breaks have 3' phosphate or phosphoglycolate ends instead of 3'-OH ends. Besides, loss of terminal base residues and fragmented sugar derivatives end up into clustered damage or single stranded gaps (288, 289). Different enzymes can process modified ends permitting those IR-induced SSBs repair. Among them, there can be found AP endonucleases, PNKP or TDP1 (290-

292). Nevertheless, an especially relevant IR-related lesion is the DSB, caused by multiple closely positioned damaged sites on both DNA strands (293), but they are generally successfully repaired by the HR pathway (294).

Regarding ionizing radiation applications, it is important to mention that IR represents an essential tool in clinical diagnosis and treatment, being especially useful in cancer treatment. In fact, around 50-60% of cancer patients are subjected to radiotherapy (295). As previously described, IR induces clustered DNA damage through oxidative stress, also affecting other cellular macromolecules (296). This kind of radiation also prevent DNA replication by activating cell-cycle checkpoints to avoid formation of toxic DNA replication lesions (297). Cell cycle checkpoints are normally regulated by effector kinases among which ATM and ATR can be found (298-300). These kinases normally modulate checkpoint proteins like CHK1 and CHK2. Flaws in DNA damage checkpoint pathways lead to increased sensitivity to a variety of anticancer treatments. For instance, ATM loss translates into sensitivity to IR (300). Another key kinase in DSB repair following ionizing radiation is PRKDC, a member of PIKK family, which joins DNA in a non-homologous way. Cells that lack this kinase are highly sensitive to IR (301), denoting that PRKDC inhibition induce a sensibilization to radiotherapy in tumors. In fact, the PIKK inhibitor wortmannin has shown antiproliferative effects in preclinical models involving IR.

4.3.5. Radiodermatitis

As previously mentioned, ionizing radiation is employed for treating around 60% of cancers (295). Despite this, radiotherapy (RT) induces a variety of side effects, among which radiodermatitis is a common one. In fact, around 95% of patients undergoing RT present skin affections because of the treatment (302). This is called radiodermatitis, radiation dermatitis, radiation injury or radiation-induced skin reactions. Symptoms of radiodermatitis include itchiness, pain, redness and lesions such as dry desquamation, erythema, and moist desquamation. This result in a decrease in patients' quality of life and survival (303). RT toxicity is complex and depends on different factors like total radiation dose, dose fractionation schedule, concurrent chemotherapy, comorbidity and volume of treated organ or tissue. Ionizing radiation from RT induces DNA damage within tumoral cells leading to cell death, but also affects skin, especially when the tumor is close to the skin, like breast, vulva, anal or head and neck cancers (304).

At lower doses, RT promotes an acute reaction that modify skin pigmentation, disrupt hair growth and damage the deeper dermis. This last effect interferes with skin cell turnover, and leads to erythema (305). When a higher dose of radiation is employed, more intense damage happens and mitotic rate of the basal keratinocyte layer increases, which leads to dry desquamation (306). At even higher doses of radiotherapy, the basal layer cannot recover and moist desquamation occurs (307). These events along with activation of proinflammatory response, result in vascular damage, promoting hypoxic condition and upregulating TGF-β (308). TGF-β-derived fibrosis and hypoxia generate ROS (308, 309) that attack DNA and cell membranes. Each subsequent fraction enhances this effect, resulting in inflammatory cell recruitment (307, 310, 311). In fact, it has been reported that chronic radiation dermatitis is caused by imbalance of proinflammatory and profibrotic cytokines, including TNF-α, TGF-β, IL1, IL6 or PDGF, among others (312-316). In addition to these mechanisms, miRNAs alteration, telomere erosion, stem cell damage and epigenetic dysregulation are also related to radiodermatitis development (317-319). Taking these data together, result important to reach a better understanding of molecular mechanisms undergoing radiodermatitis thus developing effective treatments to mitigate radiodermatitis effect in patients.

Aims

Cancer is a complex disease enhanced by alterations in signaling pathways. In fact, DNA damage response pathways play a key role in cancer development when they are deregulated. Although there is a great knowledge of the signaling pathways that take place in the DNA damage response, further research is required to assess new molecular mechanisms for fully comprehend this complex scheme. In this sense, it is essential to study how kinases like DYRK2, with a role in DDR pathway, function by identifying new substrates and characterizing their interaction. In addition, it is important to understand the network of signaling pathways activation-deactivation under DNA damage conditions, which would open a road to the development of new therapeutic strategies against cancer.

The aims of this project have been the following:

1. Identify and analyze new DYRK2 substrates.

2. Characterization of NOTCH1-DYRK2 interaction, specially focusing on DNA damage conditions.

3. Assess the implications DYRK2-dependent NOTCH1 regulation in carcinogenesis.

4. Analyze signaling pathways modulations in response to ionizing radiation in fibroblasts.

Materials and Methods

6.1.   Cell culture, transfection, and reagents

HEK-293T (wt/DYRK2$^{-/-}$/HIPK2$^{-/-}$), MDA-MB-231 (wt/DYRK2$^{-/-}$), MDA-MB-468 (wt/DYRK2$^{-/-}$), HeLa (wt/DYRK2$^{-/-}$/DYRK1A$^{-/-}$), A549, MOR, CHO and MCF7 cells were maintained in Dulbecco's Modified Eagle's Medium (DMEM) supplemented with 10% FBS (Fetal Bovine Serum) and 1% (v/v) penicillin/streptomycin (Sigma-Aldrich, St Louis, MO, USA) at 37 ºC in a humidified atmosphere containing 5% CO_2. H727 cells were maintained in Roswell Park Memorial Institute (RPMI) medium at the same conditions. Cell lines were obtained from ATCC (LGC Standards, Teddington, Middlesex, UK) and were routinely tested to be free of mycoplasma and cross contamination. Cell lines validation was performed by a multiplex PCR with Geneprint10 System (Promega, Madison, WI, USA). MG-132 was from Enzo Life Science (Lausen, Switzerland). Roti-Fect (Carl Roth, Karlsruhe, Germany) was employed for transient transfection, followed by 36 to 48 h harvesting after transfection. DNA amounts in each transfection were kept constant after the addition of empty expression vector. DYRK2 plasmids were previously described or generated in this lab by standard cloning technique (41). Point mutants were produced by conventional point mutagenesis. HeLa control and DYRK1A$^{-/-}$ cells were a gift from Dr. Susana de la Luna (Centre for Genomic Regulation, Barcelona, Spain). DYRK2-analog sensitive expression plasmid (GFP-DYRK2-AS) was previously described (66). Myc tagged NOTCH1-IC and 4xCSL vectors were provided by Dr. Hee-Sae Park (Korea Basic Science Institute, Gwang Ju, South Korea). pLentiCRISPr-V2 was a gift from Dr. Feng Zhang (Addgene plasmid # 52961). Flag tagged NOTCH2-IC and NOTCH4-IC vectors were a gift from Dr. Raphael Kopan (Addgene plasmids # 20184 and # 20186). HA tagged NOTCH3-IC plasmid was a gift from Dr. Urban Lendahl (Addgene plasmid # 47618). HA tagged NOTCH1-IC WT and mutant plasmids were kindly provided by Dr. Aifantis (NYU Langone Medical Center, New York, USA). Flag-FBXW7-WT and ∆Fbox were kindly provided by Dr. Rocío Sancho (Centre for Stem Cells & Regenerative Medicine King's College London, UK). Adriamycin (ADR), harmine, etoposide (ETP) and the rest of the reagents were from Sigma-Aldrich. PP1 analog II 1NM-PP1 (SC-203214) was obtained from Santa Cruz Biotechnology (Santa Cruz, California, USA). Scramble control oligonucleotide siRNA non-targeting pool (D-001810) and ON-TARGET plus SMARTpool against DYRK2 (L-004730-00) were purchased from Dharmacon (Waltham, MA, USA). DYRK2 human recombinant protein was purchased from Abcam (Cambridge, UK).

6.2. Generation of CRISPR/Cas9-cell lines

The endogenous DYRK2 gene was knocked-out by transfecting cells with pLentiCRISPR-v2 (which codes for Cas9 and a puromycin cassette) containing gRNAs against the first exon of the short DYRK2 isoform or a combination of gRNAs against the first and the last exon. For HeLa and MDA-MB-468 DYRK2$^{-/-}$ cells the gRNA sequence used was GCTTGCCAGTGGTGCCAGAG and for MDA-MB-231 and HEK-293T DYRK2$^{-/-}$ cells the gRNAs used were N-term sequence GCTTGCCAGTGGTGCCAGAG and C-term sequence GAAGCTGAGCTAGAAGGTGG. Control cells were transfected with the empty pLentiCRISPRV2 vector. After transfection, cells were exposed to puromycin (2 µg/ml) for two days. Surviving cells were clonally selected (in the case of control cells were used as pool population) by serial dilution, and positive clones were identified by genomic analysis and western blot.

6.3. Western blotting and antibodies

Protein fractions were obtained after lysis of cells in NP-40 buffer [20 mM Tris–HCl (pH 7.5), 150 mM NaCl, 1 mM phenylmethylsulfonyl fluoride, 10 mM NaF, 0.5 mM sodium orthovanadate, aprotinin (10 µg/ml), pepstatin (10 µg/ml), leupeptine (10 µg/ml), 1% (v/v) NP-40, and 10% (v/v) glycerol]. Proteins were diluted and boiled at 95 ºC in SDS buffer, resolved on sodium dodecyl sulfate polyacrylamide gels (SDS-PAGE), transferred to PVDF membranes, blocked with non-fat milk in TTBS buffer and incubated with primary antibodies. Membranes were incubated with the appropriate secondary antibody coupled to horseradish peroxidase, which were detected by chemiluminescence using Clarity™ Western ECL Substrate (Bio-rad, Hercules, California, USA). Antibodies against β-actin (A5316) and FLAG epitope (clone M2, A2220) were purchased from Sigma Aldrich; anti-ubiquitin (P4D1, 3936S) from Cell Signaling Technology (Danvers, Massachusetts, USA). Anti-NOTCH1 [EP1238Y] (ab52627), anti-Hes1 (ab71559) and anti-Hes5 (ab25374) were obtained from Abcam. Anti-HA (clone 3F10), anti-myc (clone 9E10), anti-GFP (11814460001) (Roche Molecular Biochemical) and anti-phosphoserine (AB1603) (Millipore, Burlington, Massachusetts, USA) were from the indicated suppliers. Anti-DYRK2 (H80; sc-66867) and anti-DYRK1A (RR7; sc-100376) antibodies were obtained from Santa Cruz Biotechnology. Antibody anti-FBXW7 (A301-720A-T) was

provided by Bethyl Laboratories (Montgomery, TX). Secondary horseradish peroxidase-coupled antibodies were purchased from Jackson ImmunoResearch Laboratories (Cambridgeshire, UK). Texas Red goat anti-rabbit IgG antibody (T-6391) was from Thermo Fisher Scientific (Waltham, Massachusetts, USA).

6.4.   Immunoprecipitation

Cells were washed in PBS and lysed in IP buffer [50 mM Hepes (pH 7.5), 50 mM NaCl, 1% (v/v) Triton X-100, 2 mM EDTA, 10 mM sodium fluoride, 0.5 mM sodium orthovanadate, 10 µg/ml aprotinin, 10 µg/ml leupeptin, and 1 mM PMSF]. Cell lysates were pre-cleared with protein A/G Sepharose (Santa Cruz) and immunoprecipitation was performed on a rotating wheel upon the addition of 1 µg of the indicated antibodies and 25 µl of protein A/G sepharose beads. Immunoprecipitated proteins were then washed for five times in IP buffer and eluted in 2× SDS sample buffer, followed by western blotting.

6.5.   Luciferase reporter assays

Cells were collected in PBS and lysed in luciferase assay buffer (25 mM Tris-phosphate pH 7.8, 8 mM $MgCl_2$, 1 mM DTT, 1 % Triton X-100 and 7 % glycerol) during 15 min at room temperature in a horizontal shaker. Luciferase assay was performed using Luciferase Assay Reagent (Promega) according to the manufacturer's instructions. Luciferase activity was measured using an Autolumat LB 953 (Berthold Technologies GmbH, Bad Wildbad, Germany) and normalized with protein concentration.

6.6.   Immunofluorescence

Cells were seeded on glass coverslips and 48 hours after transfection fixed with 3.7% of pre-warmed paraformaldehyde/PBS for 10 min, permeabilized with 0.1% Triton X-100/PBS for 15 min, blocked with 3% BSA/PBS and incubated overnight with primary antibodies. After being washed with PBS and incubated for 45 min with the secondary antibody, cells were mounted on glass slides with mounting medium containing DAPI

(Vectashield Burlingame, CA, USA). Fluorescence images were captured using an LSM 5 EXCITER (Carl Zeiss MicroImaging GmbH, Oberkochen, Germany) confocal laser scanning microscope using a 40×/1.30 oil objective (EC Plan-Neofluar) and ZEN 2008 software (Carl Zeiss MicroImaging GmbH). To determine fluorescent signal colocalization between different channels the Coloc_2 module was used. The degree of channel colocalization was analyzed by considering the following indexes: thresholded Manders' coefficients A and B and Pearson's coefficient. To evaluate the spatial relations between channel intensity we used the ImageJ tool RGB Profiler to create a profile of fluorescence intensity values across a line drawn on the image.

6.7. mRNA extraction and qPCR

Total RNA was extracted using the High Pure RNA Isolation kit (Roche Diagnostics, Switzerland), reverse transcription performed with the iScript cDNA Synthesis kit (Bio-Rad) and real-time PCR carried out in an iCYCLER detection system (Bio-Rad) with iQTM SYBR Green Supermix (Bio-Rad). Amplification efficiencies were validated and normalized against HPRT, and fold change in gene expression was calculated using the $2^{-\Delta\Delta Ct}$ method. Primer sequences are available upon request.

6.8. *In vitro* phosphorylation

Immunoprecipitated Myc-tagged NOTCH1-IC endogenous protein was incubated with 50 ng of commercial recombinant DYRK2 protein (Millipore, 14-669) in kinase buffer (20 mM Hepes pH 7.5, 10 mM $MgCl_2$, 1 mM DTT) with or without ATP (0.1 µM). After 60 min of incubation at 37 °C, reactions were stopped by using 1M glycine pH 2.5 in agitation for 20 min at room temperature and A/G beads (Santa Cruz Biotecnology) were removed by centrifugation. Finally, readjustment of pH levels of the supernatant was performed employing 1 M Tris-HCl pH 7.5.

6.9.   Cell viability and flow cytometry analyses

For apoptosis studies, cells were harvested and washed in cold PBS and then resuspended in binding buffer consisting of 10 mM Hepes, 140 mM NaCl and 2.5 mM CaCl$_2$ pH 7.4. Cells were stained with Annexin V, Alexa Fluor 488 conjugate (Molecular Probes by Life Technologies, Carlsbad, CA, USA) and propidium iodide. Cell cycle distribution and apoptosis were determined by BD FACSCanto™ flow cytometer (BD Biosciences, San Jose, CA, USA) using BD FACSDiva™ software. For cytotoxicity assay, cells were seeded in a 96-well plate and after 12 hours YOYO-1 (Life Technologies) was added to a final concentration of 0.1 µM. Object counting analysis was performed using the cell imaging system IncuCyte HD (Essen BioScience).

6.10.   Cell motility assay

Cells were seeded in a 96-well Essen ImageLock plate (Essen BioScience, Ann Arbor, Michigan, USA) 24 hours after transfection and grown to confluence. After 12 hours, the scratches were made using the 96-pin WoundMaker (Essen BioScience), followed by incubation with 10 ng/ml of mitomycin C. Wound images were taken every 60 min for 24 h and the data analysed by the integrated metric Relative Wound Density part of the live content cell imaging system IncuCyte HD (Essen BioScience).

6.11.   Cell invasion assay

Invasion assays were performed in Boyden chamber using a 48-well Neuro Probe, Inc. insert system (Gaithersburg, MD, USA). Polyethylene membrane inserts (8.0 µm pore size) were precoated with 200 µg/µl of Matrigel® Matrix (Corning®, Corning, NY, USA) (in coating buffer 0.01 M Tris and 0.7 % NaCl). Cells were subcultured in an mw6 plate, and 24 hours prior the assay, FBS was removed from the media and ADR was added in the specific conditions. Then, cells were seeded with 2.5×10^4 cells per insert (cells suspended in 50 µl in DMEM, in addition to 25 µl FBS free DMEM in the bottom side of the chamber) and incubated at 37 ºC, 5% CO$_2$ for 12 h. Then, the membrane was washed at least three times for 10 min with PBS. The membranes were then cut out of the inserts by a scalpel, dyed in methyl violet for 30 minutes and mounted between two

thin cover slips. The total number of migrated cells was counted for each group (n=4) with an inverted microscope. Only cells which had completely migrated through the membrane were counted.

6.12.   Enrichment of His-tagged proteins

Cells were collected in PBS and pellets resuspended in lysis buffer (6 M guanidinium-HCl, 0.1 M Na_2HPO_4/NaH_2PO_4, 0.01 M Tris-HCl [pH 8], 5 mM imidazol and 0.01 M β-mercaptoethanol). Samples were sonicated and cell debris was removed by centrifugation. Supernatants were mixed with 75 □l of equilibrated Ni-NTA resin (Quiagen, Hilden, Germany), followed by incubation for 4 h at room temperature on a rotating wheel. Precipitates were washed once with lysis buffers, once in wash buffer (8 M urea, 0.1 M Na_2HPO_4/NaH_2PO_4, 0.01 M Tris-HCl [pH 6.8], 5 mM imidazol, and 0.01 M β-mercaptoethanol), and twice in wash buffer plus 0.1% Triton X-100. Proteins were eluted in 75 □l of 0.2 M imidazol, 0.15 M Tris-HCl (pH 6.8), 30% glycerol, 0.72 M β-mercaptoethanol and 5% SDS for 20 min at room temperature with gentle agitation and further analysed by immunoblotting.

6.13.   Data analysis

Protein abundance in tumor tissue was obtained from The Human Protein Atlas database as antibody staining level (not detected, low, medium, and high) per patient (320). Data were accessed via the R hpar package. Gene alteration frequencies were calculated using the TCGA PanCancer dataset that includes 10967 samples across 33 different tumor types (321). To calculate the alteration frequencies, the number of samples containing a missense/non-sense mutation or a deep deletion for a given gene was divided by the total number of samples in each cancer type. Data were accessed via the cBioPortal web service using the R cgdsr package (322). Images were evaluated and quantified using the Image J (http://rsbweb. nih.gov/ij/). Data are expressed as mean ± SD. Differences were analysed by Student's t test. $P < 0.05$ was considered significant. Statistical analysis was performed using GraphPad Prism® version 6.01 (GraphPad, San Diego, CA, USA).

6.14. Immunoprecipitation coupled to mass spectrometry

6.14.1. Immunoprecipitation

HEK-293T cells were washed in PBS and lysed in IP buffer [50 mM Hepes (pH 7.5), 50 mM NaCl, 1% (v/v) Triton X-100, 2 mM EDTA, 10 mM sodium fluoride, 0.5 mM sodium orthovanadate, 10 μg/ml aprotinin, 10 □g/ml leupeptin, and 1 mM PMSF]. Cell lysates were pre-cleared with protein A/G sepharose beads (Santa Cruz) and immunoprecipitation was performed on a rotating wheel upon the addition of 1 μg of anti-DYRK2 or IgG control. Immunoprecipitated proteins were then washed ten times in IP buffer and eluted in elution buffer (0.2 M glycine, pH 2.3/ 0.5% Igepal CA-630). Experiments were performed and analysed in triplicate.

6.14.2. Sample preparation for LC-MS analysis

Lysed cells were cleaned to remove contaminants by protein precipitation with TCA/acetone and solubilized in 50 μl of 0.2% RapiGest (Waters, Milford, MA, USA) in 50 mM ammonium bicarbonate. Total protein was quantified using Qubit Protein Assay Kit (Thermo Fisher Scientific, Waltham, MA, USA) and 50 μg proteins from each sample were digested with trypsin. Briefly, protein samples were incubated with 5 mM DTT at 60 °C for 30 min, and then with 10 mM iodoacetamide at room temperature for 30 min in darkness. Sequencing Grade Modified Trypsin (Promega, Madison, WI, USA) was added (ratio 1:40 trypsin:protein) and samples were incubated at 37 °C for 2 h. Afterwards, trypsin was added again (ratio 1:40) and samples were incubated at 37 °C for 15 h. RapiGest was suppressed by precipitation with 0.5% TFA at 37 °C for 1 h and centrifugation. The final volume was adjusted with milliQ water and ACN to a final concentration of 0.5 μg peptide/μL (2.25% ACN and 0.2% TFA), and 1× of the iRT peptides (Biognosis AG, Schlieren/Zurich, Switzerland) were spiked in each sample.

6.14.3. LC-MS analysis

Peptide solutions were analysed in triplicate by a shotgun approach by nanoLC-MS/MS. Samples (3 μl) were analysed with a nano-LC system Ekspert nLC415 (Eksigent,

Dublin, CA, USA) using an Acclaim PepMap RSLC C18 column (75 μm × 25 cm, 3 μm, 100 Å) (Thermo Fisher Scientific) at a flow rate of 300 nl/min. Water and ACN, both containing 0.1% formic acid, were used as solvents A and B, respectively. The gradient run consisted of 5% to 30% B for 120 min. Peptides eluted were directly injected into a hybrid quadrupole-TOF mass spectrometer Triple TOF 5600+ (Sciex, Redwood City, CA, USA) operated with a top 65 data-dependent acquisition system (DDA) using positive ion mode. A NanoSpray III ESI source (Sciex) was used for the interface between nano-LC and MS, applying 2600 V. The acquisition mode consisted of a 250 ms survey MS scan from 350 to 1250 m/z, followed by an MS/MS scan from 230 to 1700 m/z (60 ms acquisition time, 350 mDA mass tolerance, rolling collision energy) of the top 65 precursor ions from the survey scan. The fragmented precursors were then added to a dynamic exclusion list for 15 s, excluding any singly charged ions from the MS/MS analysis. Peptide and protein identifications were performed using Protein Pilot software v5.0 (Sciex) with a human UniProtKB concatenated target-reverse decoy database, specifying cysteines as modification and trypsin as enzyme used for digestion. The false discovery rate (FDR) was set to 1% for peptides and proteins. Those peptide proteins identified in the IgG control samples were subtracted from the later analysis. Protein were scores analysing Total ProtScore, Unused ProtScore, confident peptides and % Cov (95).

6.15. Fibroblast culture, SILAC labelling and sample management

6.15.1. Cell culture for SILAC labelling

A culture of human adult dermal fibroblasts from 4 different donors was employed for the SILAC and RNAseq essays. Cells were obtained from Tebu-Bio® (Le-Perray-en-Yvelines, France) and cultured as a pool under two different conditions: light and heavy. All the reagents were provided by Thermo Fisher Scientific® (Waltham, MA). We employed DMEM for SILAC (#88364), supplemented with 10% dialyzed FBS (#26400044) and 1% (v/v) penicillin/streptomycin. Cell culture was carried out at 37 ºC in a humidified atmosphere containing 5% CO_2. These conditions were maintained until during the whole experiment and labeling was validated by mass spectrometry (MS). For labeling, 0.01% (p/v) of the pertinent aminoacids were added:

- Light fibroblasts (control group):
  - L-Lysine-2HCl, $^{13}C_6$, $^{15}N_2$ for SILAC (#88209).

- o   L-Arginine-HCl, $^{13}C_6$, $^{15}N_4$ for SILAC (#89990).
- Heavy fibroblasts (irradiated group):
  - o   L-Lysine-2HCl for SILAC (#89987).
  - o   L-Arginine-HCl for SILAC (#89989).

Donor	Age	Gender	Race	BMI	Smoker	Diabetic	Depot	Reference
#1	26	F	C	27,6	No	No	Abdomen	DFM0218116B
#2	62	F	C	23,3	No	No	Eye	DFM110210B
#3	48	F	H	26,2	No	No	Abdomen	DFM102014A
#4	35	F	H	33,9	No	No	Abdomen	DFM102715B

Table 1. Fibroblasts' donor characteristics. Four different donors were selected to carry out the experiments using primary fibroblasts. BMI: Body mass index. F: Female. C: Caucasian. H: Hispanic.

6.15.2.   Stimuli and cell lysis

Cells were treated by using two different stimuli simulating either acute or accumulative radiation. To allow this, a X ray irradiator 43855F-CP160 (Faxitron X-Ray LLC, Lincolnshire, IL) was employed. For the acute dose, cells were irradiated with 2 Gy and lysed 30 minutes after the treatment. In the other hand, cells for the accumulative stimulus were exposed at 5 Gy four times, once every 12 hours, and lysed 2 hours after the last stimulus. For proteomic and phosphoproteomic analysis, after treatments cells were washed using PBS and grinded at 4 ºC. Protein fraction was obtained using urea lysis buffer (6 M urea, 50 mM Tris-HCl (pH=8),1 mM phenylmethylsulfonyl fluoride, 10 mM NaF, 0.5 mM sodium orthovanadate, leupeptine (10 µg/ml), pepstatin (10 µg/ml), aprotinin (10 µg/ml). In the case of the samples for RNAseq, cells were exposed to radiation as previously described and total RNA was purified using GenElute™ Mammalian Total RNA Miniprep Kit (RTN70-1KT, Sigma Aldrich).

6.16.   Proteomic and phosphoproteomic analysis of fibroblast samples

6.16.1. Protein sample preparation

Samples (700 µg) were dissolved in 6 M urea with mM ammonium bicarbonate, reduced with dithiothreitol (2100 nmol, 37 ºC, 60 min) and alkylated in the dark with

iodoacetamide (4200 nmol, 25 ºC, 30 min). The resulting protein extract was first diluted to 2M urea with 200 mM ammonium bicarbonate for digestion with endoproteinase LysC (1:100 w:w, 37ºC, o/n, Wako, cat # 129-02541), and then diluted 2-fold with 200 mM ammonium bicarbonate for trypsin digestion (1:100 w:w, 37ºC, 8h, Promega cat #V5113). After digestion, peptide mix was acidified with formic acid and desalted with a Hypersep C18 column (The Nest Group, Inc) prior to LCMS/MS analysis. In the one hand, 90 µg of each sample was fractionated by strong cation exchange chromatography (3M, cat # 66889-U), procedure adapted from Rappsilber et al1. The peptides were eluted into six different concentration of ammonium acetate (40, 80, 120, 160, 200 and 500mM). Each fraction was cleaned up with a MicroSpin C18 column (The Nest Group, Inc) prior to LC-MS/MS analysis. In the other hand, 455 µg of each sample was enriched in phosphopeptides with the High-Select™ TiO$_2$ Phosphopeptide Enrichment Kit (Thermo Scientific, cat # A32993).

6.16.2. Chromatographic and mass spectrometry analysis

Samples were analyzed using an LTQ-Orbitrap Fusion Lumos mass spectrometer (Thermo Fisher Scientific, San Jose, CA, USA) coupled to an EASY-nLC 1000 (Thermo Fisher Scientific (Proxeon), Odense, Denmark). Peptides were loaded directly onto the analytical column and were separated by reversed-phase chromatography using a 50-cm column with an inner diameter of 75 µm, packed with 2 µm C18 particles spectrometer (Thermo Scientific, San Jose, CA, USA). Chromatographic gradients started at 95% buffer A and 5% buffer B with a flow rate of 300 nl/min for 5 minutes and gradually increased to 25% buffer B and 78% A in 158 min and then to 40% buffer B and 65% A in 22 min. After each analysis, the column was washed for 10 min with 10% buffer A and 90% buffer B. Buffer A: 0.1% formic acid in water. Buffer B: 0.1% formic acid in acetonitrile.

The mass spectrometer was operated in positive ionization mode with nanospray voltage set at 2.4 kV and source temperature at 275°C. Ultramark 1621 for the was used for external calibration of the FT mass analyzer prior the analyses, and an internal calibration was performed using the background polysiloxane ion signal at m/z 445.1200. The acquisition was performed in data-dependent acquisition (DDA) mode and full MS scans with 1 micro scans at resolution of 120,000 were used over a mass range of m/z

350-1500 with detection in the Orbitrap mass analyzer. Auto gain control (AGC) was set to 1E5 and charge state filtering disqualifying singly charged peptides was activated. In each cycle of data-dependent acquisition analysis, following each survey scan, the most intense ions above a threshold ion count of 10000 were selected for fragmentation. The number of selected precursor ions for fragmentation was determined by the "Top Speed" acquisition algorithm and a dynamic exclusion of 60 seconds. Fragment ion spectra were produced via high-energy collision dissociation (HCD) at normalized collision energy of 28% and they were acquired in the ion trap mass analyzer. AGC was set to 1E4, and an isolation window of 1.6 m/z and a maximum injection time of 50 ms were used. All data were acquired with Xcalibur software v3.0.63. Digested bovine serum albumin (New England biolabs cat # P8108S) was analyzed between each sample to avoid sample carryover and to assure stability of the instrument and QCloud2 has been used to control instrument longitudinal performance during the project.

6.16.3. Data analysis

Acquired spectra were analyzed using the MaxQuant3 software suite (v1.6.0.16) and the Andromeda4 search engine. The data were searched against a Swiss-Prot human database (as in April 2018, 20341 entries) plus a list of common contaminants and all the corresponding decoy entries. For peptide identification a precursor ion mass tolerance of 7 ppm was used for MS1 level, trypsin was chosen as enzyme, and up to three missed cleavages were allowed. The fragment ion mass tolerance was set to 0.5 Da for MS2 spectra. Arg10;Lys8 were used as a label, oxidation of methionine and N-terminal protein acetylation were used as variable modifications whereas carbamidomethylation on cysteines was set as a fixed modification. In phosphorylated samples phosphorylation (STY) also was used as variable modifications. False discovery rate (FDR) in peptide identification was set to a maximum of 5%. Protein and phosphopeptide quantification data were retrieved from the ratio light versus heavy and fold-changes, p-value and adjusted p-values was calculated with Perseus5 1.6.2.1.

6.16.4. TruSeq Stranded Total RNA library preparation and sequencing

Libraries were prepared using the TruSeq Stranded Total RNA Library Prep Kit with Ribo-Zero Human/Mouse/Rat Kit (RS-122-2201/2202, Illumina) according to the manufacturer's protocol. Briefly, 300 ng of total RNA were used for ribosomal RNA depletion. Then, ribosomal depleted RNA was fragmented for 4.5 min at 94 ºC. The remaining steps of the library preparation were followed according to the manufacturer's instructions. Final libraries were analyzed on an Agilent Technologies 2100 Bioanalyzer system using the Agilent DNA 1000 chip to estimate the quantity and validate the size distribution and were then quantified by qPCR using the KAPA Library Quantification Kit KK4835 (REF. 07960204001, Roche) prior to the amplification with Illumina's cBot. Finally, libraries were sequenced on the Illumina HiSeq 2500 sequencing system using single reads, 50 base long reads (1x50, v4).

Results

7.1. Phosphorylation-dependent regulation of NOTCH1-IC by DYRK2

7.1.1. DYRK2 modulates NOTCH1-IC protein levels

We analyzed DYRK2 interactome by mass spectrometry following an immunoprecipitation (IP) assay with the aim of identify novel potential DYRK2 interactors (Figure 15). Various members of NOTCH family of receptors were present in these results. We focused our research on NOTCH1 and its potential relationship with DYRK2.

Representative Accession	Name	Control IGs Peptides	IP DYRK2 Peptides	Unused ProtScore	Total ProtScore	Confident Peptides	%Seq Cov - peptides >95% conf
sp|Q92630|DYRK2_HUMAN	Dual specificity tyrosine-phosphorylation-regulated kinase 2 OS=Homo sapiens GN=DYRK2 PE=1 SV=3	0|0|0	18|8|11	28,06	28,08	18	32,4
sp|P46531|NOTC1_HUMAN	Neurogenic locus notch homolog protein 1 OS=Homo sapiens GN=NOTCH1 PE=1 SV=4	0|0|0	11|10|11	14,60	25,07	12	33,1
sp|Q04721|NOTC2_HUMAN	Neurogenic locus notch homolog protein 2 OS=Homo sapiens GN=NOTCH2 PE=1 SV=3	0|0|0	22|44|19	54,31	54,31	44	23,3
sp|Q9UM47|NOTC3_HUMAN	Neurogenic locus notch homolog protein 3 OS=Homo sapiens GN=NOTCH3 PE=1 SV=2	0|0|0	13|8|9	21,95	21,99	13	6,1

Figure 8. NOTCH1 as a potential DYRK2 interactor. Endogenous DYRK2 was immunoprecipitated from HEK-293T cells using anti-DYRK2 antibody and rabbit IgG for controls. Eluted DYRK2 was detected by immunoblot, as well as its presence in the original lysate (INPUT). Triplicates for this experiment were performed (upper panel). Results from IP for DYRK2 and NOTCH family members are summarized in the table. These data include the number of peptides identified after IP for each assay. Finally, an example of DYRK2. NOTCH1, NOTCH2 and NOTCH3 peptides spectrums are shown.

To study this interaction in detail, we first co-expressed HA-NOTCH1-IC plasmid, either alone or together with growing concentrations of Flag tagged DYRK2, in HEK-293T cells. This resulted in a decrease of NOTCH1-IC protein levels in a DYRK2 dose-dependent manner. In addition, this decrease went with a delay in migration of the bans (Figure 9A). As shown in Figure 9B, where the potential effect of all DYRK subfamily members on NOTCH1 was checked, only DYRK1A and DYRK1B presented similar results to those observed with DYRK2. Similarly, the whole NOTCH family of receptors (NOTCH1-4) was analyzed in presence or absence of DYRK2 overexpression, resulting in a reduction of protein levels for all of them (Figure 9C).
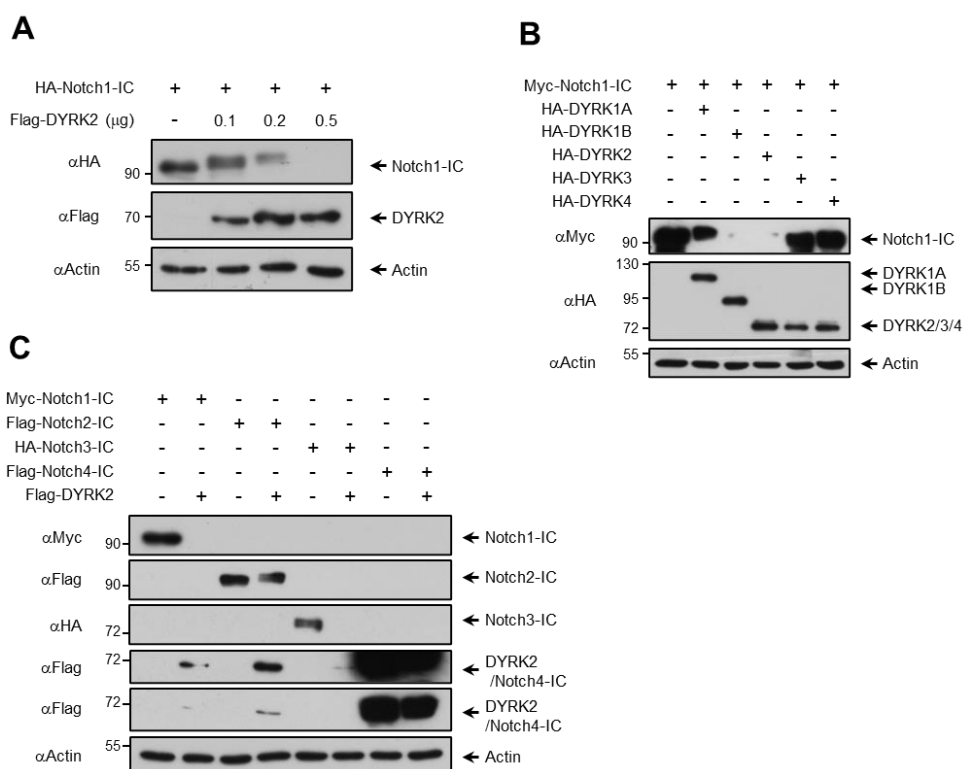
Figure 9. DYRK2 modulates NOTCH1 protein levels. (A) The indicated constructs were transfected into HEK-293T cells and protein expression was checked by western blot 36 h after transfection. **(B)** Co-transfection of HEK-293T cells was carried out using the indicated plasmids. Cells were lysed 36 h later and protein expression was evaluated by immunoblotting. **(C)** HEK-293T cells were co-transfected using the denoted plasmids. Protein expression was evaluated by western blot 36 h after transfection using the indicated antibodies. Representative blots of three independent replicates are shown for each figure.

Next, we studied the effect of DYRK2 expression on endogenous NOTCH1-IC endogenous levels. We observed (Figure 10A) that increased concentrations of

transfected DYRK2 resulted in a progressive decrease of NOTCH1-IC protein levels with no effect on *NOTCH* mRNA levels. As shown in Figure 10B, where endogenous protein levels of NOTCH1-IC were tested while over-expressing all members of DYRK subfamily, DYRK1B also leads to NOTCH1-IC decrease. Since DYRK1A has been previously described to phosphorylate NOTCH1 (149), we checked the specificity of DYRK2 antibodies and plasmids (Figure 11A). Besides, an experiment comparing knockout and wild type cells for DYRK1A transfected with increasing levels of DYRK2, demonstrated that the effect of DYRK2 on NOTCH1 is DYRK1A independent (Figure 11B). To further study the specificity of DYRK2 on NOTCH1-IC levels, we analyzed the effect of knocking down DYRK2 by using a specific siRNA (Figure 12). According with the obtained before, DYRK2 depletion resulted in increased NOTCH1-IC levels (Figure 12A), as well as in augmented NOTCH1-IC half-life (Figure 12B), supporting that DYRK2 regulates NOTCH1-IC endogenous levels.
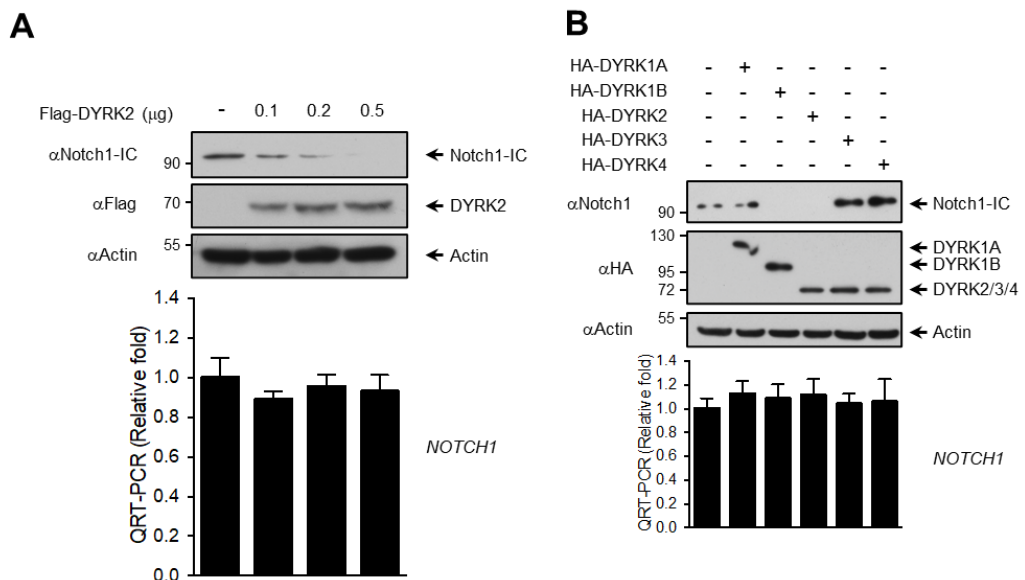

Figure 10. DYRK2 modulates NOTCH1 at a post-transcriptional level. (A) The showed amounts of DYRK2 were transfected into HEK-293T cells. After cell lysis al protein extraction, one fraction was analyzed for endogenous NOTCH1-IC protein levels, while another aliquot was destinated to study NOTCH1-IC mRNA levels by qPCR. **(B)** All members of DYRK family were transfected in HEK-293T cells. Protein levels were analyzed by western blot and NOTCH1 mRNA levels were studied by qPCR. Data are mean ± SD of n = 3. We show a representative blot of three independent experiments.
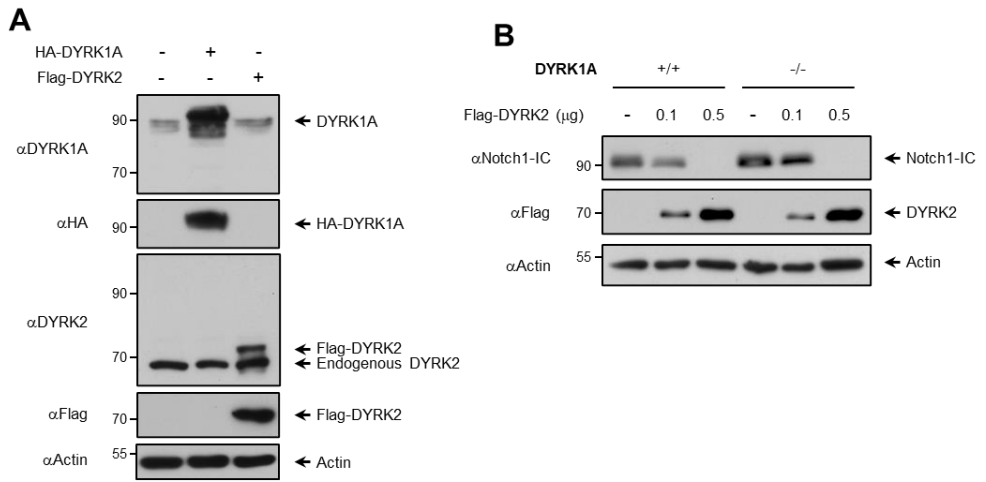
Figure 11. NOTCH1 regulation is DYRK1A independent. (A) HEK-293T cells were transfected using the indicated plasmids and protein expression was evaluated by western blot with the indicated antibodies. **(B)** HeLa WT and DYRK1A$^{-/-}$ cells were transfected with increasing levels of DYRK2. Protein levels were studied by immunoblot with the indicated antibodies. We show representative blots of three independent experiments.
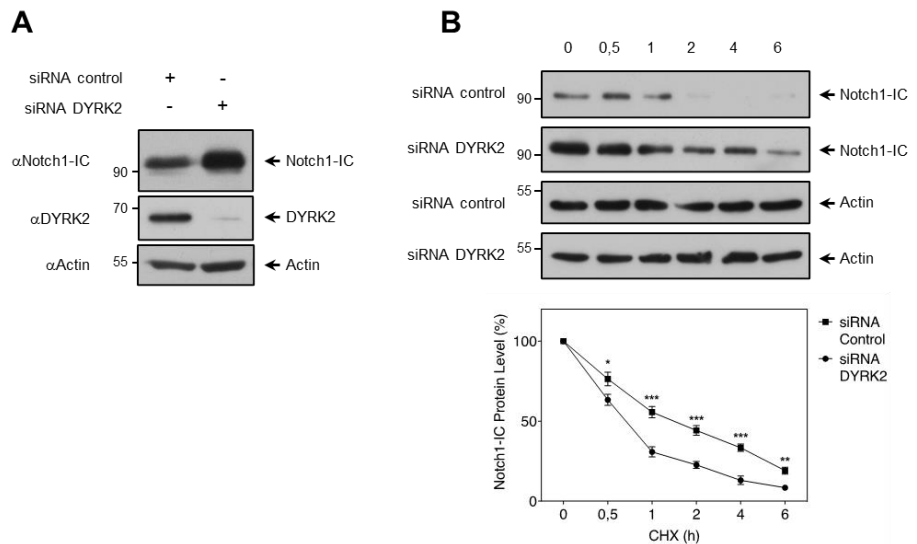

Figure 12. Silencing of DYRK2 promotes NOTCH1-IC protein stabilization. (A) DYRK2 or scrambled (control) siRNAs were transfected into HEK-293T cells. After 4 days of culture, NOTCH1-IC or DYRK2 protein levels were checked by immunoblot. **(B)** HEK-293T cells were transfected with DYRK2 or scrambled (control) siRNAs. 3 days after transfection, cells were treated with the protein synthesis inhibitor cycloheximide (CHX) (50 μg/ml) for the indicated hours, and lysed. NOTCH1-IC levels examined by immunoblot, using actin expression as the loading control. The graph represents the mean ± SD of band density from 3 different experiments. We show representative blots of three independent experiments. *P < 0.05, **P < 0.01, ***P < 0.001

Taken together, our data suggest that DYRK2 might negatively modulate NOTCH-IC protein levels. Then, we questioned if endogenous levels of DYRK2 and NOTCH1 might also show a correlation. To assess this idea, we studied these two proteins in 8 different cell lines (Figure 13A), observing a negative correlation between NOTCH1-IC and DYRK2. To further analyze NOTCH1-IC regulation by DYRK2, 4 different KO cell lines for the kinase were generated by CRISPR/Cas9 gene-editing techniques and NOTCH1-IC protein levels were evaluated. We observed that stable DYRK2 knockout presented increased levels of NOTCH1-IC in three of the four cell lines tested (Figure 13B). NOTCH1-IC bands presented higher electrophoretic mobility in HeLa DYRK2$^{-/-}$ comparing to the WT cells, which might be due to unphosphorylated NOTCH1-IC. These results demonstrate a negative regulation of NOTCH1-IC in a DYRK2-dependent way.
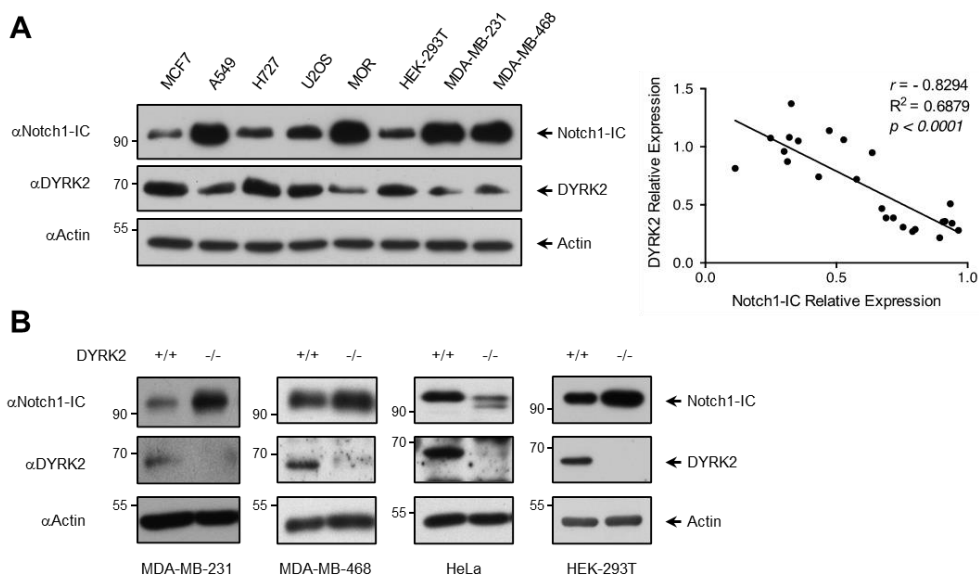

Figure 13. Inverse correlation of DYRK2 and NOTCH1 protein levels. (A) Endogenous expression of NOTCH1-IC and DYRK2 was studied by western blot in the indicated cell lines (left panel). Band signal from three independent experiments were quantified and normalized to actin, and correlation was analyzed (right panel). **(B)** DYRK2 and NOTCH1-IC endogenous levels were analyzed in MDA-MB-231, MDA-MB-468, HeLa and HEK-293T cell lines both WT and DYRK2$^{-/-}$ by western blot. We show representative blots of three independent experiments.

7.1.2. NOTCH1-IC is phosphorylated by DYRK2 *in* vivo and *in vitro*

As observed in Figure 2A, DYRK2 affects to NOTCH1-IC bands mobility. This could be due to the appearance of phosphorylated forms of NOTCH1-IC, so we analyzed

if DYRK2 kinase activity was necessary for this modification. To study this, we co-expressed NOTCH1-IC with increasing amounts of either wild type DYRK2 (DYRK2 WT) or a mutant with no kinase activity (DYRK2 KM). DYRK2 overexpression resulted in NOTCH1-IC protein levels decrease, as well as the appearance of upshifted bands. By contrast, this effect on NOTCH1-IC was not observed when transfecting DYRK2 KM. This experiment was carried out checking NOTCH1-IC both overexpressed (Figure 14A) and endogenous (Figure 14B) levels. To assess if that NOTCH1-IC protein levels reduction was due to proteasomal degradation, we co-expressed NOTCH1-IC and DYRK2 (either WT or KM) in the presence or absence of the proteasome inhibitor MG-132. As shown in Figure 14C, MG132 considerably reduced DYRK2-dependent NOTCH1-IC decrease with no effect on band mobility.
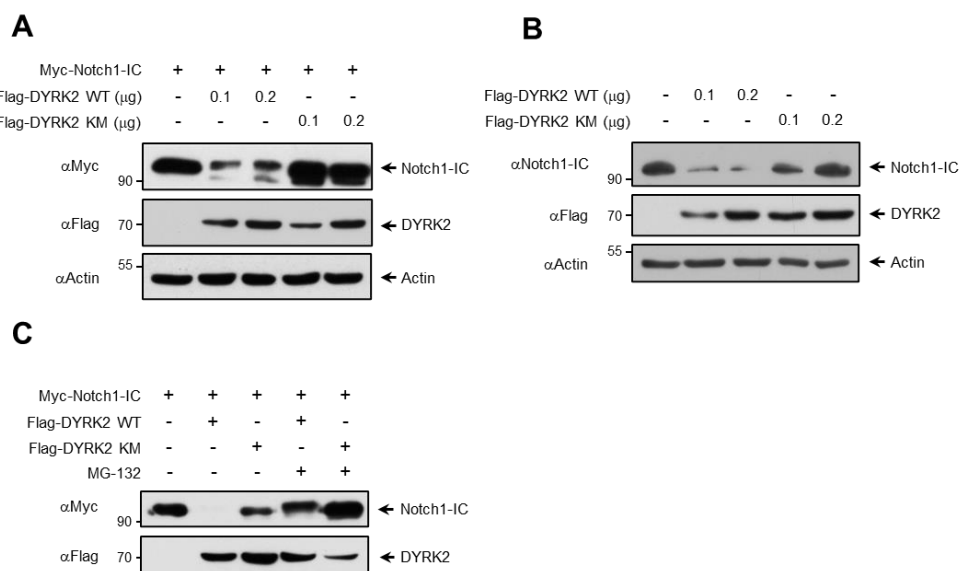

Figure 14. NOTCH1-IC regulation by DYRK2 depends on its kinase activity. (A) Myc-NOTCH1-IC and increasing amounts of Flag-DYRK2 wild type (WT) or kinase mutant (KM) were co-transfected in HEK-293T cells. Levels of proteins of interest were analyzed by western blot using the indicated antibodies. **(B)** HEK-293T cells were transfected with DYRK2 WT or KM plasmids, as indicated. Cell lysates were studied by immunoblot with the indicated antibodies. **(C)** HEK-239T cells were co-transfected with the indicated plasmids24 h after transfection, cells were treated with MG-132 (10 µM) for 12 hours and protein levels were analyzed by immunoblotting with the indicated antibodies. We show representative blots of three independent experiments.

Since reduced electrophoretic mobility of NOTCH1-IC bands in presence of DYRK2 could be due to the existence of phosphorylated forms, we exposed cell lysates to λ-phosphatase. As shown in Figure 15A, λ-phosphatase treatment reverted the upshift

promoted by DYRK2 similarly to the effect observed in response to DYRK2 KM expression. In addition, to evaluate if DYRK2 directly phosphorylates NOTCH1-IC, we carried out an *in vitro* kinase assay (Figure 15B). The presence of DYRK2 recombinant protein led to retarded migration of NOTCH1-IC bands, only when adding ATP to the reaction. Besides, we tested different chemical inhibitors of DYRK2 to assess the importance of DYRK2 kinase activity on NOTCH1-IC. Treatment with harmine in presence of DYRK2 WT (Figure 16A) resulted in a stabilization of NOTCH1-IC levels, similarly to the effect of DYRK2 KM. In addition, treatment with rising concentrations of harmine increased electrophoretic motility of NOTCH1-IC bands (Figure 16B). As shown in Figure 16C, similar results were obtained with curcumin, another DYRK2 inhibitor (77). Taken together, these results demonstrate that NOTCH1-IC is directly phosphorylated by DYRK2.
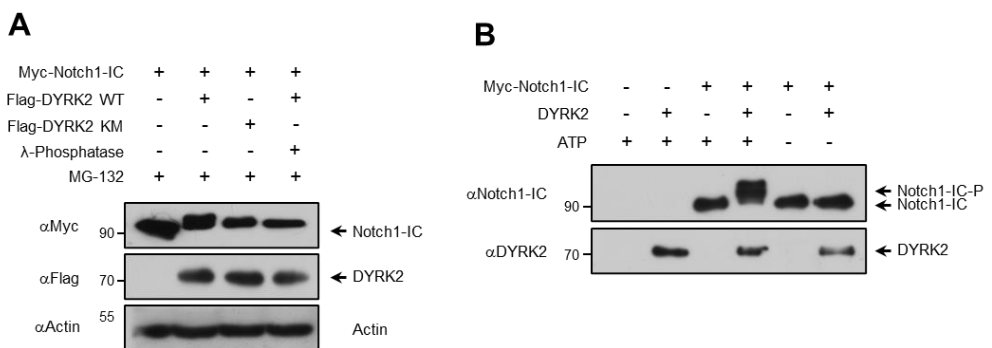

Figure 15. DYRK2 phosphorylates NOTCH1. (A) The indicated plasmids were co-expressed in HEK-293T cells. Cells were treated with MG-132 for 12 h prior to lysis and protein extracts were incubated wither in presence or absence of λ-phosphatase. Proteins of interest were analyzed by western blot. **(B)** NOTCH1-IC endogenous protein was immunoprecipitated from HEK-293T cells and then incubated with DYRK2 recombinant protein, in presence or absence of ATP (0.1 μM). Electrophoretic mobility was determined by western blot. We show representative blots of three independent experiments.
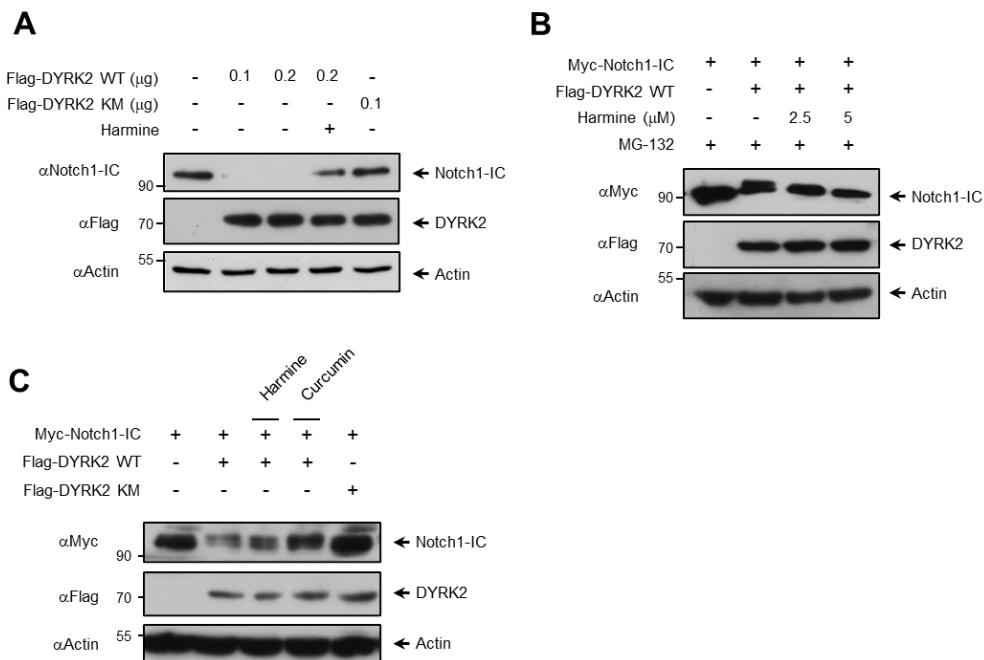
Figure 16. Pharmacological inhibition of DYRK2 reverts its effect on NOTCH1. (A) HEK-293T cells were co-transfected with the indicated plasmids and then incubated with harmine (5 µM) following the scheme for 12 h before lysis. Protein fractions were studied by immunoblotting using the indicated antibodies. **(B)** The indicated plasmids were co-expressed in HEK-239T cells. 36 hours after transfection, cells were treated with MG-132 in presence or absence of harmine for 12 h before lysis. Protein expression was studied by western blot **(C)** HEK-293T cells were co-transfected using the indicated constructs and exposed to harmine (5 µM, 12 h) or curcumin (5 µM, 6 h) before lysis. Cell lysates were analyzed by western blot. We show representative blots of three independent experiments. Figure authorship (C): Alejandro Correa Sáez.

Once proven the direct phosphorylation of NOTCH1-IC by DYRK2, next step would be identifying the residue(s) implicated in this process. To determine the NOTCH1-IC sites phosphorylated by DYRK2, we studied different residues already published to be phosphorylated and involved in NOTCH1-IC regulation. Then, mutants of these residues to alanine (323) were co-transfected with DYRK2 and its electrophoretic mobility was analyzed by western blot. As shown in Figure 17A, mutation of Thr2512 reduced DYRK2-mediated NOTCH1-IC degradation. Similar results were obtained comparing NOTCH1-IC Thr2512 to the WT co-expressed together with DYRK2 (Figure 17B). These data point out that phosphorylation of Thr2512 is necessary for DYRK2 effect on NOTCH1-IC stability. Next, we analyzed if DYRK2 phosphorylates Thr2512 of NOTCH1-IC in cells by co-expressing NOTCH1-IC, both WT and T2512A, and DYRK2, both WT and KM, following the scheme in Figure 17C. Phosphorylation pattern of NOTCH1-IC (WT and

T2512A) was analyzed using a phospho-serine/threonine antibody since there was no specific antibody against phospho-T2512 NOTCH1 available. As shown in the figure, phosphorylation was clearly reduced for T2512A mutant compared to the WT form (lanes 2 and 4). Nevertheless, as observed in lane 4, DYRK2 still promotes NOTCH1-IC T2512A phosphorylation, suggesting that DYRK2 might be phosphorylating NOTCH1-IC in several residues besides Thr2512. Taken together, these data demonstrate that NOTCH1-IC phosphorylation by DYRK2 at Thr2512 is key for its degradation.
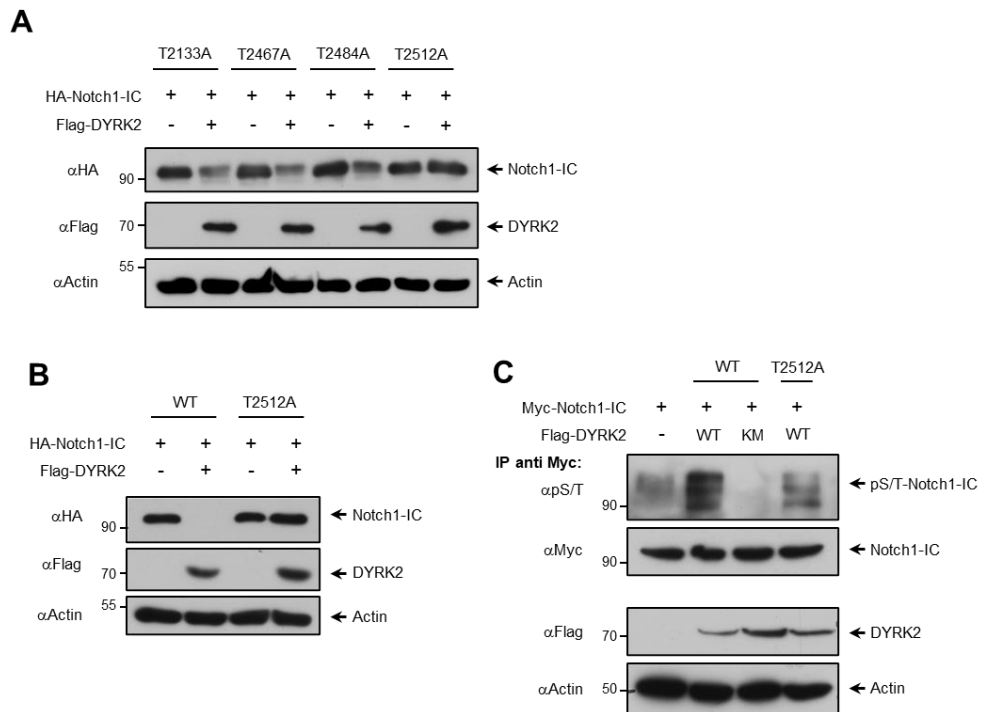

Figure 17. DYRK2 phosphorylates NOTCH1-IC at Thr2512. (A) NOTCH1-IC constructs, either WT or the indicated mutants, were overexpressed in HEK-293T cells in presence or absence of DYRK2. Cell lysates were obtained 36 h after transfection and protein expression pattern was studied by western blot. with the indicated antibodies. We show a representative blot of three independent experiments. **(B)** HEK-293T cells were transfected using the indicated plasmids and incubated 36 h before lysis. Protein levels were analyzed by immunoblot using the indicated antibodies. **(C)** Myc-NOTCH1-IC (WT or T2512) and Flag-DYRK2 (WT or KM) plasmids were co-transfected in HEK-293T cells following the indicated scheme. 24 h after transfection, cells were treated with MG132 for 8 h and then lysed. A part of the lysate was employed for immunoprecipitation (IP) using anti-Myc antibody, and phosphorylation status of eluted samples were analyzed by immunoblot using anti-phospho-Ser/Thr antibody (upper panel). At the same time, exogenous NOTCH1-IC levels were studied also by western blot but using anti-Myc antibody (second panel). The rest of the lysate extract was tested for the occurrence of the proteins of interest (lower panels). For each figure we show representative blots of three independent experiments. Figure authorship (C): Alejandro Correa Sáez.

7.1.3. NOTCH1-IC proteasomal degradation is regulated by DYRK2

As previously observed in Figure 14C, treatment with the proteasome inhibitor MG-132 reverted NOTCH1-IC decrease by DYRK2 (lanes 2 and 4). This indicates that DYRK2 reduces NOTCH1-IC stability in a proteasome-dependent manner. NOTCH1-IC proteasomal degradation after phosphorylation of Thr2512 has been previously reported to be dependent on FBXW7 ubiquitin ligase activity (163). Thus, we evaluated the potential implications of this ubiquitin-ligase in NOTCH1-IC degradation process triggered by DYRK2. First, we co-transfected constructs of NOTCH1-IC, DYRK2 and FBXW7ΔFbox (a dominant-negative mutant of FBXW7 which lacks the F-box, essential for its activity). As observed in Figure 18A, NOTCH1-IC protein levels were not decreased in presence of FBXW7ΔFbox even when co-expressing DYRK2. Similar data were obtained at endogenous levels (Figure 18B). These data confirm the relevance of FBXW7 in NOTCH1-IC degradation mediated by DYRK2.

Next, we analyzed if NOTCH1-IC ubiquitination status is modulated by DYRK2. In Figure 18C, we can observe that NOTCH1-IC polyubiquitination is augmented under increasing concentrations of DYRK2 WT but is not affected by the KM version of this kinase. Moreover, we studied the effect of DYRK2 absence on endogenous NOTCH1-IC polyubiquitination by comparing basal ubiquitination levels of NOTCH1-IC in both WT and DYRK2 knocked-out cells (Figure 18D). Data show that NOTCH1-IC ubiquitination levels were importantly decreased in DYRK2$^{-/-}$ cells. Taken together, these results imply that, following phosphorylation by DYRK2, NOTCH1-IC is ubiquitinated by FBXW7 and later degraded in a proteasomal dependent way.
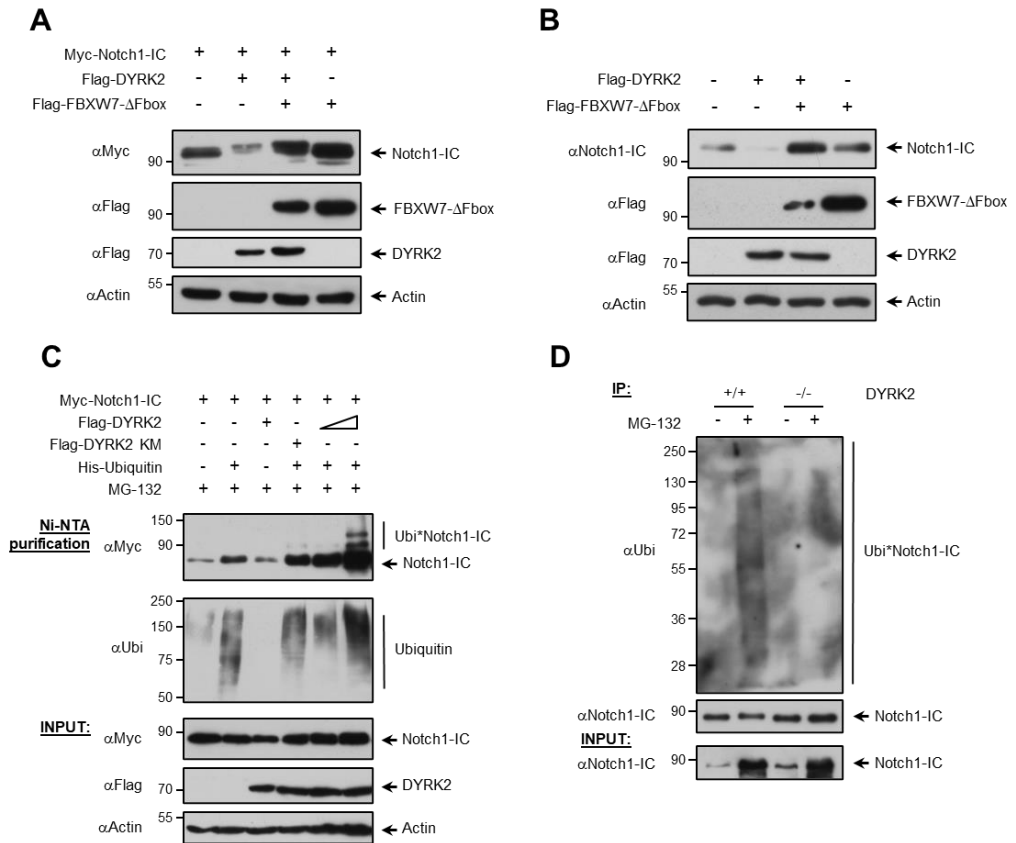
Figure 18. DYRK2 modulates NOTCH1-IC proteasomal degradation triggered by FBXW7. (A) NOTCH1-IC and DYRK2 plasmids were overexpressed in HEK-293T cells in presence or absence of FBXW7-ΔFbox (FBXW7 mutant that lacks the Fbox domain) and harvested for 36 h. Protein levels were analyzed by western blot after cell lysis. **(B)** HEK-293T cells were transfected with the indicated plasmids to evaluate NOTCH1-IC endogenous protein levels. 36 h after transfection protein analysis was carried out by immunoblotting. **(C)** HEK-293T were transfected following the showed scheme and incubated for 24 h before being treated with MG-132 (10 μM) proteasome inhibitor for another 12 h. After lysis, His-Ubiquitin was purified using Ni-NTA agarose beads and proteins of interest were checked by western blot. A small fraction of total protein lysate was employed to assess the presence of the indicated proteins (INPUT). **(D)** DYRK2 knocked-out (DYRK2$^{-/-}$) and WT cells were treated with MG-132 (10 μM) for 12 h following the indicated scheme and lysed. Endogenous NOTCH-IC was immunoprecipitated and the eluted fraction was analyzed by immunoblotting with the indicated antibodies. A small fraction of the total protein extract was used to test the presence of NOTCH-IC (INPUT). We show representative blots of three independent experiments for each figure. Figure (C) authorship: Alejandro Correa Sáez.

7.1.4. NOTCH1-IC and DYRK2 interact and colocalize

Next, we wondered about the potential DYRK2-NOTCH1-IC interaction, so we analyzed it by coimmunoprecipitation (coIP) assays after overexpressing both proteins.

As shown in Figure 19A, NOTCH-IC successfully coimmunoprecipitated with DYRK2. We also studied the subcellular location of both proteins by confocal microscopy and the effect of DNA damage on it. As it can be observed in Figures 12B and 12C, under DNA damage conditions induced by etoposide (ETP) treatment GFP-DYRK2 and endogenous NOTCH1-IC colocalize in the nucleus (Pearson's coefficient = 0.65 and Manders' coefficients of A=0.789; B=0.773).
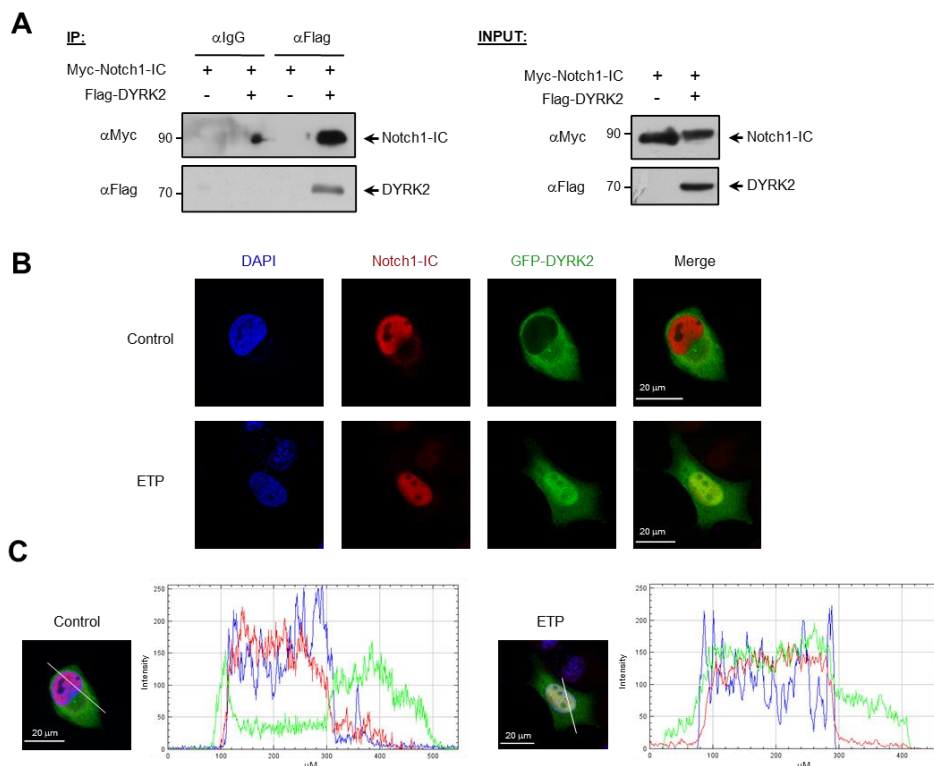

Figure 19. DYRK2 and NOTCH-IC interaction and colocalization. (A) The indicated plasmids were transfected in HEK-293T cells, which were harvested by 24 h before being treated with MG-132 (10 µM) for 12 h. Immunoprecipitation (IP) of DYRK2 was performed using anti-Flag antibody. Eluted samples were analyzed by western blot using the indicated antibodies. A small fraction of the total protein extract was used to assess the proteins of interest expression (INPUT). **(B)** CHO cells were transfected with GFP-DYRK2 construct and treated or not with ETP 10 µM for 6 h. Protein subcellular location was analyzed by confocal microscopy. Nuclear DNA was stained with DAPI. Overlapping of GFP-DYRK2 and NOTCH-IC signals in merged pictures is shown in yellow. **(C)** GFP-DYRK2 and NOTCH-IC fluorescence intensity profiles at both control and ETP treatment conditions along the white line are shown. Thresholded Manders' coefficients A and B (A=0.789; B=0.773) and Pearson's coefficient (0.65) were calculated for both conditions. Representative blots and images three independent experiments for each figure. Figure (A) authorship: Alejandro Correa Sáez.

To determine the interaction sites of NOTCH1-IC and DYRK2, we first carried out an *in vitro* interaction peptide array (Figure 20A and 20B). A library of overlapping

peptides of complete NOTCH1-IC and DYRK2 was exposed to GST-tagged DYRK2 or NOTCH1-IC recombinant proteins, respectively. Binding was detected using specific antibodies, which resulted in 6 potential interacting regions of NOTCH1-IC with DYRK2. On the other hand, DYRK2 array showed 3 candidate regions for NOTCH1-IC interaction, all of them at the C-terminal domain of the kinase.
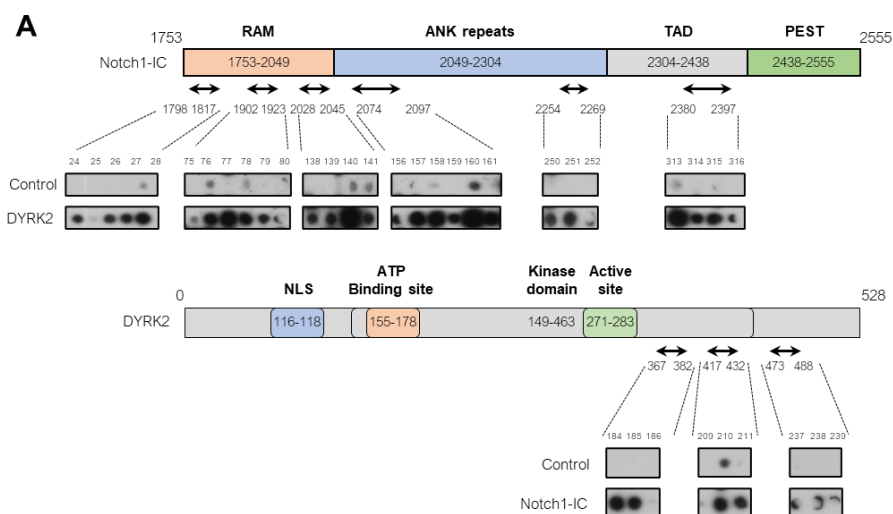

B

Notch-IC		DYRK2	
24	KNASDGALMDDN	184	MPSQKLLDASKR
25	ASDGALMDDNQN	185	SQKLLDASKRAK
26	DGALMDDNQNEW	186	KLLDASKRAKNF
27	ALMDDNQNEWGD	209	PPESREWGNALK
28	MDDNQNEWGDED	210	ESREWGNALKGC
75	EEEDAPAVISDF	211	REWGNALKGCDD
76	EDAPAVISDFIY	237	EKTSVKRITEST
77	APAVISDFIYQG	238	TSVKRITESTGA
78	AVISDFIYQGAS	239	VKRITESTGAIT
79	ISDFIYQGASLH		
80	DFIYQGASLHNQ		
138	GKSALHWAAAVN		
139	SALHWAAAVNNV		
140	LHWAAAVNNVDA		
141	WAAAVNNVDAAV		
156	YETAKVLLDHFA		
157	TAKVLLDHFANR		
158	KVLLDHFANRDI		
159	LLDHFANRDITD		
160	DHFANRDITDHM		
161	FANRDITDHMDR		
162	NRDITDHMDRLP		
250	EMAALGGGGRLA		
251	AALGGGGRLAFE		
252	LGGGGRLAFETG		
313	VQTQQVQPQNLQ		
314	TQQVQPQNLQMQ		
315	QVQPQNLQMQQQ		
316	QPQNLQMQQQNL		

Figure 20. Binding regions involved in NOTCH1-IC-DYRK2 interaction. (A) Schemes of NOTCH1-IC and DYRK2 proteins with regions responsible of interaction indicated. A peptide-array library membrane covering NOTCH1-IC or DYRK2 whole sequences were treated with either GST-tagged DYRK2 or NOTCH1-IC recombinant proteins, respectively. GST recombinant protein was employed as control. Recombinant protein-membrane binding spots were detected by western blot. Representative blots of two independent experiments are shown. (B) Sequences of NOTCH1-IC and DYRK2 peptides recognized in peptide array assay. Figure authorship (A and B): Alejandro Correa Sáez.

To validate the functional relevance of different NOTCH1-IC regions, we generated NOTCH1-IC mutants (Figure 21A) and tested their interaction with DYRK2 (Figure 21B). As exposed in figure 14B, mutations in the RAM and ANK (ankyrin) domains caused a reduction in the capacity to coimmunoprecipitated with DYRK2. In addition, DYRK2-dependent decrease of protein levels was also affected for these specific mutations (Figure 22A and 22B). Taken together, these data prove the direct interaction between both proteins and suggest the implication of more than one region. Nevertheless, RAM domain seems to be particularly important in this binding process.
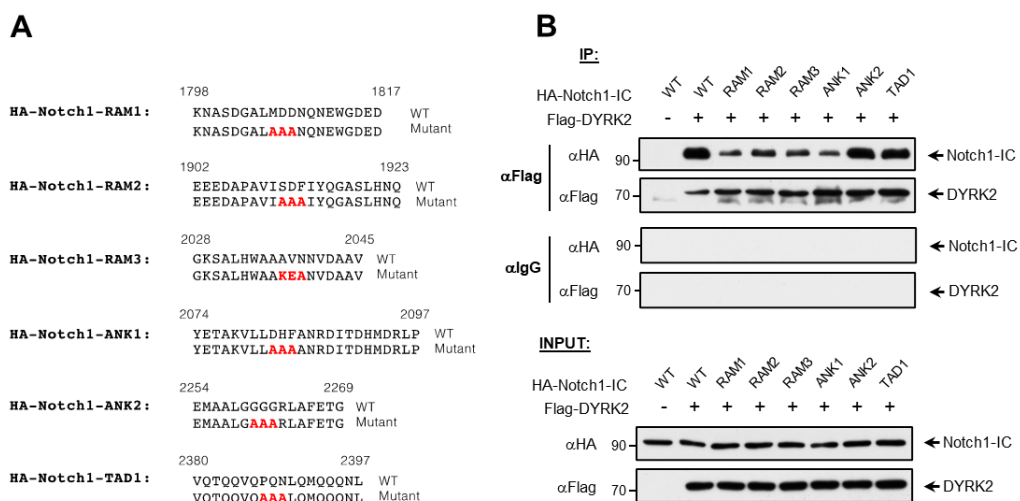

Figure 21. DYRK2 interaction with NOTCH1-IC mutants. (A) Aminoacids located on the center of each interaction region identified in the previous peptide array were mutated to alanine (A). For HA-NOTCH1-RAM3, alanine and valine (V) aminoacids were mutated to lysine (K) and glutamic acid (E), respectively. **(B)** HA-NOTCH1-IC constructs, both WT and mutants were co-transfected in HEK-293T cells together with Flag-DYRK2 and harvested for 36 h. Cells were treated with MG-132 (10 µM) for the last 12 h of incubation. After cell lysis, overexpressed DYRK2 was immunoprecipitated using anti-Flag antibody and coIP of NOTCH1-IC (WT and mutants) was assessed by western blot (upper panel). Proper expression of transfected plasmids was analyzed by immunoblot in a small fraction of the initial protein extract (INPUT, lower panel). Here we show representative blots of three independent experiments.
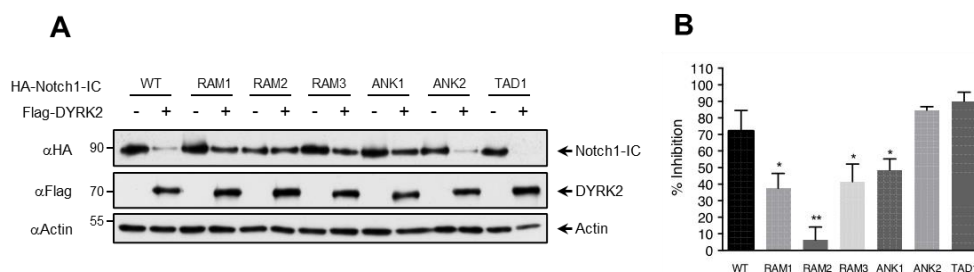
Figure 22. DYRK2 effect on NOTCH1-IC mutants. (A) HA-NOTCH1-IC (WT and mutants) and Flag-DYRK2 plasmids were co-expressed in HEK-293T cells as shown. Cells were lysed 36 h after transfection and protein levels were studied by immunoblotting using the indicated antibodies. **(B)** Inhibition of NOTCH1-IC WT and mutants protein levels (%) in response to co-expression of DYRK2. NOTCH1-IC signals were quantified and normalized to actin signal using ImageJ. *$P <$ 0.05, **$P <$ 0.01. Three independent experiments were carried out to generate this figure, a representative blot was selected for 22A.

7.1.5. NOTCH1-IC modulation by DYRK2 in response to genotoxic stress

Next, we studied the DYRK2 effect on NOTCH1-IC under physiological conditions. As previously exposed, there exist several stimuli that regulate DYRK2 activity. Among them, DNA damage stands out (31, 41, 61). According to this, we assessed NOTCH1-IC modulation by DYRK2 in response to genotoxic stress by stimulating cells with increasing concentrations of the cytotoxic drug adriamycin (ADR). As shown in Figure 16A, DYRK2 accumulation triggered by ADR treatment in HEK-293T cells results in lower levels of NOTCH1-IC. Similar results were obtained using MDA-MB-231 cells (Figure 23B), DYRK1A$^{-/-}$ cells (Figure 23C) or with other DNA-damaging agents like etoposide (ETP) or cis-platin (CPT) (Figures 23D and 23E, respectively).

Additionally, we studied the potential effect of DNA damage on NOTCH1-IC transcriptional activity. According to previous results, treatment with increasing concentrations of ADR resulted in a NOTCH1-IC protein lost as well as a reduction of its transcriptional activity (Figure 24A). Since similar results were previously described under HIPK2 influence, were carried out the same experiment using HIPK2 knocked out cells (Figure 24B) obtaining similar results, proving that is a HIPK2-independent process. Next, we analyzed if DYRK2 levels would directly affect NOTCH1-IC transcriptional activity. As observed in Figures 25A and 25B, DYRK2 not only affects NOTCH1-IC activity on 4xCSL reporter construct, but also on its physiological target genes Hes1 and Hes5. In summary, these data support NOTCH1-IC modulation by DYRK2 in response to DNA damage.
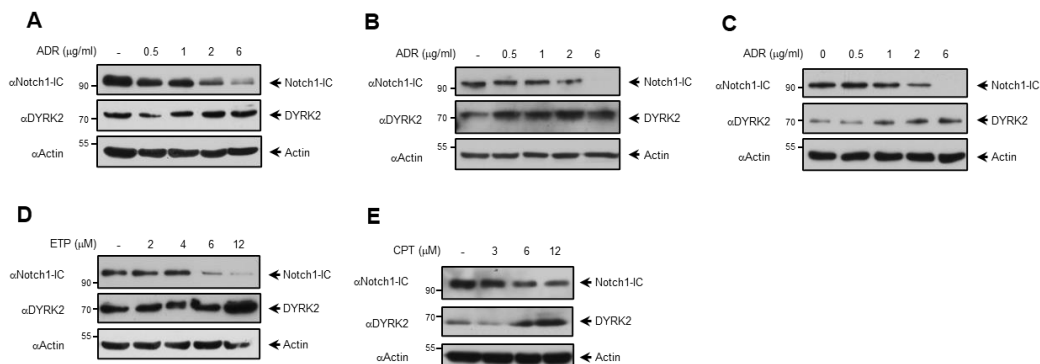
Figure 23. DNA damage modulates NOTCH1-IC in a DYRK2-dependent way. Increasing concentrations of ADR were employed to stimulate **(A)** HEK-293-T, **(B)** MDA-MB-231 and **(C)** HeLa DYRK1A$^{-/-}$ cells. After 12 h of treatment, cells were lysed and endogenous levels of proteins of interest were assessed by western blot. **(D)** H727 cells were stimulated with increasing concentrations of etoposide (ETP) for 12 h. After treatment and cell lysis, endogenous protein levels of NOTCH1.IC and DYRK2 were analyzed by immunoblotting. **(E)** MDA-MB-231 cells were treated with the indicated concentrations of cis-platin (CPT) for 12 h. Next, they were lysed, and protein levels were studied using specific antibodies. We show representative blots of three independent experiments for each figure.
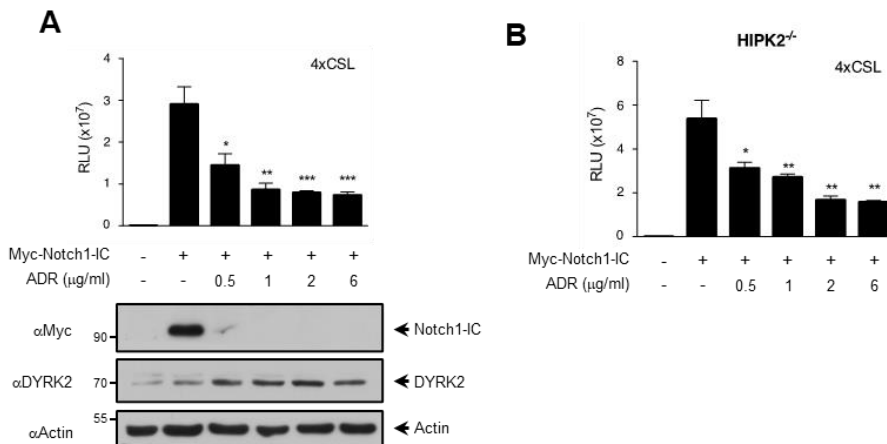

Figure 24. Genotoxic stress-triggered DYRK2 modulates NOTCH1-IC transcriptional activity. **(A)** 24 h after being transfected with the indicated plasmids, cells were treated with ADR for 12 h and then lysed. A fraction was employed for analyze protein levels by western blotting, while the other one was used in a luciferase reporter assay (top panel). **(B)** HEK-293T HIPK2$^{-/-}$ cells were transfected following the indicated scheme and later treated with ADR for 12 h. After cell lysis, NOTCH1-IC transcriptional activity was assessed by luciferase reporter assay. We show representative blots of three independent experiments. Data are mean ± SD of n = 3 experiments. *P < 0.05, **P < 0.01, ***P < 0.001

To further consolidate the role of DYRK2 kinase activity on NOTCH1-IC modulation, we employed an analogue-sensitive DYRK2 mutant (DYRK2-AS). According to Bishop et. al technique description (324), DRYK2-AS construct presents a mutation in the gatekeeper residue that turns DYRK2-AS into a selectively sensitive kinase to PP1 inhibitors. As observed in Figure 26A, DYRK2-AS kinase activity inhibition by PP1 analog reverts the effect of the kinase on NOTCH1-IC protein levels and its transcriptomic activity, as Hes5 mRNA and protein levels demonstrate. In addition, we evaluated over-expressed NOTCH1-IC protein levels and activity in DYRK2 knocked out cells (Figure 26B). As shown, overexpression of NOTCH1-IC is significantly higher in DYRK2$^{-/-}$ cells comparing to the control ones.
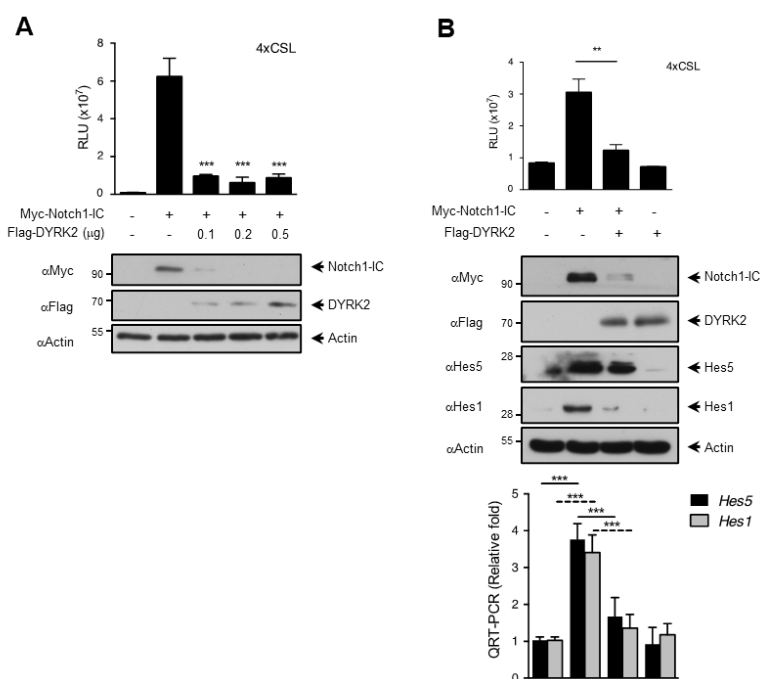

Figure 25. NOTCH1-IC activity is modulated by DYRK2 expression. (A) HEK-293T cells were transfected according to the indicated scheme and harvested for 36 h. After cell lysis, one aliquot of the protein extract was employed to analyze NOTCH1-IC activity on luciferase reporter assay (top panel) and the other one was analyzed by western blot to study levels of proteins of interest. **(B)** the indicated plasmids were transfected on HEK-293T cells. 36 h after transfection, cell lysis was performed and a fraction of the extract was used for luciferase reporter assay and western blotting (upper panels), while the rest of the sample was destined to qPCR analyses to assess Hes1 and Hes5 mRNA levels (lower panel). We show representative blots of three independent experiments. Data are mean ± SD of n = 3 experiments. **P < 0.01, ***P < 0.001
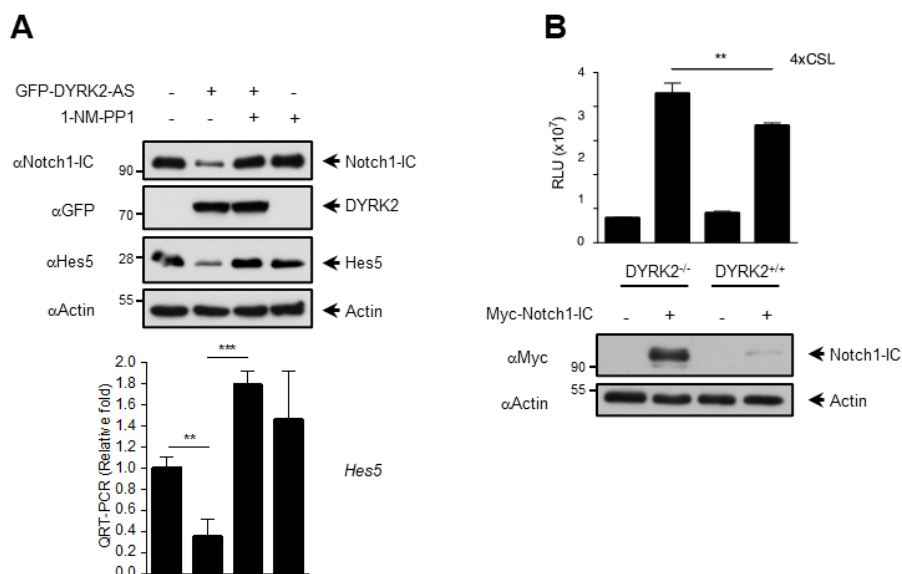
Figure 26. NOTCH1-IC modulation depends on DYRK2 kinase activity. (A) GFP-DYRK2-AS (analog sensitive) mutant was transfected into HEK-293T cells following the scheme. Cells were harvested for 36 h and the indicated points were treated using PP1 analog 1-NM-PP1 (3 μM) during the 3 last ones. Cells were then split in two different aliquots. One of them was employed for checking protein levels by western blot (first panel) and the other one was subjected to qPCR analysis to check Hes5 mRNA levels (second panel). **(B)** MDA-MB-231 cells, both WT and DYRK2 knocked out, were transfected using Myc-NOTCH1-IC and 4xCSL luciferase reporter constructs and incubated for 36 h. Once lysed, an aliquot was used for analyzing NOTCH1-IC transcriptional activity using a luciferase reporter assay (upper panel), while the other aliquot was employed to analyze the indicated protein levels by immunoblotting (lower panel). For each figure we show representative blots of three independent experiments. Data are mean ± SD of n = 3 experiments. **$P < 0.01$ ***P < 0.001

At this point, we analyzed the effect of silencing DYRK2 using siRNA to consolidate the importance on NOTCH1-IC regulation after DNA damage. As observed in Figure 27, decrease of NOTCH1-IC in response to ADR (adriamycin) treatment was reversed silencing DYRK2 (lanes 2 and 5). Similarly, expression of NOTCH1-IC target genes Hes1 and 5 (both mRNA and protein levels) was restored by harmine treatment or DYRK2 knock down (lanes 2m 3 and 5) in MDA-MB-231 and HEK293T cells (Figures 27A and 27B, respectively). Taken together, these results indicate that NOTCH1-IC protein levels and activity are modulated in response to DNA damage in a DYRK2-dependent manner.
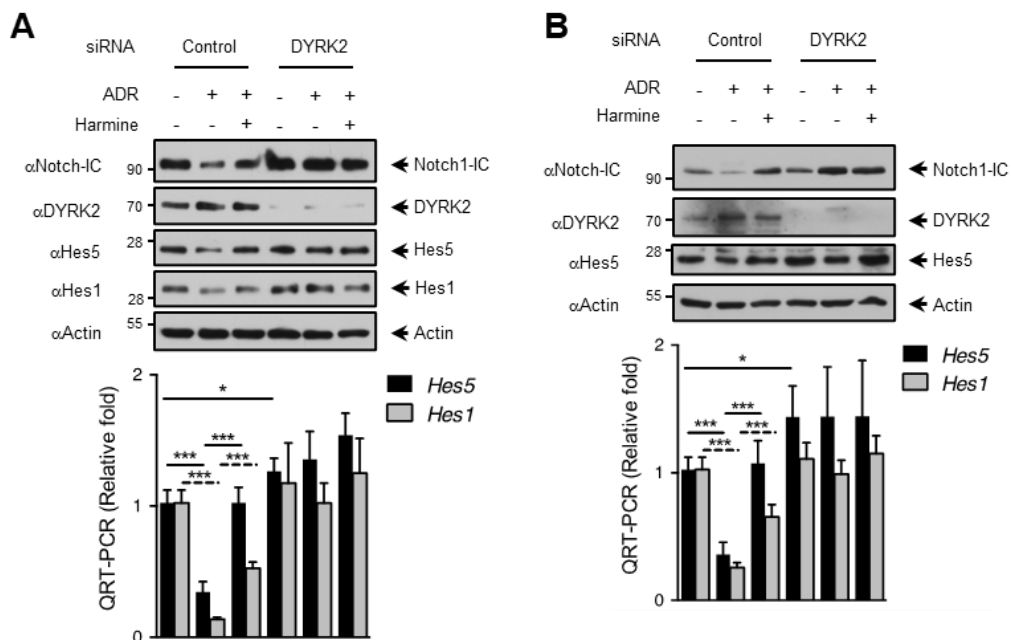
Figure 27. DYRK2 is involved in NOTCH1-IC modulation by DNA damage. (A) MDA-MB-231 or **(B)** HEK-293T cells were transfected using specific DYRK2 siRNA or scrambled (control) and incubated for 3 days. Treatments with ADR (2 µg/ml) and harmine (5 µM) for 12 h were performed following the scheme. An aliquot of the cells was used to analyze the levels of the proteins of interest by immunoblot with specific antibodies (upper panel), while another one was employed to analyze Hes5 and Hes1 mRNA levels by qPCR (lower panel). We show representative blots of three independent experiments for each figure. Data are mean ± SD of n = 3 experiments. $*P <$ 0.05, $***P < 0.001$.

7.1.6. NOTCH1-IC physiological functions are affected by DYRK2

Finally, and to try to elucidate the clinical relevance of our findings, we first analyzed DYRK2 and NOTCH1 data from the public database *"The Human Protein Atlas".* According to previous results, a significantly high number of patients present high levels of NOTCH1 and low levels of DYRK2 in different tissues, from which several tumoral tissues as cervical, ovarian, colorectal, or pancreatic cancer stand out (Figure 28A). In the same way, we analyzed the frequency of loss-of-function mutations of DYRK2 and NOTCH1 in tumors, observing that mutations of both genes rarely happen together, pointing out that both proteins might act in the same pathway (Figure 28B).
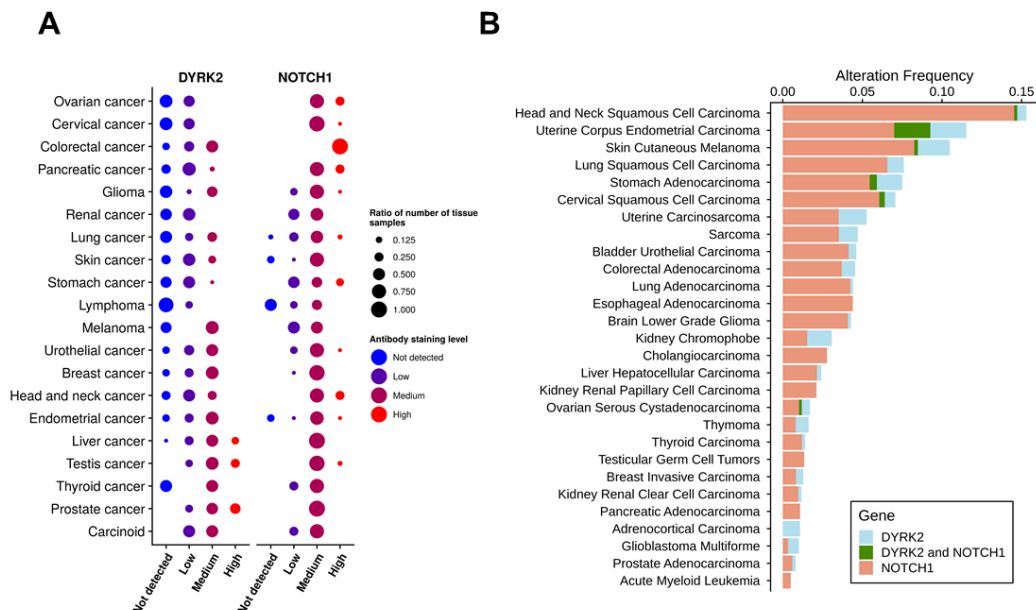
Figure 28. DYRK2 and NOTCH1 mutations and protein levels in different cancer databases. **(A)** Representative scheme of DYRK2 and NOTCH1 protein expression in different tumor tissues. Data obtained from The Human Protein Atlas database. Columns and colors represent the antibody stain levels. Circle size shows the ratio of patients expressing that level of protein comparing to the total number of patients. Tumor tissues are shown based on the score of differences between DYRK2 and NOTCH1 expression patterns. This score was calculated by assigning a number (1-4) to every staining level (Not detected, Low, Medium, and High, respectively), and multiplying it by the total number of patients for each tissue and protein. Absolute mean differences were finally calculated for every tumor tissue. **(B)** Mutation frequency (missense, non-sense, or deep deletions) of DYRK2 and NOTCH1 either independently or together for every tumor type included in the TCGA PanCancer database**.**

We also studied apoptosis and cell viability modulation under genotoxic stress by ADR mediated by DYRK2. In these experiments, we observed that MDA-MB-231 DYRK2$^{-/-}$ cells showed increased viability in response to ADR than the WT ones (Figure 29A), but the opposite result was obtained overexpressing DYRK2. Similarly, DYRK2 overexpression induced a raise on the percentage of apoptotic cells when treating them with ADR, while the use of harmine significantly reduced this percentage, in both MDA-MB-231 (Figure 29B) and MDA-MB-468 (Figure 29C) cells. Additionally, as shown in Figure 29D, DYRK2 affected the expression of relevant genes for cell viability like *BLC2*.
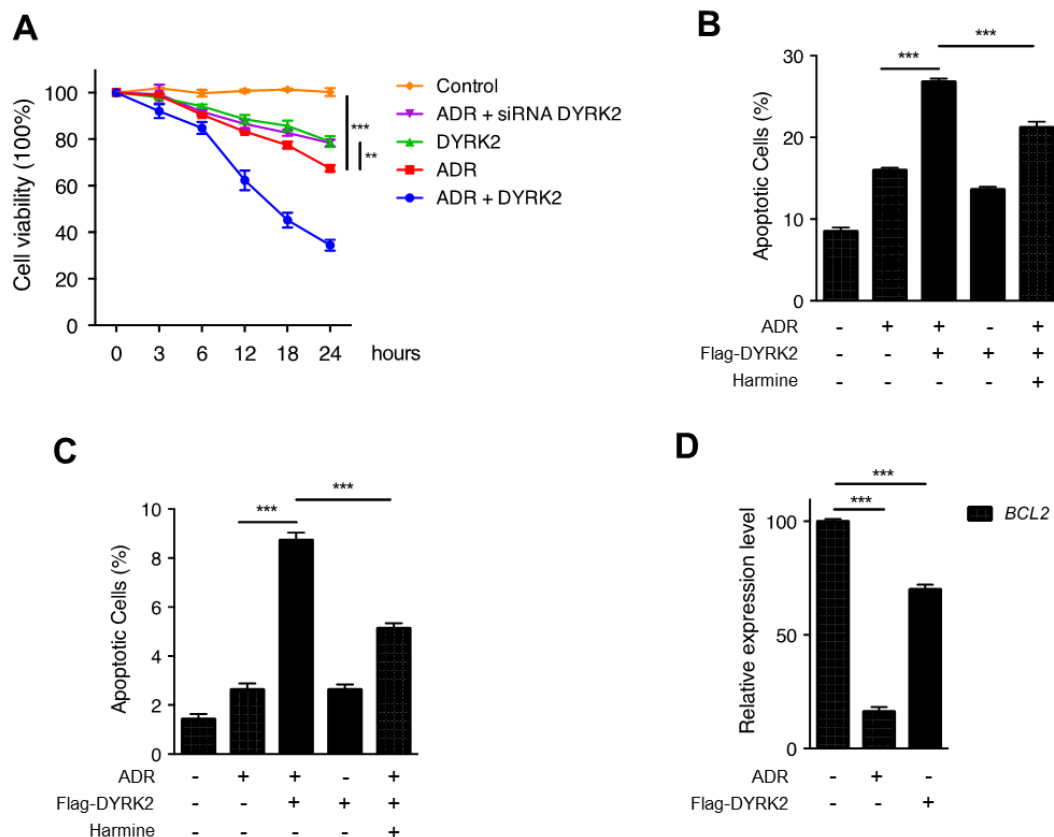
Figure 29. Cell viability and survival of breast cancer cells are affected by DYRK2 modulation. (A) MDA-MB-231 cells were transfected following the scheme and the indicated points were stimulated using ADR (2 µg/ml) for 12 h. YOYO-1 fluorescence technique was carried out to analyze cell viability. MDA-MB-231 **(B)** and MDA-MB-468 **(C)** cells were transfected or not with Flag-DYRK2 construct and the indicated points were subjected to ADR (2 µg/ml) and/or harmine (5 µM) for 12 h. Next, apoptotic rate was assessed by Annexin V/PI staining coupled to flow cytometry. **(D)** MDA-MB-231 cells were transfected with Flag-DYRK2 and treated with ADR (2 µg/ml) following the scheme. 12 h after treatment, mRNA was extracted and BCL2 expression levels were measured by qPCR. For all the 4 figures: data are mean ± SD of n = 3 experiments. $**P < 0.01$, $***P < 0.001$.

In addition, as shown in Figure 30A, DYRK2 is necessary for adriamycin-induced suppression of cell invasion (Figure 23A). In the same sense, cell motility assays showed how NOTCH1-IC overexpression significantly increased cell migration of DYRK2$^{-/-}$ cells comparing to the same conditions on DYRK2 WT cells (Figures 30B and 30C, respectively). In this sence, expression of some key genes involved in cell mobility and invasion (*FGF, TFG-β, TNFα* and *OCT-4)* were analyzed (Figure 31), supporting the mentioned effect of DYRK2-NOTCH1 expression combination. Taken together, these

data imply a novel role of DYRK2 modulating cancer cell migration and invasion by affecting NOTCH1-IC expression levels.
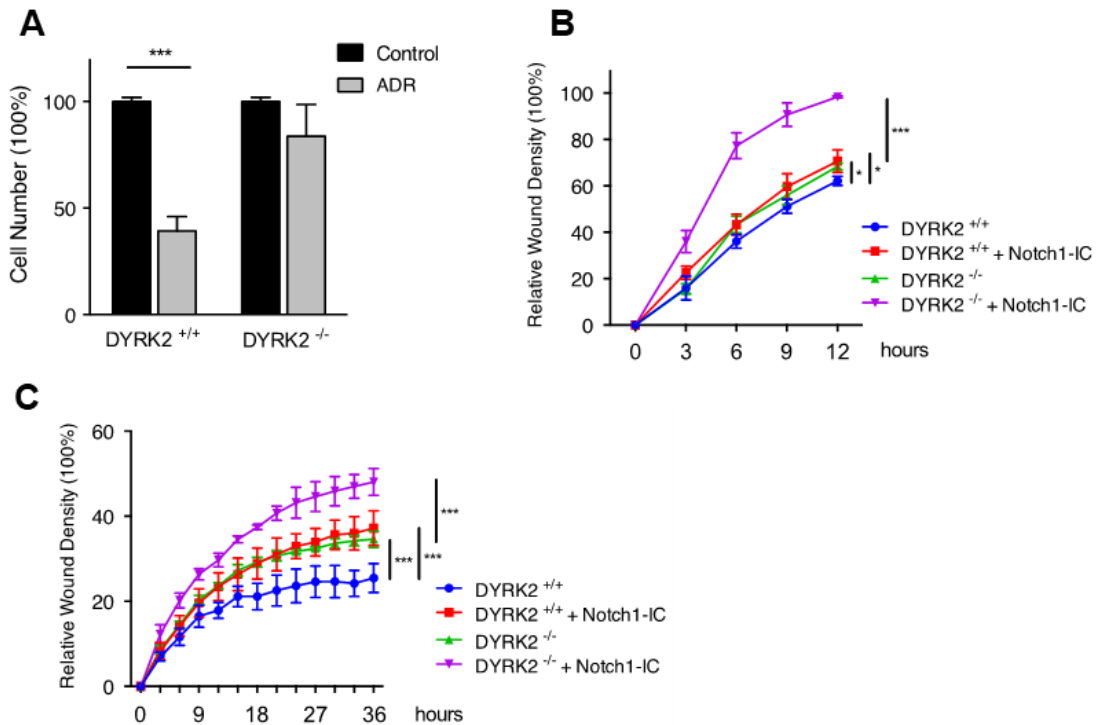
Figure 30. Breast cancer cells invasiveness and motility is modulated by the axis DYRK2-NOTCH1-IC. (A) Both WT and DYRK2 knocked-out MDA-MB-231 cells were treated or not with ADR (2 µg/ml) for 12 h and invasion potential was assessed by matrigel motility analysis. MDA-MB-231 **(B)** and MDA-MB-231 **(C)** cells both WT or DYRK2-/- were transfected or not using Flag-NOTCH1-IC construct. 36 h after transfection, cells were subjected to wound healing motility assays. For all the 3 figures, data are mean ± SD of n = 3 experiments. *** $P < 0.001$. Figure (A) authorship: Alejandro Correa Sáez.

Figure 31. Expression of invasiveness and motility-related genes is affected by DYRK2 and NOTCH1-IC. MDA-MB-231 both WT and DYRK2-/- cells were transfected or not with Flag-NOTCH1-IC. 36 h after transfection, mRNA levels of the indicated genes were studied by qPCR. Data are mean ± SD of n = 3 experiments. **$P < 0.01$, ***$P < 0.001$.

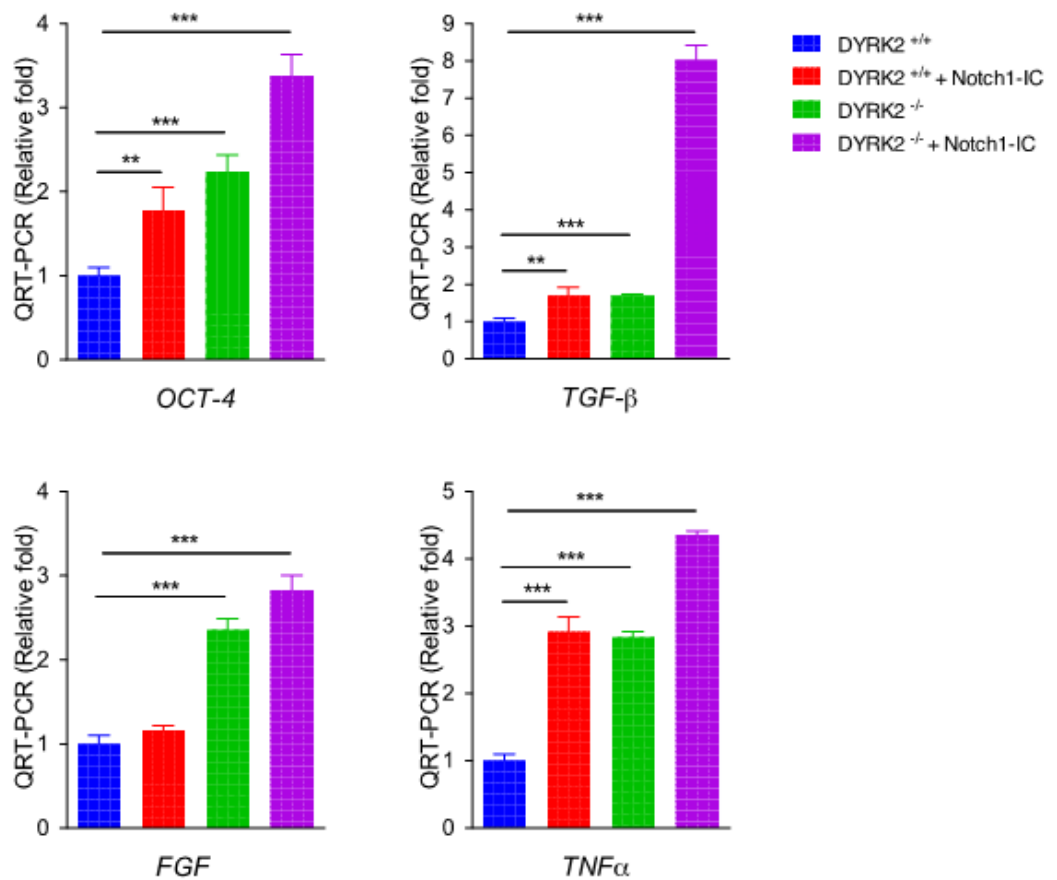## 7.2. Modulation of signaling pathways in response to X ray in human dermal fibroblasts

7.2.1. Different patterns of ionizing radiation induce DNA damage in human dermal fibroblasts

As previously commented, further research about DDR pathways is required to assess new molecular mechanisms for fully comprehend this complex scheme. To allow this, we analyzed the signaling changes that occur in dermal fibroblast of patients who are treated with radiation. These patients can be normally subjected to two different patterns of radiation: acute or accumulative (302, 325). To analyze the molecular mechanisms that participate in response to this treatment, we followed the scheme shown in Figure 25. First, primary fibroblasts from 4 different donors (Table 1) were cultured as a unique pool and labelled or not using SILAC techniques. Finally, cells were subjected to different radiation patterns (either acute or accumulative) and proteomic, phosphoproteomic and transcriptomic data were analyzed. To choose the best X ray dose and pattern for the experiments, we irradiated primary human dermal fibroblasts using different schemes. In the one hand, we used a unique dose that would represent the acute dose; in the other hand, 4 stimuli, one each 12 h, as equivalent for accumulative doses. To report the consequent DNA damage after radiation, levels of γH2AX and phosphorylation in Thr68 of CHK2 were checked by western blot. As shown in Figure 26A, the most appropriate dose for acute radiation was 2 Gy (Figure 33A), while in the case of accumulative radiation the most effective procedure was to irradiate the cells with 5 Gy (Figure 33B).
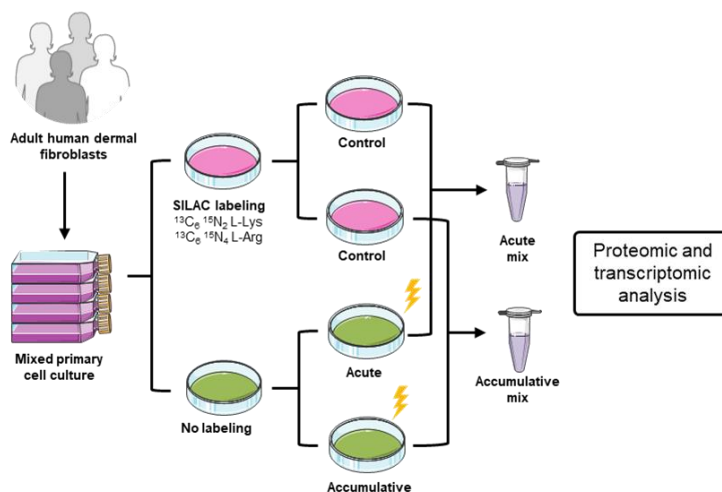

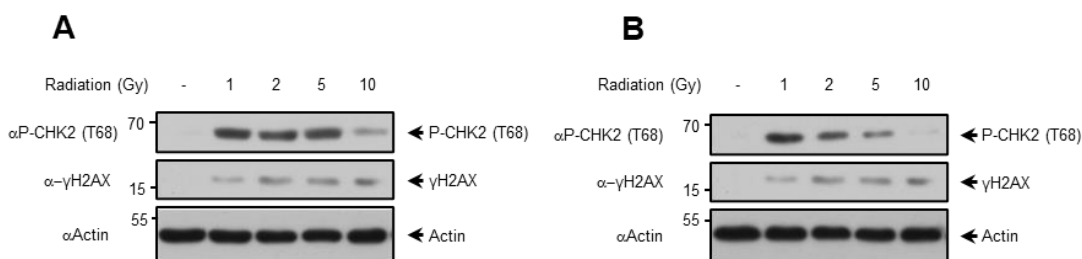**Figure 32. Schematic representation of the experimental design.**

Figure 33. Acute and accumulative doses of radiation were adjusted for the subsequent experiments. (A) Adult human dermal fibroblasts from 4 different donors were irradiated using one only dose of each indicated intensity of radiation and lysed 2 h after stimulation. Protein expression was evaluated by immunoblotting. **(B)** Adult human dermal fibroblasts were stimulated every 12 h using the indicated doses (4 times per dose in total). Cells were lysed 30 min after the last stimulus and protein levels were analyzed by immunoblotting with the indicated antibodies. We show a representative blot of three independent experiments.

Next, cells were expanded to maximize the amount of sample while labelling them using SILAC (Stable Isotope Labelling with Amino acids in Cell culture). In this sense, two different subcultures were prepared: one labelled using SILAC and another one unlabeled, following the conditions specified in *Materials and Methods*. Before carrying out the experiment, labelling of the cells was properly verified, as it can be confirmed in Figure 34. Unlabeled cells were treated with the acute or accumulative dose as required, while labelled cells were kept as a control of the experiment. After stimulation with X rays, cells were lysed to obtain protein and total RNA samples for the proteomic, phosphoproteomic and transcriptomic analysis. In the case of proteomic and phosphoproteomic studies, samples were treated as shown in Figure 34, mixing each irradiated sample with it correspondent untreated sample in a 1:1 ratio. At the same time, while purifying proteomic samples we also isolated total RNA of those treated and untreated fibroblasts. This would permit us to carry out RNA-seq analysis, which improved the quality and strength of the data obtained when crossed with proteomic and phosphoproteomic results.
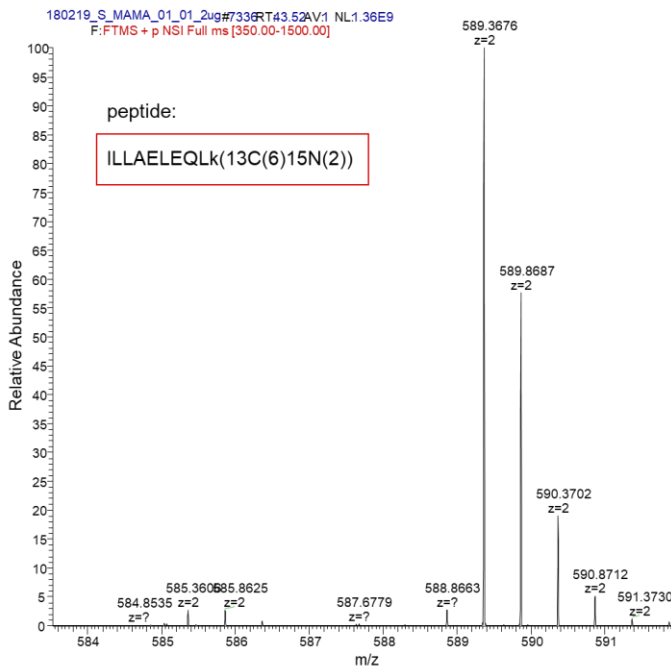
Figure 34. SILAC labelling example. Spectrum of one of the peptides from the SILAC-labelled samples, in which intense signal of heavily labeled peptide is shown where barely no signal of the light one is present. Peptide: ILLAELEQLk(13C(6)15N(2)).

7.2.2. Analysis of changes in proteome, phosphoproteome and transcriptome in response to ionizing radiation

Once we had the protein and RNA samples, we proceeded to analyze them. First, we studied proteome and phosphoproteome of those fibroblasts. In a first try, we obtained 1496 proteins and 3785 phosphopeptides, which means a proteome and phosphoproteome coverage of 7%. Besides, between 27-28% of phosphoproteins were also found in the proteomic results, indicating two main things: 1) coverage of the proteome of reference was not very high and 2) approximately 1/3 of the detected proteins in the phosphoproteomic analysis were also identified in the proteomic one. After an intense data analysis, we concluded that the low coverage was not due to the extraction method, but to the specific features of the sample and the limitations of the spectrometry analysis. That made us carry out a fractionation of the samples of up to 6 times, resulting in a significant improvement of the data. After fractioning, we obtained more than 6000 proteins and phosphopeptides, which implies around 25% of coverage

of the whole proteome. Proteomic data were analyzed to differentiate phosphopeptides with one, two o more than two phosphorylations. From this analysis 4639 different phosphosites were identified, either in mono- or poly-phosphorylated peptides corresponding to 1687 phosphoproteins. Only 3 proteins showed up at both proteomic and phosphoproteomic studies. In addition, transcriptomic analysis by RNA-seq were performed and resulting data were integrated with proteomics and phosphoproteomic ones. As shown in Figure 35 (A and B), 15749 transcripts were detected. From them, 3947 transduce for proteins obtained in proteomic analysis, 293 represent proteins that appear phosphorylated and 1353 proteins, phosphoproteins and ARN sequences emerge in all the three techniques employed.
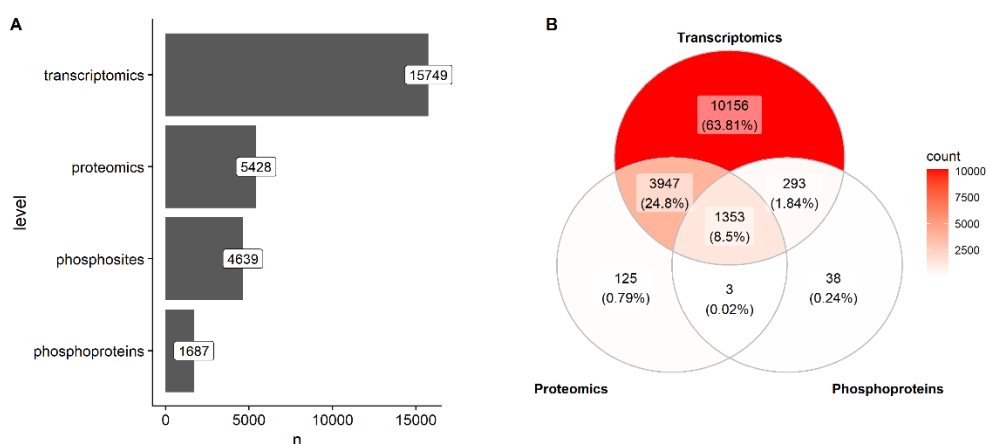
Figure 35. SkinXCare dataset overview. (A) Bar plot representing the number of quantified features per omic level. **(B)** Venn diagram showing the overlap between quantified genes, proteins, and phosphoproteins. Color indicates the number of features in each intersection. Figure authorship: Martín Garrido-Rodriguez Córdoba.

7.2.3. Analysis of proteins and signaling pathways altered in response to ionizing radiation

RNA-seq, proteomic and phosphoproteomic data were then analyzed to evaluate the main up- and down-regulated signaling pathways in response to the different patterns of radiation employed. To this, gene set variation analysis (GSVA) was carried out and results compared to mutil-omic data. The 5 most upregulated and downregulated pathways after either acute or accumulative radiation stimuli are presented in Figure 36. As observed, NOTCH signaling pathway is the most upregulated pathway for both

radiation patterns (Figure 36A and C), especially represented at transcriptomic analysis (Figure 36B and D). Similarly, apoptosis pathway is one of the most upregulated ones under both stimuli (Figure 36A and C), being transcriptomic results the most important dataset to assess this affirmation for acute radiation and proteomic one in the case of accumulative radiation. On the other hand, AMPK signaling pathway, as well as Hippo pathway, are downregulated under both acute and accumulative radiation treatments (Figure 36A and C). Among the pathways that specifically show up under acute radiation we can find cell cycle, sphingolipid signaling pathway and TNF signaling pathway as the most upregulated ones. On the other hand, the most representative pathways among the downregulated ones we can observe Ras, Phospholipase D, mTOR and hippo signaling pathways (Figure 36A). All downregulated pathways are supported by proteomic and phosphoproteomic data (Figure 36B), except hippo pathway which is also represented by transcriptomic data. Regarding accumulative radiation, the most representative upregulated pathways are the same as for acute treatment except for cell cycle pathway, which is not that relevant in response to accumulative radiation and Jak-STAT signaling pathway appears instead (Figure 36C). Despite this, only 2 signaling pathways (Hippo and AMPK) are downregulated at both stimuli, being TGF-beta, cGMP-PKG and Rap1 signaling pathways specifically downregulated after accumulative radiation (Figure 36C). Anyhow, transcriptomic data are the main supporters of these up and downregulations, except for Cell cycle, TNF, or apoptosis pathways modulation, which is especially represented at proteomic levels (Figure 36B and D).
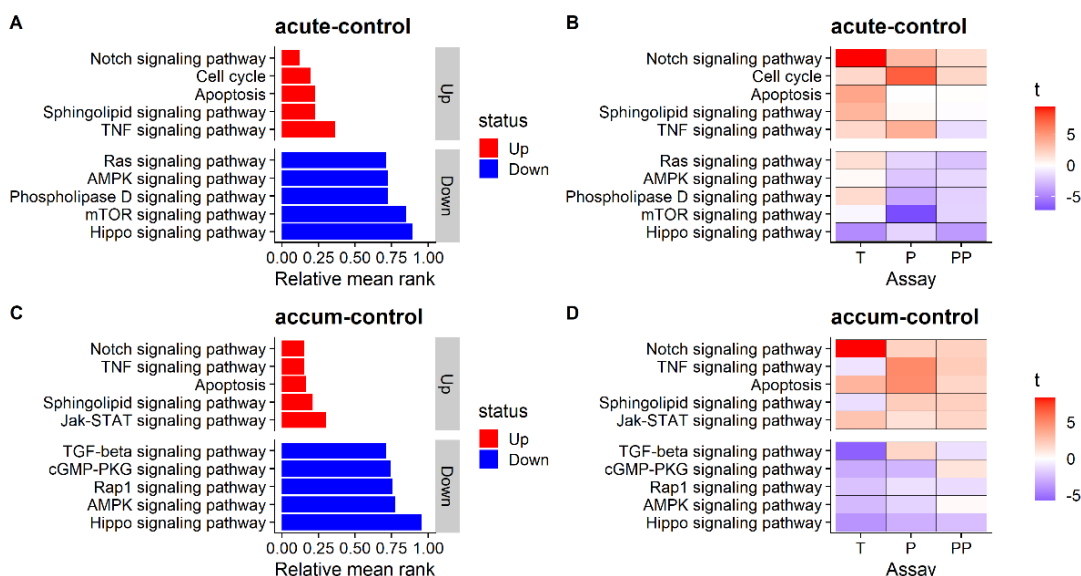
Figure 36. GSVA mean rank multi-omic combination result. Left side plots represent the relative mean rank across the three molecular levels for the top 5 up and down regulated pathways. Right side plots represent the individual limma moderated T values on each molecular level as a heatmap. T: Transcriptomics; P: Proteomics; PP: Phosphoproteins. Subfigures **(A)** and **(B)** depicts the results for the acute radiation vs control comparison and subfigures **(C)** and **(D)** for the accumulative radiation vs control comparison. Figure authorship: Martín Garrido-Rodriguez Córdoba.

Finally, some of altered proteins from the multi-omic analysis were checked by western blot to validate the robustness of the methodology (Figure 37A). A normalization of the increase of decrease of protein compared to control conditions was calculated and expressed from -1 to 1. As shown in Figure 37B, most of the tested proteins agree with the up or down regulated data from proteomic, phosphoproteomic and transcriptomic analysis. In example, under acute and accumulative radiation stimuli, γH2AX is increased in our data, but also in the validation western blot. Same situation occurs with PRKDC. On the other hand, we find down-regulated proteins that decrease in the western blot, like RAP1A or CCN2.

Further analysis should be performed to validate the bioinformatic results and elucidate a map of signaling pathways and axes that are altered in response to ionizing radiation.
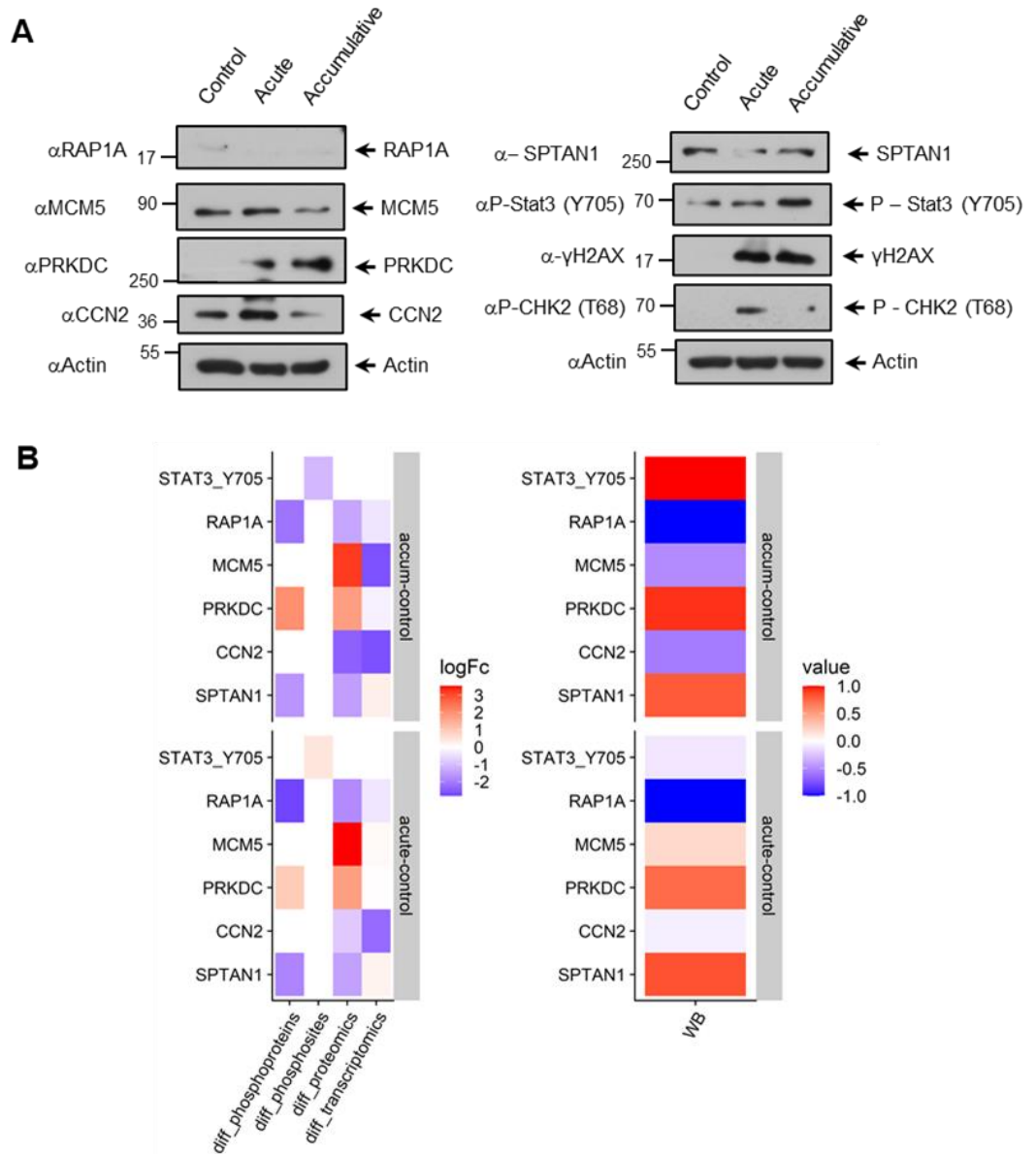
Figure 37. Validation of multi-omic results. Adult human fibroblasts were exposed to either acute or accumulative radiation stimuli emulating the multi-omic experimental conditions. **(A)** Endogenous levels of proteins and phosphoproteins of interest were evaluated by western blot. **(B)** Up and down-regulated proteins compared to control conditions at different omic levels (left panel) were compared to their levels detected by western blot (right panel).

Discussion

8.1. NOTCH1-IC protein is regulated by DYRK2 in a phosphorylation-dependent way

NOTCH1, the most widely studied member of NOTCH receptors family, regulates the expression of key genes in processes such as proliferation, angiogenesis, cell survival and migration (115, 326). In fact, functional studies implicate NOTCH1 in most of the hallmarks of cancer, being associated with its abnormal expression, high mutation rate and poor survival in several cancers such as lung, breast, gastric or lymphoid cancer (139, 172, 176, 311, 327). These data have triggered an interest of the scientific community in finding pharmacologic strategies to inhibit NOTCH1 signaling in tumors (328). Numerous works have described different ways to modulate NOTCH1 signaling activity by regulating its stability or activity by post-translational modifications (ubiquitination and phosphorylation, mainly) (150, 329). From among them, NOTCH1 ubiquitination by FBXW7 E3 ubiquitin ligase is the most relevant (330), requiring a previous phosphorylation of NOTCH1 Thr2512. In this work, we show how DYRK2 can modify NOTCH1 signaling by phosphorylating its Thr2512 residue, thus inducing FBXW7-dependent proteasomal degradation of NOTCH1-IC.

As previously reported in this thesis, NOTCH1 present a PEST domain in its C-terminal region. It has been reported that NOTCH1-IC phosphorylation, and specifically those phosphorylations affecting to the PEST region, are crucial in NOTCH signaling pathway regulation (134). PEST phosphorylation leads to NOTCH1-IC proteasomal degradation, which compromises not only NOTCH1-IC protein levels but also its transcriptional activity. It has been previously described that NOTCH1-IC phosphorylated PEST domain is recognized by FBXW7 E3 ubiquitin ligase, which triggers NOTCH1-IC proteasomal degradation (135, 136, 150, 158-160). Previous research works have reported that some kinases that promote this process like Cyclin C and some CDKs (CDK1, 3, 8 and 19) require previous phosphorylation of residue Thr2512 (135-138). To date, only HIPK2 and MEKK1 (150) have been described to phosphorylate NOTCH1 at Thr-2512, promoting its subsequent proteasomal degradation. In this sense, this thesis shows how DYRK2 also regulates NOTCH1-IC by phosphorylating T2512 residue that leads to NOTCH1-IC proteasomal degradation. In this regard, it is particularly relevant to highlight the evolutionary closeness between DYRK2 and HIPK2, since they belong to the same kinase family (DYRK family, in CMGC group) (3). Besides, the two of them are

regulated by MDM2 (31, 331) and SIAH2 (41, 332) ubiquitin ligases. Also, both are triggered by the same stimuli, including DNA damage that promotes p53 Ser46 phosphorylation by both DYRK2 and HIPK2, leading to apoptosis (61, 333).

Our data suggest that NOTCH1-IC modulation is also common for both DYRK2 and HIPK2 kinase (150), although the DYRK2 effect described in this work is HIPK2 independent. Anyhow, NOTCH1-IC regulation by DYRK2 and HIPK2 in response to DNA damage may represent ¡a contingence mechanism to ensure ¡a proper decrease of NOTCH1-IC levels in this situation. Further studies should be accomplished to clear out the relationship between these two signaling pathways. In the same way, it would be interesting to study NOTCH1-IC affection after other DYRK2 triggering stimuli such as hypoxia (41), β-adrenergic stimulation (334); serum starvation (69) or heat shock (66), among others. Besides, here we also show NOTCH1-IC and DYRK2 colocalization in the nucleus after DNA damage, as well as their interaction. Data suggest that NOTCH1-IC RAM region plays an essential role for NOTCH1-IC-DYRK2 interaction. Is has been previously demonstrated that this RAM domain is critical for NOTCH1-IC interaction with CSL, allowing the transcription activity of the complex over target genes like MAML1 (335, 336). Further works should be accomplished to elucidate the potential role of this interaction downstream NOTCH1-IC signaling.

Some previous works have demonstrated that a disturbed NOTCH1 signaling is related to several lung diseases pathogenesis, like lung cancer (337) and lung lesions (64). Additionally, NOTCH signaling role in breast and prostate cancer has been demonstrated (328, 338, 339), as well as NOTCH1-IC overexpression in leukemia (178). Despite this, DYRK2 role in carcinogenesis is not that clear and there exists controversy about its potential protumoral or antitumoral functions, although several works have demonstrated that DYRK2 downregulation is related to breast, prostate, colon, or lung tumors, as well as poor prognosis (68-70, 76, 82, 340, 341). Data showing a correlation in both DYRK2 and NOTCH1 protein levels in tumor tissues (Figure 21A) concur to our data supporting our idea that NOTCH1-IC degradation by DYRK2 could be relevant in cancer patients. Besides, our results demonstrate that NOTCH1-IC Thr2512 phosphorylation by DYRK2 is key for NOTCH1-IC regulation. Therefore, our results might clear up previous studies focused on the importance of Thr2512 mutation in cancers such as human T cell acute lymphoblastic leukemia (T-ALL) (342).

Regarding one of the major problems in cancer treatment, chemotherapy resistance, it is critical to understand the molecular mechanisms that take place in the DNA damage response (DDR). In fact, several works have reported that resistance to cisplatin of lung and liver tumorous cells is related to NOTCH1-IC overexpression (303, 343). In example, cisplatin-induced NOTCH1-IC expression occurs in a dose-dependent way in cervical cancer cells (30). Besides, Adamowicz and collaborators demonstrated in 2016 that, after ionizing radiation treatment, NOTCH1 has a negative regulatory role in DNA damage response (344). Despite this evidence, some types of tumors like skin cancer, hepatocellular carcinoma, or small cell lung cancer (SCLC), there exist contradictory data suggesting that NOTCH1 might play an anti-proliferative role rather than a pro-tumoral one (345). Here in this work, we procure new insights into the NOTCH1 signaling pathway response to DNA damage exposure, considering that the employment of different chemotherapeutic agents seems to promote DYRK2 driven NOTCH1-IC inhibition in different cell lines.

In summary, there results demonstrate that DYRK2 phosphorylate NOTCH1-IC regulating its stability and therefore affecting its transcriptional activity. Besides, DYRK2 increase under DNA damage conditions empathize NOTCH1-IC phosphorylation and promotes its proteasomal degradation by FBXW7 dependent ubiquitination (Figure 38). Therefore, we propose that this new molecular mechanism induced by DNA damage might have an influence on cancer cells behavior. Nevertheless, further studies must be accomplished to completely understand the implications of this process in tumors overexpressing NOTCH1-IC.
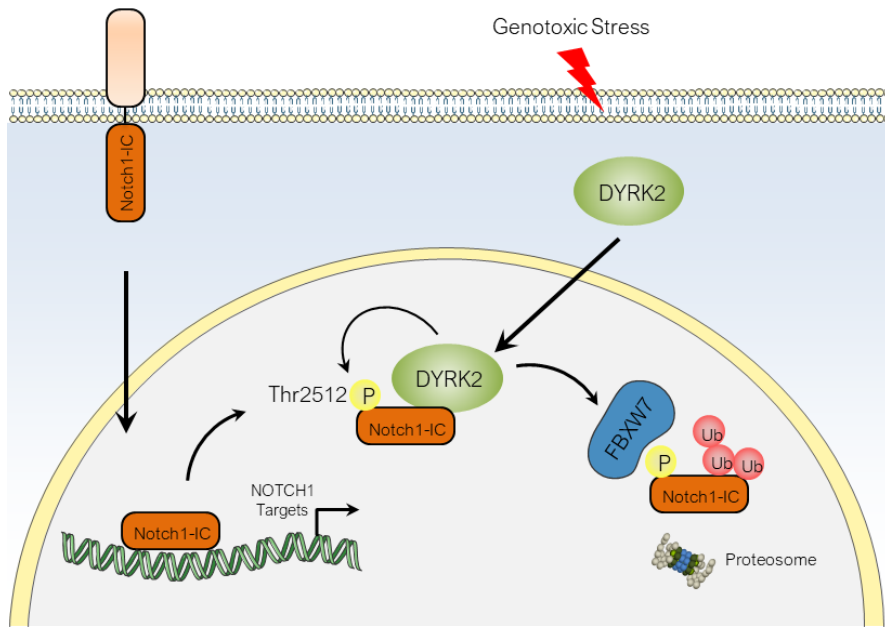
Figure 38. Schematic model for the modulation of NOTCH1-IC by DYRK2 action. Under genotoxic stress situations, DYRK2 phosphorylates NOTCH1-IC Thr2512, inducing NOTCH1-IC recognition by FBXW7 and thus promoting its ubiquitination-dependent proteasome degradation.

8.2. Modulation of signaling pathways in response to X ray in human dermal fibroblasts

This work attempts to obtain an overview of cellular circuits that are involved in ionizing radiation triggered DNA damage response. These data pretend to represent a realistic view of fibroblasts' molecular response to two different radiation patterns. To allow this, we employed RNA-seq techniques for assess transcriptional changes and proteomic analysis such as SILAC labelling coupled to LC-MS/MS to detect alterations at proteomic and phosphoproteomic levels. The main aim of this project is that profiling these molecular levels (transcriptomic, proteomic and phosphoproteomic) would permit to get the whole picture of most of the signaling events that happens in fibroblasts in response to ionizing radiation. There exist some factors that interfere in a perfect congruence among gene expression, protein levels, and post-translational modifications that encompass cellular signaling. Despite them, we have tried to infer altered signaling circuits in response to radiation by employing a variety of techniques and the available

omic profiles. These methods sum up RNAs levels, proteins and phosphosites at both a basal (non-radiated cells) or two different perturbed conditions (differently radiated cells). To our knowledge, this is the first work that compare these 3 different functional approaches to this aim, that clearly differ both in the way prior knowledge and omic data are used.

Regarding the results we obtained, we can evaluate if the most importantly altered pathways for each model are consistent with previous works. In this sense, we would expect to observe mainly pathways that are traditionally related to DNA damage response after ionizing radiation (346). On the one hand, we found that NOTCH signaling pathway was the top up-regulated pathway in response to both acute and accumulative radiation treatments. According to this, Oh and collaborators demonstrated using animal models that NOTCH signaling is up-regulated under radiation conditions (both acute and accumulative patterns) in tumor-associated macrophages {Oh, 2016}. Besides, Giuranno et al. described that NOTCH signaling also induces cell survival in response to X-ray, analyzing basal airway stem cells (347). Another signaling pathway that appeared upregulated in response to both acute and accumulative radiation treatments is "Apoptosis signaling pathway", represented, among others by Fodrin protein. Regarding this, it is worth to mention that Fodrin proteolysis has been described as a critical step in apoptosis following ionizing radiation (348).

On the other hand, the most down-regulated pathway under both radiation schemes was the Hippo signaling pathway. CTGF (connective tissue growth factor), a key effector of Hippo pathway, has been reported to be down-regulated in response to ionizing radiation by miRNA-26 action (349). Besides, it has been described in two different publications that one of the key proteins in this pathway, YAP1, is crucial in the activation of proapoptotic genes in response to DNA damage (350, 351). Therefore, Hippo pathway down-regulation could be a clue of the lack of proapoptotic mechanisms activation in fibroblasts. Another down-regulated signaling pathway under both acute and accumulative doses of radiation is the AMPK signaling pathway, being PPAR-GC1A (a PPARG cofactor) the top up-regulated circuit in response to the acute dose of radiation. In fact, it has been reported a protective role of PPAR-GC1A against DNA damage and telomere malfunction in different studies (352, 353).

We also discovered different up- and down-regulated circuits specifically upregulated in response to either the acute or accumulative radiation stimulus, demonstrating a higher "stimulus-specificity" of the method. Among them the Jak-stat signaling pathway is up-regulated after accumulative treatment, being CDKN1A (p21) its top up-regulated component. CDKN1A has been described as a modulator of cell cycle, apoptosis, and gene transcription in response to DNA damage (354). This upregulation suggests a more prominent cell cycle arrest in response to the accumulation to the radiation doses. Additionally, Jak-stat signaling pathway has been related to breast cancer radioresistance, which would agree with its up-regulation after recurrent doses of irradiation (37).

Further validations of the results should be carried out to achieve a solid data compilation that permits a deeper understanding of the pathways that take place in response to ionizing radiation. This will provide new therapeutic opportunities for radiodermatitis prevention and treatment.

Conclusions

1. It exists a direct physical interaction between DYRK2 and NOTCH1 being several domains responsible for binding in both proteins. This interaction, as well as their co-localization, is enhanced by DNA damage.

2. DYRK2 negatively regulates NOTCH1 expression through ubiquitin/proteasome and DYRK2 kinase activity dependent process, affecting its half-life.

3. DYRK2 directly phosphorylates NOTCH1 at least at residue Thr2512, triggering its recognition by FBXW7 and subsequent ubiquitination.

4. DYRK2-dependent phosphorylation reduces NOTCH1 transcriptional activity.

5. DYRK2 is the most effective in degrading NOTCH1 among the members of its subfamily, and its activity is HIPK2 independent.

6. DYRK2 directly phosphorylates NOTCH1-IC *in vitro.* Data suggest that RAM region of NOTCH1-IC plays an essential role for NOTCH1-IC-DYRK2 interaction.

7. Different DNA damage stimuli result in an inverse correlation of DYRK2 and NOTCH1 expression, which is also reported at endogenous levels in human lung cancer cell lines and human lung cancer tissues.

8. There is an apparent poor agreement between the changes happening at transcriptomic, proteomic and phosphoproteomic levels for irradiated fibroblasts.

References

1.   Becker W, Weber Y, Wetzel K, Eirmbter K, Tejedor FJ, Joost HG. Sequence characteristics, subcellular localization, and substrate specificity of DYRK-related kinases, a novel family of dual specificity protein kinases. J Biol Chem. 1998;273(40):25893-902.

2.   Soppa U, Becker W. DYRK protein kinases. Curr Biol. 2015;25(12):R488-9.

3.   Aranda S, Laguna A, de la Luna S. DYRK family of protein kinases: evolutionary relationships, biochemical properties, and functional roles. FASEB J. 2011;25(2):449-62.

4.   Lindberg MF, Meijer L. Dual-Specificity, Tyrosine Phosphorylation-Regulated Kinases (DYRKs) and cdc2-Like Kinases (CLKs) in Human Disease, an Overview. Int J Mol Sci. 2021;22(11).

5.   Ryoo SR, Jeong HK, Radnaabazar C, Yoo JJ, Cho HJ, Lee HW, et al. DYRK1A-mediated hyperphosphorylation of Tau. A functional link between Down syndrome and Alzheimer disease. J Biol Chem. 2007;282(48):34850-7.

6.   Ackeifi C, Swartz E, Kumar K, Liu H, Chalada S, Karakose E, et al. Pharmacologic and genetic approaches define human pancreatic beta cell mitogenic targets of DYRK1A inhibitors. JCI Insight. 2020;5(1).

7.   Kumar K, Suebsuwong C, Wang P, Garcia-Ocana A, Stewart AF, DeVita RJ. DYRK1A Inhibitors as Potential Therapeutics for beta-Cell Regeneration for Diabetes. J Med Chem. 2021;64(6):2901-22.

8.   Nalls MA, Blauwendraat C, Vallerga CL, Heilbron K, Bandres-Ciga S, Chang D, et al. Identification of novel risk loci, causal insights, and heritable risk for Parkinson's disease: a meta-analysis of genome-wide association studies. Lancet Neurol. 2019;18(12):1091-102.

9.   Gwack Y, Sharma S, Nardone J, Tanasa B, Iuga A, Srikanth S, et al. A genome-wide Drosophila RNAi screen identifies DYRK-family kinases as regulators of NFAT. Nature. 2006;441(7093):646-50.

10. Woods YL, Cohen P, Becker W, Jakes R, Goedert M, Wang X, et al. The kinase DYRK phosphorylates protein-synthesis initiation factor eIF2Bepsilon at Ser539 and the microtubule-associated protein tau at Thr212: potential role for DYRK as a glycogen synthase kinase 3-priming kinase. Biochem J. 2001;355(Pt 3):609-15.

11. Matsuo R, Ochiai W, Nakashima K, Taga T. A new expression cloning strategy for isolation of substrate-specific kinases by using phosphorylation site-specific antibody. J Immunol Methods. 2001;247(1-2):141-51.

12. Lee HK, Barbarosie M, Kameyama K, Bear MF, Huganir RL. Regulation of distinct AMPA receptor phosphorylation sites during bidirectional synaptic plasticity. Nature. 2000;405(6789):955-9.

13. Mercer SE, Ewton DZ, Deng X, Lim S, Mazur TR, Friedman E. Mirk/Dyrk1B mediates survival during the differentiation of C2C12 myoblasts. J Biol Chem. 2005;280(27):25788-801.

14. Mercer SE, Friedman E. Mirk/Dyrk1B: a multifunctional dual-specificity kinase involved in growth arrest, differentiation, and cell survival. Cell Biochem Biophys. 2006;45(3):303-15.

15. Abu Jhaisha S, Widowati EW, Kii I, Sonamoto R, Knapp S, Papadopoulos C, et al. DYRK1B mutations associated with metabolic syndrome impair the chaperone-dependent maturation of the kinase domain. Sci Rep. 2017;7(1):6420.

16. Geiger SM, Abrahams-Sandi E, Soboslay PT, Hoffmann WH, Pfaff AW, Graeff-Teixeira C, et al. Cellular immune responses and cytokine production in BALB/c and C57BL/6 mice during the acute phase of Angiostrongylus costaricensis infection. Acta Trop. 2001;80(1):59-68.

17. Guo X, Williams JG, Schug TT, Li X. DYRK1A and DYRK3 promote cell survival through phosphorylation and activation of SIRT1. J Biol Chem. 2010;285(17):13223-32.

18.   Sacher F, Moller C, Bone W, Gottwald U, Fritsch M. The expression of the testis-specific Dyrk4 kinase is highly restricted to step 8 spermatids but is not required for male fertility in mice. Mol Cell Endocrinol. 2007;267(1-2):80-8.

19.   Soundararajan M, Roos AK, Savitsky P, Filippakopoulos P, Kettenbach AN, Olsen JV, et al. Structures of Down syndrome kinases, DYRKs, reveal mechanisms of kinase activation and substrate recognition. Structure. 2013;21(6):986-96.

20.   Lochhead PA, Sibbet G, Kinstrie R, Cleghon T, Rylatt M, Morrison DK, et al. dDYRK2: a novel dual-specificity tyrosine-phosphorylation-regulated kinase in Drosophila. Biochem J. 2003;374(Pt 2):381-91.

21.   Houlgatte R, Mariage-Samson R, Duprat S, Tessier A, Bentolila S, Lamy B, et al. The Genexpress Index: a resource for gene discovery and the genic map of the human genome. Genome Res. 1995;5(3):272-304.

22.   Hossain D, Javadi Esfehani Y, Das A, Tsang WY. Cep78 controls centrosome homeostasis by inhibiting EDD-DYRK2-DDB1(Vpr)(BP). EMBO Rep. 2017;18(4):632-44.

23.   Correa-Saez A, Jimenez-Izquierdo R, Garrido-Rodriguez M, Morrugares R, Munoz E, Calzado MA. Updating dual-specificity tyrosine-phosphorylation-regulated kinase 2 (DYRK2): molecular basis, functions and role in diseases. Cell Mol Life Sci. 2020;77(23):4747-63.

24.   Park CS, Lewis AH, Chen TJ, Bridges CS, Shen Y, Suppipat K, et al. A KLF4-DYRK2-mediated pathway regulating self-renewal in CML stem cells. Blood. 2019;134(22):1960-72.

25.   Kumamoto T, Yamada K, Yoshida S, Aoki K, Hirooka S, Eto K, et al. Impairment of DYRK2 by DNMT1mediated transcription augments carcinogenesis in human colorectal cancer. Int J Oncol. 2020;56(6):1529-39.

26.   Wang J, Jia Z, Zhang C, Sun M, Wang W, Chen P, et al. miR-499 protects cardiomyocytes from H_2O_2-induced apoptosis via its effects on Pdcd4 and Pacs2. RNA Biol. 2014;11(4):339-50.

27.   Wang Y, Sun J, Wei X, Luan L, Zeng X, Wang C, et al. Decrease of miR-622 expression suppresses migration and invasion by targeting regulation of DYRK2 in colorectal cancer cells. Onco Targets Ther. 2017;10:1091-100.

28.   Yang J, Yu X, Xue F, Li Y, Liu W, Zhang S. Exosomes derived from cardiomyocytes promote cardiac fibrosis via myocyte-fibroblast cross-talk. Am J Transl Res. 2018;10(12):4350-66.

29.   Haenisch S, von Ruden EL, Wahmkow H, Rettenbeck ML, Michler C, Russmann V, et al. miRNA-187-3p-Mediated Regulation of the KCNK10/TREK-2 Potassium Channel in a Rat Epilepsy Model. ACS Chem Neurosci. 2016;7(11):1585-94.

30.   Banerjee S, Wei T, Wang J, Lee JJ, Gutierrez HL, Chapman O, et al. Inhibition of dual-specificity tyrosine phosphorylation-regulated kinase 2 perturbs 26S proteasome-addicted neoplastic progression. Proc Natl Acad Sci U S A. 2019;116(49):24881-91.

31.   Taira N, Yamamoto H, Yamaguchi T, Miki Y, Yoshida K. ATM augments nuclear stabilization of DYRK2 by inhibiting MDM2 in the apoptotic response to DNA damage. J Biol Chem. 2010;285(7):4909-19.

32.   Kinstrie R, Luebbering N, Miranda-Saavedra D, Sibbet G, Han J, Lochhead PA, et al. Characterization of a domain that transiently converts class 2 DYRKs into intramolecular tyrosine kinases. Sci Signal. 2010;3(111):ra16.

33.   Bai X, He T, Liu Y, Zhang J, Li X, Shi J, et al. Acetylation-Dependent Regulation of Notch Signaling in Macrophages by SIRT1 Affects Sepsis Development. Front Immunol. 2018;9:762.

34.   Nolen B, Taylor S, Ghosh G. Regulation of protein kinases; controlling activity through activation segment conformation. Mol Cell. 2004;15(5):661-75.

35.   Han J, Miranda-Saavedra D, Luebbering N, Singh A, Sibbet G, Ferguson MA, et al. Deep evolutionary conservation of an intramolecular protein kinase activation mechanism. PLoS One. 2012;7(1):e29702.

36.   Ashford AL, Dunkley TP, Cockerill M, Rowlinson RA, Baak LM, Gallo R, et al. Identification of DYRK1B as a substrate of ERK1/2 and characterisation of the kinase activity of DYRK1B mutants from cancer and metabolic syndrome. Cell Mol Life Sci. 2016;73(4):883-900.

37.   Lu L, Dong J, Wang L, Xia Q, Zhang D, Kim H, et al. Activation of STAT3 and Bcl-2 and reduction of reactive oxygen species (ROS) promote radioresistance in breast cancer and overcome of radioresistance with niclosamide. Oncogene. 2018;37(39):5292-304.

38.   Kaczmarski W, Barua M, Mazur-Kolecka B, Frackowiak J, Dowjat W, Mehta P, et al. Intracellular distribution of differentially phosphorylated dual-specificity tyrosine phosphorylation-regulated kinase 1A (DYRK1A). J Neurosci Res. 2014;92(2):162-73.

39.   Alvarez M, Altafaj X, Aranda S, de la Luna S. DYRK1A autophosphorylation on serine residue 520 modulates its kinase activity via 14-3-3 binding. Mol Biol Cell. 2007;18(4):1167-78.

40.   Lara-Chica M, Correa-Saez A, Jimenez-Izquierdo R, Garrido-Rodriguez M, Ponce FJ, Moreno R, et al. A novel CDC25A/DYRK2 regulatory switch modulates cell cycle and survival. Cell Death Differ. 2022;29(1):105-17.

41.   Perez M, Garcia-Limones C, Zapico I, Marina A, Schmitz ML, Munoz E, et al. Mutual regulation between SIAH2 and DYRK2 controls hypoxic and genotoxic signaling pathways. J Mol Cell Biol. 2012;4(5):316-30.

42.   Varjosalo M, Bjorklund M, Cheng F, Syvanen H, Kivioja T, Kilpinen S, et al. Application of active and kinase-deficient kinome collection for identification of kinases regulating hedgehog signaling. Cell. 2008;133(3):537-48.

43.   Xu L, Sun Y, Li M, Ge X. Dyrk2 mediated the release of proinflammatory cytokines in LPS-induced BV2 cells. Int J Biol Macromol. 2018;109:1115-24.

44.   Campbell LE, Proud CG. Differing substrate specificities of members of the DYRK family of arginine-directed protein kinases. FEBS Lett. 2002;510(1-2):31-6.

45.   Singh R, Lauth M. Emerging Roles of DYRK Kinases in Embryogenesis and Hedgehog Pathway Control. J Dev Biol. 2017;5(4).

46.   Mimoto R, Taira N, Takahashi H, Yamaguchi T, Okabe M, Uchida K, et al. DYRK2 controls the epithelial-mesenchymal transition in breast cancer by degrading Snail. Cancer Lett. 2013;339(2):214-25.

47.   Taira N, Mimoto R, Kurata M, Yamaguchi T, Kitagawa M, Miki Y, et al. DYRK2 priming phosphorylation of c-Jun and c-Myc modulates cell cycle progression in human cancer cells. J Clin Invest. 2012;122(3):859-72.

48.   Nishi Y, Lin R. DYRK2 and GSK-3 phosphorylate and promote the timely degradation of OMA-1, a key regulator of the oocyte-to-embryo transition in C. elegans. Dev Biol. 2005;288(1):139-49.

49.   Cole AR, Causeret F, Yadirgi G, Hastie CJ, McLauchlan H, McManus EJ, et al. Distinct priming kinases contribute to differential regulation of collapsin response mediator proteins by glycogen synthase kinase-3 in vivo. J Biol Chem. 2006;281(24):16591-8.

50.   Tanaka H, Morimura R, Ohshima T. Dpysl2 (CRMP2) and Dpysl3 (CRMP4) phosphorylation by Cdk5 and DYRK2 is required for proper positioning of Rohon-Beard neurons and neural crest cells during neurulation in zebrafish. Dev Biol. 2012;370(2):223-36.

51.   Doble BW, Woodgett JR. GSK-3: tricks of the trade for a multi-tasking kinase. J Cell Sci. 2003;116(Pt 7):1175-86.

52.   Thomas GM, Frame S, Goedert M, Nathke I, Polakis P, Cohen P. A GSK3-binding peptide from FRAT1 selectively inhibits the GSK3-catalysed phosphorylation of axin and beta-catenin. FEBS Lett. 1999;458(2):247-51.

53.   Beurel E, Grieco SF, Jope RS. Glycogen synthase kinase-3 (GSK3): regulation, actions, and diseases. Pharmacol Ther. 2015;148:114-31.

54.   Jope RS, Johnson GV. The glamour and gloom of glycogen synthase kinase-3. Trends Biochem Sci. 2004;29(2):95-102.

55.   Maddika S, Chen J. Protein kinase DYRK2 is a scaffold that facilitates assembly of an E3 ligase. Nat Cell Biol. 2009;11(4):409-19.

56.   Jung HY, Wang X, Jun S, Park JI. Dyrk2-associated EDD-DDB1-VprBP E3 ligase inhibits telomerase by TERT degradation. J Biol Chem. 2013;288(10):7252-62.

57.   Himpel S, Tegge W, Frank R, Leder S, Joost HG, Becker W. Specificity determinants of substrate recognition by the protein kinase DYRK1A. J Biol Chem. 2000;275(4):2431-8.

58.   Wang X, Li W, Parra JL, Beugnet A, Proud CG. The C terminus of initiation factor 4E-binding protein 1 contains multiple regulatory features that influence its function and phosphorylation. Mol Cell Biol. 2003;23(5):1546-57.

59.   Skurat AV, Dietrich AD. Phosphorylation of Ser640 in muscle glycogen synthase by DYRK family protein kinases. J Biol Chem. 2004;279(4):2490-8.

60.   Auld GC, Campbell DG, Morrice N, Cohen P. Identification of calcium-regulated heat-stable protein of 24 kDa (CRHSP24) as a physiological substrate for PKB and RSK using KESTREL. Biochem J. 2005;389(Pt 3):775-83.

61.   Taira N, Nihira K, Yamaguchi T, Miki Y, Yoshida K. DYRK2 is targeted to the nucleus and controls p53 via Ser46 phosphorylation in the apoptotic response to DNA damage. Mol Cell. 2007;25(5):725-38.

62.   Slepak TI, Salay LD, Lemmon VP, Bixby JL. Dyrk kinases regulate phosphorylation of doublecortin, cytoskeletal organization, and neuronal morphology. Cytoskeleton (Hoboken). 2012;69(7):514-27.

63.   An T, Li S, Pan W, Tien P, Zhong B, Shu HB, et al. DYRK2 Negatively Regulates Type I Interferon Induction by Promoting TBK1 Degradation via Ser527 Phosphorylation. PLoS Pathog. 2015;11(9):e1005179.

64.   Guo X, Wang X, Wang Z, Banerjee S, Yang J, Huang L, et al. Site-specific proteasome phosphorylation controls cell proliferation and tumorigenesis. Nat Cell Biol. 2016;18(2):202-12.

65.   Woo Y, Kim SJ, Suh BK, Kwak Y, Jung HJ, Nhung TTM, et al. Sequential phosphorylation of NDEL1 by the DYRK2-GSK3beta complex is critical for neuronal morphogenesis. Elife. 2019;8.

66.   Moreno R, Banerjee S, Jackson AW, Quinn J, Baillie G, Dixon JE, et al. The stress-responsive kinase DYRK2 activates heat shock factor 1 promoting resistance to proteotoxic stress. Cell Death Differ. 2021;28(5):1563-78.

67.   Yamamoto T, Taira Nihira N, Yogosawa S, Aoki K, Takeda H, Sawasaki T, et al. Interaction between RNF8 and DYRK2 is required for the recruitment of DNA repair molecules to DNA double-strand breaks. FEBS Lett. 2017;591(6):842-53.

68.   Yan H, Hu K, Wu W, Li Y, Tian H, Chu Z, et al. Low Expression of DYRK2 (Dual Specificity Tyrosine Phosphorylation Regulated Kinase 2) Correlates with Poor Prognosis in Colorectal Cancer. PLoS One. 2016;11(8):e0159954.

69.   Zhang X, Xu P, Ni W, Fan H, Xu J, Chen Y, et al. Downregulated DYRK2 expression is associated with poor prognosis and Oxaliplatin resistance in hepatocellular carcinoma. Pathol Res Pract. 2016;212(3):162-70.

70.   Ito D, Yogosawa S, Mimoto R, Hirooka S, Horiuchi T, Eto K, et al. Dual-specificity tyrosine-regulated kinase 2 is a suppressor and potential prognostic marker for liver metastasis of colorectal cancer. Cancer Sci. 2017;108(8):1565-73.

71.   Yamashita S, Chujo M, Moroga T, Anami K, Tokuishi K, Miyawaki M, et al. DYRK2 expression may be a predictive marker for chemotherapy in non-small cell lung cancer. Anticancer Res. 2009;29(7):2753-7.

72.   Yamashita S, Chujo M, Tokuishi K, Anami K, Miyawaki M, Yamamoto S, et al. Expression of dual-specificity tyrosine-(Y)-phosphorylation-regulated kinase 2 (DYRK2) can be a favorable prognostic marker in pulmonary adenocarcinoma. J Thorac Cardiovasc Surg. 2009;138(6):1303-8.

73.   Nomura S, Suzuki Y, Takahashi R, Terasaki M, Kimata R, Terasaki Y, et al. Dual-specificity tyrosine phosphorylation-regulated kinase 2 (DYRK2) as a novel

marker in T1 high-grade and T2 bladder cancer patients receiving neoadjuvant chemotherapy. BMC Urol. 2015;15:53.

74.   Wang Y, Wu Y, Miao X, Zhu X, Miao X, He Y, et al. Silencing of DYRK2 increases cell proliferation but reverses CAM-DR in Non-Hodgkin's Lymphoma. Int J Biol Macromol. 2015;81:809-17.

75.   Uhl KL, Schultz CR, Geerts D, Bachmann AS. Harmine, a dual-specificity tyrosine phosphorylation-regulated kinase (DYRK) inhibitor induces caspase-mediated apoptosis in neuroblastoma. Cancer Cell Int. 2018;18:82.

76.   Enomoto Y, Yamashita S, Yoshinaga Y, Fukami Y, Miyahara S, Nabeshima K, et al. Downregulation of DYRK2 can be a predictor of recurrence in early stage breast cancer. Tumour Biol. 2014;35(11):11021-5.

77.   Banerjee S, Ji C, Mayfield JE, Goel A, Xiao J, Dixon JE, et al. Ancient drug curcumin impedes 26S proteasome activity by direct inhibition of dual-specificity tyrosine-regulated kinase 2. Proc Natl Acad Sci U S A. 2018;115(32):8155-60.

78.   Zhou W, Lv R, Qi W, Wu D, Xu Y, Liu W, et al. Snail contributes to the maintenance of stem cell-like phenotype cells in human pancreatic cancer. PLoS One. 2014;9(1):e87409.

79.   Ryu KJ, Park SM, Park SH, Kim IK, Han H, Kim HJ, et al. p38 Stabilizes Snail by Suppressing DYRK2-Mediated Phosphorylation That Is Required for GSK3beta-betaTrCP-Induced Snail Degradation. Cancer Res. 2019;79(16):4135-48.

80.   Shen Y, Zhang L, Wang D, Bao Y, Liu C, Xu Z, et al. Regulation of Glioma Cells Migration by DYRK2. Neurochem Res. 2017;42(11):3093-102.

81.   Mrugala MM. Advances and challenges in the treatment of glioblastoma: a clinician's perspective. Discov Med. 2013;15(83):221-30.

82.   Imawari Y, Mimoto R, Hirooka S, Morikawa T, Takeyama H, Yoshida K. Downregulation of dual-specificity tyrosine-regulated kinase 2 promotes tumor cell proliferation and invasion by enhancing cyclin-dependent kinase 14 expression in breast cancer. Cancer Sci. 2018;109(2):363-72.

83.   Tandon V, de la Vega L, Banerjee S. Emerging roles of DYRK2 in cancer. J Biol Chem. 2021;296:100233.

84.   Gockler N, Jofre G, Papadopoulos C, Soppa U, Tejedor FJ, Becker W. Harmine specifically inhibits protein kinase DYRK1A and interferes with neurite formation. FEBS J. 2009;276(21):6324-37.

85.   Ogawa Y, Nonaka Y, Goto T, Ohnishi E, Hiramatsu T, Kii I, et al. Development of a novel selective inhibitor of the Down syndrome-related kinase Dyrk1A. Nat Commun. 2010;1:86.

86.   Matthay KK, Maris JM, Schleiermacher G, Nakagawara A, Mackall CL, Diller L, et al. Neuroblastoma. Nat Rev Dis Primers. 2016;2:16078.

87.   Nelson KM, Dahlin JL, Bisson J, Graham J, Pauli GF, Walters MA. The Essential Medicinal Chemistry of Curcumin. J Med Chem. 2017;60(5):1620-37.

88.   Cuny GD, Robin M, Ulyanova NP, Patnaik D, Pique V, Casano G, et al. Structure-activity relationship study of acridine analogs as haspin and DYRK2 kinase inhibitors. Bioorg Med Chem Lett. 2010;20(12):3491-4.

89.   Cuny GD, Ulyanova NP, Patnaik D, Liu JF, Lin X, Auerbach K, et al. Structure-activity relationship study of beta-carboline derivatives as haspin kinase inhibitors. Bioorg Med Chem Lett. 2012;22(5):2015-9.

90.   Morgan THJTAN. The theory of the gene. 1917;51(609):513-44.

91.   Artavanis-Tsakonas S, Rand MD, Lake RJ. Notch signaling: cell fate control and signal integration in development. Science. 1999;284(5415):770-6.

92.   Kovall RA, Gebelein B, Sprinzak D, Kopan R. The Canonical Notch Signaling Pathway: Structural and Biochemical Insights into Shape, Sugar, and Force. Dev Cell. 2017;41(3):228-41.

93.   Weinmaster G, Fischer JA. Notch ligand ubiquitylation: what is it good for? Dev Cell. 2011;21(1):134-44.

94.   D'Souza B, Miyamoto A, Weinmaster G. The many facets of Notch ligands. Oncogene. 2008;27(38):5148-67.

95.   Sanchez-Irizarry C, Carpenter AC, Weng AP, Pear WS, Aster JC, Blacklow SC. Notch subunit heterodimerization and prevention of ligand-independent proteolytic activation depend, respectively, on a novel domain and the LNR repeats. Mol Cell Biol. 2004;24(21):9265-73.

96.   Gordon WR, Vardar-Ulu D, L'Heureux S, Ashworth T, Malecki MJ, Sanchez-Irizarry C, et al. Effects of S1 cleavage on the structure, surface export, and signaling activity of human Notch1 and Notch2. PLoS One. 2009;4(8):e6613.

97.   Borggrefe T, Oswald F. The Notch signaling pathway: transcriptional regulation at Notch target genes. Cell Mol Life Sci. 2009;66(10):1631-46.

98.   Rogers S, Wells R, Rechsteiner M. Amino acid sequences common to rapidly degraded proteins: the PEST hypothesis. Science. 1986;234(4774):364-8.

99.   Gordon WR, Vardar-Ulu D, Histen G, Sanchez-Irizarry C, Aster JC, Blacklow SC. Structural basis for autoinhibition of Notch. Nat Struct Mol Biol. 2007;14(4):295-300.

100.   Lu P, Bai XC, Ma D, Xie T, Yan C, Sun L, et al. Three-dimensional structure of human gamma-secretase. Nature. 2014;512(7513):166-70.

101.   Steiner H, Fluhrer R, Haass C. Intramembrane proteolysis by gamma-secretase. J Biol Chem. 2008;283(44):29627-31.

102.   Logeat F, Bessia C, Brou C, LeBail O, Jarriault S, Seidah NG, et al. The Notch1 receptor is cleaved constitutively by a furin-like convertase. Proc Natl Acad Sci U S A. 1998;95(14):8108-12.

103.   Lieber T, Kidd S, Young MW. kuzbanian-mediated cleavage of Drosophila Notch. Genes Dev. 2002;16(2):209-21.

104. Chillakuri CR, Sheppard D, Lea SM, Handford PA. Notch receptor-ligand binding and activation: insights from molecular studies. Semin Cell Dev Biol. 2012;23(4):421-8.

105. Mumm JS, Kopan R. Notch signaling: from the outside in. Dev Biol. 2000;228(2):151-65.

106. Schroeter EH, Kisslinger JA, Kopan R. Notch-1 signalling requires ligand-induced proteolytic release of intracellular domain. Nature. 1998;393(6683):382-6.

107. Conner SD. Regulation of Notch Signaling Through Intracellular Transport. Int Rev Cell Mol Biol. 2016;323:107-27.

108. Krejci A, Bray S. Notch activation stimulates transient and selective binding of Su(H)/CSL to target enhancers. Genes Dev. 2007;21(11):1322-7.

109. Polacheck WJ, Kutys ML, Yang J, Eyckmans J, Wu Y, Vasavada H, et al. A non-canonical Notch complex regulates adherens junctions and vascular barrier function. Nature. 2017;552(7684):258-62.

110. Oswald F, Winkler M, Cao Y, Astrahantseff K, Bourteele S, Knochel W, et al. RBP-Jkappa/SHARP recruits CtIP/CtBP corepressors to silence Notch target genes. Mol Cell Biol. 2005;25(23):10379-90.

111. McElhinny AS, Li JL, Wu L. Mastermind-like transcriptional co-activators: emerging roles in regulating cross talk among multiple signaling pathways. Oncogene. 2008;27(38):5138-47.

112. Wallberg AE, Pedersen K, Lendahl U, Roeder RG. p300 and PCAF act cooperatively to mediate transcriptional activation from chromatin templates by notch intracellular domains in vitro. Mol Cell Biol. 2002;22(22):7812-9.

113. Fryer CJ, Lamar E, Turbachova I, Kintner C, Jones KA. Mastermind mediates chromatin-specific transcription and turnover of the Notch enhancer complex. Genes Dev. 2002;16(11):1397-411.

114.	Gomez-Lamarca MJ, Falo-Sanjuan J, Stojnic R, Abdul Rehman S, Muresan L, Jones ML, et al. Activation of the Notch Signaling Pathway In Vivo Elicits Changes in CSL Nuclear Dynamics. Dev Cell. 2018;44(5):611-23 e7.

115.	Kopan R, Ilagan MX. The canonical Notch signaling pathway: unfolding the activation mechanism. Cell. 2009;137(2):216-33.

116.	Acar M, Jafar-Nejad H, Takeuchi H, Rajan A, Ibrani D, Rana NA, et al. Rumi is a CAP10 domain glycosyltransferase that modifies Notch and is required for Notch signaling. Cell. 2008;132(2):247-58.

117.	Luo Y, Haltiwanger RS. O-fucosylation of notch occurs in the endoplasmic reticulum. J Biol Chem. 2005;280(12):11289-94.

118.	Takeuchi H, Haltiwanger RS. Significance of glycosylation in Notch signaling. Biochem Biophys Res Commun. 2014;453(2):235-42.

119.	LeBon L, Lee TV, Sprinzak D, Jafar-Nejad H, Elowitz MB. Fringe proteins modulate Notch-ligand cis and trans interactions to specify signaling states. Elife. 2014;3:e02950.

120.	Boskovski MT, Yuan S, Pedersen NB, Goth CK, Makova S, Clausen H, et al. The heterotaxy gene GALNT11 glycosylates Notch to orchestrate cilia type and laterality. Nature. 2013;504(7480):456-9.

121.	Moloney DJ, Shair LH, Lu FM, Xia J, Locke R, Matta KL, et al. Mammalian Notch1 is modified with two unusual forms of O-linked glycosylation found on epidermal growth factor-like modules. J Biol Chem. 2000;275(13):9604-11.

122.	Chen J, Moloney DJ, Stanley P. Fringe modulation of Jagged1-induced Notch signaling requires the action of beta 4galactosyltransferase-1. Proc Natl Acad Sci U S A. 2001;98(24):13716-21.

123.	Gustafsson MV, Zheng X, Pereira T, Gradin K, Jin S, Lundkvist J, et al. Hypoxia requires notch signaling to maintain the undifferentiated cell state. Dev Cell. 2005;9(5):617-28.

124.   Coleman ML, McDonough MA, Hewitson KS, Coles C, Mecinovic J, Edelmann M, et al. Asparaginyl hydroxylation of the Notch ankyrin repeat domain by factor inhibiting hypoxia-inducible factor. J Biol Chem. 2007;282(33):24027-38.

125.   Zheng X, Linke S, Dias JM, Zheng X, Gradin K, Wallis TP, et al. Interaction with factor inhibiting HIF-1 defines an additional mode of cross-coupling between the Notch and hypoxia signaling pathways. Proc Natl Acad Sci U S A. 2008;105(9):3368-73.

126.   Wilkins SE, Hyvarinen J, Chicher J, Gorman JJ, Peet DJ, Bilton RL, et al. Differences in hydroxylation and binding of Notch and HIF-1alpha demonstrate substrate selectivity for factor inhibiting HIF-1 (FIH-1). Int J Biochem Cell Biol. 2009;41(7):1563-71.

127.   Kurooka H, Honjo T. Functional interaction between the mouse notch1 intracellular region and histone acetyltransferases PCAF and GCN5. J Biol Chem. 2000;275(22):17211-20.

128.   Oswald F, Tauber B, Dobner T, Bourteele S, Kostezka U, Adler G, et al. p300 acts as a transcriptional coactivator for mammalian Notch-1. Mol Cell Biol. 2001;21(22):7761-74.

129.   Ma CY, Yao MJ, Zhai QW, Jiao JW, Yuan XB, Poo MM. SIRT1 suppresses self-renewal of adult hippocampal neural stem cells. Development. 2014;141(24):4697-709.

130.   Collesi C, Felician G, Secco I, Gutierrez MI, Martelletti E, Ali H, et al. Reversible Notch1 acetylation tunes proliferative signalling in cardiomyocytes. Cardiovasc Res. 2018;114(1):103-22.

131.   Marcel N, Perumalsamy LR, Shukla SK, Sarin A. The lysine deacetylase Sirtuin 1 modulates the localization and function of the Notch1 receptor in regulatory T cells. Sci Signal. 2017;10(473).

132.   Hein K, Mittler G, Cizelsky W, Kuhl M, Ferrante F, Liefke R, et al. Site-specific methylation of Notch1 controls the amplitude and duration of the Notch1 response. Sci Signal. 2015;8(369):ra30.

133.   Foltz DR, Nye JS. Hyperphosphorylation and association with RBP of the intracellular domain of Notch1. Biochem Biophys Res Commun. 2001;286(3):484-92.

134.   Lee HJ, Kim MY, Park HS. Phosphorylation-dependent regulation of Notch1 signaling: the fulcrum of Notch1 signaling. BMB Rep. 2015;48(8):431-7.

135.   Fryer CJ, White JB, Jones KA. Mastermind recruits CycC:CDK8 to phosphorylate the Notch ICD and coordinate activation with turnover. Mol Cell. 2004;16(4):509-20.

136.   Li N, Fassl A, Chick J, Inuzuka H, Li X, Mansour MR, et al. Cyclin C is a haploinsufficient tumour suppressor. Nat Cell Biol. 2014;16(11):1080-91.

137.   Espinosa L, Ingles-Esteve J, Aguilera C, Bigas A. Phosphorylation by glycogen synthase kinase-3 beta down-regulates Notch activity, a link for Notch and Wnt pathways. J Biol Chem. 2003;278(34):32227-35.

138.   Carrieri FA, Murray PJ, Ditsova D, Ferris MA, Davies P, Dale JK. CDK1 and CDK2 regulate NICD1 turnover and the periodicity of the segmentation clock. EMBO Rep. 2019;20(7):e46436.

139.   Ranganathan P, Vasquez-Del Carpio R, Kaplan FM, Wang H, Gupta A, VanWye JD, et al. Hierarchical phosphorylation within the ankyrin repeat domain defines a phosphoregulatory loop that regulates Notch transcriptional activity. J Biol Chem. 2011;286(33):28844-57.

140.   Mo JS, Kim MY, Han SO, Kim IS, Ann EJ, Lee KS, et al. Integrin-linked kinase controls Notch1 signaling by down-regulation of protein stability through Fbw7 ubiquitin ligase. Mol Cell Biol. 2007;27(15):5565-74.

141.   LaFoya B, Munroe JA, Pu X, Albig AR. Src kinase phosphorylates Notch1 to inhibit MAML binding. Sci Rep. 2018;8(1):15515.

142.   Ishitani T, Hirao T, Suzuki M, Isoda M, Ishitani S, Harigaya K, et al. Nemo-like kinase suppresses Notch signalling by interfering with formation of the Notch active transcriptional complex. Nat Cell Biol. 2010;12(3):278-85.

143.   Santio NM, Landor SK, Vahtera L, Yla-Pelto J, Paloniemi E, Imanishi SY, et al. Phosphorylation of Notch1 by Pim kinases promotes oncogenic signaling in breast and prostate cancer cells. Oncotarget. 2016;7(28):43220-38.

144.   Song J, Park S, Kim M, Shin I. Down-regulation of Notch-dependent transcription by Akt in vitro. FEBS Lett. 2008;582(12):1693-9.

145.   Ramakrishnan G, Davaakhuu G, Chung WC, Zhu H, Rana A, Filipovic A, et al. AKT and 14-3-3 regulate Notch4 nuclear localization. Sci Rep. 2015;5:8782.

146.   Sjoqvist M, Antfolk D, Ferraris S, Rraklli V, Haga C, Antila C, et al. PKCzeta regulates Notch receptor routing and activity in a Notch signaling-dependent manner. Cell Res. 2014;24(4):433-50.

147.   Jin YH, Kim H, Oh M, Ki H, Kim K. Regulation of Notch1/NICD and Hes1 expressions by GSK-3alpha/beta. Mol Cells. 2009;27(1):15-9.

148.   Foltz DR, Santiago MC, Berechid BE, Nye JS. Glycogen synthase kinase-3beta modulates notch signaling and stability. Curr Biol. 2002;12(12):1006-11.

149.   Fernandez-Martinez J, Vela EM, Tora-Ponsioen M, Ocana OH, Nieto MA, Galceran J. Attenuation of Notch signalling by the Down-syndrome-associated kinase DYRK1A. J Cell Sci. 2009;122(Pt 10):1574-83.

150.   Ann EJ, Kim MY, Yoon JH, Ahn JS, Jo EH, Lee HJ, et al. Tumor Suppressor HIPK2 Regulates Malignant Growth via Phosphorylation of Notch1. Cancer Res. 2016;76(16):4728-40.

151.   Itoh M, Kim CH, Palardy G, Oda T, Jiang YJ, Maust D, et al. Mind bomb is a ubiquitin ligase that is essential for efficient activation of Notch signaling by Delta. Dev Cell. 2003;4(1):67-82.

152.   Lai EC, Deblandre GA, Kintner C, Rubin GM. Drosophila neuralized is a ubiquitin ligase that promotes the internalization and degradation of delta. Dev Cell. 2001;1(6):783-94.

153.   Bielskiene K, Bagdoniene L, Mozuraitiene J, Kazbariene B, Janulionis E. E3 ubiquitin ligases as drug targets and prognostic biomarkers in melanoma. Medicina (Kaunas). 2015;51(1):1-9.

154.   Qiu L, Joazeiro C, Fang N, Wang HY, Elly C, Altman Y, et al. Recognition and ubiquitination of Notch by Itch, a hect-type E3 ubiquitin ligase. J Biol Chem. 2000;275(46):35734-7.

155.   McGill MA, McGlade CJ. Mammalian numb proteins promote Notch1 receptor ubiquitination and degradation of the Notch1 intracellular domain. J Biol Chem. 2003;278(25):23196-203.

156.   Sapir T, Levy T, Kozer N, Shin I, Zamor V, Haffner-Krausz R, et al. Notch Activation by Shootin1 Opposing Activities on 2 Ubiquitin Ligases. Cereb Cortex. 2018;28(9):3115-28.

157.   Moretti J, Chastagner P, Liang CC, Cohn MA, Israel A, Brou C. The ubiquitin-specific protease 12 (USP12) is a negative regulator of notch signaling acting on notch receptor trafficking toward degradation. J Biol Chem. 2012;287(35):29429-41.

158.   Hubbard EJ, Wu G, Kitajewski J, Greenwald I. sel-10, a negative regulator of lin-12 activity in Caenorhabditis elegans, encodes a member of the CDC4 family of proteins. Genes Dev. 1997;11(23):3182-93.

159.   Oberg C, Li J, Pauley A, Wolf E, Gurney M, Lendahl U. The Notch intracellular domain is ubiquitinated and negatively regulated by the mammalian Sel-10 homolog. J Biol Chem. 2001;276(38):35847-53.

160.   Wu G, Lyapina S, Das I, Li J, Gurney M, Pauley A, et al. SEL-10 is an inhibitor of notch signaling that targets notch for ubiquitin-mediated protein degradation. Mol Cell Biol. 2001;21(21):7403-15.

161.   Carrieri FA, Dale JK. Turn It Down a Notch. Front Cell Dev Biol. 2016;4:151.

162.   Hsu KW, Fang WL, Huang KH, Huang TT, Lee HC, Hsieh RH, et al. Notch1 pathway-mediated microRNA-151-5p promotes gastric cancer progression. Oncotarget. 2016;7(25):38036-51.

163.   O'Neil J, Grim J, Strack P, Rao S, Tibbitts D, Winter C, et al. FBW7 mutations in leukemic cells mediate NOTCH pathway activation and resistance to gamma-secretase inhibitors. J Exp Med. 2007;204(8):1813-24.

164.   Li L, Guturi KKN, Gautreau B, Patel PS, Saad A, Morii M, et al. Ubiquitin ligase RNF8 suppresses Notch signaling to regulate mammary development and tumorigenesis. J Clin Invest. 2018;128(10):4525-42.

165.   Thomas JJ, Abed M, Heuberger J, Novak R, Zohar Y, Beltran Lopez AP, et al. RNF4-Dependent Oncogene Activation by Protein Stabilization. Cell Rep. 2016;16(12):3388-400.

166.   Pettersson S, Sczaniecka M, McLaren L, Russell F, Gladstone K, Hupp T, et al. Non-degradative ubiquitination of the Notch1 receptor by the E3 ligase MDM2 activates the Notch signalling pathway. Biochem J. 2013;450(3):523-36.

167.   Zhang J, Liu M, Su Y, Du J, Zhu AJ. A targeted in vivo RNAi screen reveals deubiquitinases as new regulators of Notch signaling. G3 (Bethesda). 2012;2(12):1563-75.

168.   Chen F, Zhang C, Wu H, Ma Y, Luo X, Gong X, et al. The E3 ubiquitin ligase SCF(FBXL14) complex stimulates neuronal differentiation by targeting the Notch signaling factor HES1 for proteolysis. J Biol Chem. 2017;292(49):20100-12.

169.   Wu HC, Lin YC, Liu CH, Chung HC, Wang YT, Lin YW, et al. USP11 regulates PML stability to control Notch-induced malignancy in brain tumours. Nat Commun. 2014;5:3214.

170.   Hellstrom M, Phng LK, Hofmann JJ, Wallgard E, Coultas L, Lindblom P, et al. Dll4 signalling through Notch1 regulates formation of tip cells during angiogenesis. Nature. 2007;445(7129):776-80.

171.   High FA, Epstein JA. The multifaceted role of Notch in cardiac development and disease. Nat Rev Genet. 2008;9(1):49-61.

172.   Aster JC, Pear WS, Blacklow SC. The Varied Roles of Notch in Cancer. Annu Rev Pathol. 2017;12:245-75.

173.   Tamagnone L, Zacchigna S, Rehman M. Taming the Notch Transcriptional Regulator for Cancer Therapy. Molecules. 2018;23(2).

174.   Thurston G, Kitajewski J. VEGF and Delta-Notch: interacting signalling pathways in tumour angiogenesis. Br J Cancer. 2008;99(8):1204-9.

175.   Nguyen BC, Lefort K, Mandinova A, Antonini D, Devgan V, Della Gatta G, et al. Cross-regulation between Notch and p63 in keratinocyte commitment to differentiation. Genes Dev. 2006;20(8):1028-42.

176.   Koch U, Radtke F. Notch and cancer: a double-edged sword. Cell Mol Life Sci. 2007;64(21):2746-62.

177.   Siebel C, Lendahl U. Notch Signaling in Development, Tissue Homeostasis, and Disease. Physiol Rev. 2017;97(4):1235-94.

178.   Weng AP, Ferrando AA, Lee W, Morris JPt, Silverman LB, Sanchez-Irizarry C, et al. Activating mutations of NOTCH1 in human T cell acute lymphoblastic leukemia. Science. 2004;306(5694):269-71.

179.   Kridel R, Meissner B, Rogic S, Boyle M, Telenius A, Woolcock B, et al. Whole transcriptome sequencing reveals recurrent NOTCH1 mutations in mantle cell lymphoma. Blood. 2012;119(9):1963-71.

180.   Frierson HF, Jr., Moskaluk CA. Mutation signature of adenoid cystic carcinoma: evidence for transcriptional and epigenetic reprogramming. J Clin Invest. 2013;123(7):2783-5.

181.   Wang WM, Zhao ZL, Ma SR, Yu GT, Liu B, Zhang L, et al. Epidermal growth factor receptor inhibition reduces angiogenesis via hypoxia-inducible factor-1alpha and Notch1 in head neck squamous cell carcinoma. PLoS One. 2015;10(2):e0119723.

182.   Stephens PJ, Davies HR, Mitani Y, Van Loo P, Shlien A, Tarpey PS, et al. Whole exome sequencing of adenoid cystic carcinoma. J Clin Invest. 2013;123(7):2965-8.

183.   Westhoff B, Colaluca IN, D'Ario G, Donzelli M, Tosoni D, Volorio S, et al. Alterations of the Notch pathway in lung cancer. Proc Natl Acad Sci U S A. 2009;106(52):22293-8.

184.   Ellisen LW, Bird J, West DC, Soreng AL, Reynolds TC, Smith SD, et al. TAN-1, the human homolog of the Drosophila notch gene, is broken by chromosomal translocations in T lymphoblastic neoplasms. Cell. 1991;66(4):649-61.

185.   Ferrando AA. The role of NOTCH1 signaling in T-ALL. Hematology Am Soc Hematol Educ Program. 2009:353-61.

186.   Jhappan C, Gallahan D, Stahle C, Chu E, Smith GH, Merlino G, et al. Expression of an activated Notch-related int-3 transgene interferes with cell differentiation and induces neoplastic transformation in mammary and salivary glands. Genes Dev. 1992;6(3):345-55.

187.   Kiaris H, Politi K, Grimm LM, Szabolcs M, Fisher P, Efstratiadis A, et al. Modulation of notch signaling elicits signature tumors and inhibits hras1-induced oncogenesis in the mouse mammary epithelium. Am J Pathol. 2004;165(2):695-705.

188.   Somasundaram K, Reddy SP, Vinnakota K, Britto R, Subbarayan M, Nambiar S, et al. Upregulation of ASCL1 and inhibition of Notch signaling pathway characterize progressive astrocytoma. Oncogene. 2005;24(47):7073-83.

189.   Santagata S, Demichelis F, Riva A, Varambally S, Hofer MD, Kutok JL, et al. JAGGED1 expression is associated with prostate cancer metastasis and recurrence. Cancer Res. 2004;64(19):6854-7.

190.   Zhu H, Zhou X, Redfield S, Lewin J, Miele L. Elevated Jagged-1 and Notch-1 expression in high grade and metastatic prostate cancers. Am J Transl Res. 2013;5(3):368-78.

191.   Xu A, Haines N, Dlugosz M, Rana NA, Takeuchi H, Haltiwanger RS, et al. In vitro reconstitution of the modulation of Drosophila Notch-ligand binding by Fringe. J Biol Chem. 2007;282(48):35153-62.

192.   Zhang C, Zhao H, Zhang L. Fringe order error in multifrequency fringe projection phase unwrapping: reason and correction. Appl Opt. 2015;54(32):9390-9.

193.   Lopez-Arribillaga E, Rodilla V, Colomer C, Vert A, Shelton A, Cheng JH, et al. Manic Fringe deficiency imposes Jagged1 addiction to intestinal tumor cells. Nat Commun. 2018;9(1):2992.

194.   Haines N, Irvine KD. Glycosylation regulates Notch signalling. Nat Rev Mol Cell Biol. 2003;4(10):786-97.

195.   Bigas A, Espinosa L. The multiple usages of Notch signaling in development, cell differentiation and cancer. Curr Opin Cell Biol. 2018;55:1-7.

196.   Lim KJ, Brandt WD, Heth JA, Muraszko KM, Fan X, Bar EE, et al. Lateral inhibition of Notch signaling in neoplastic cells. Oncotarget. 2015;6(3):1666-77.

197.   Corada M, Morini MF, Dejana E. Signaling pathways in the specification of arteries and veins. Arterioscler Thromb Vasc Biol. 2014;34(11):2372-7.

198.   Shawber CJ, Funahashi Y, Francisco E, Vorontchikhina M, Kitamura Y, Stowell SA, et al. Notch alters VEGF responsiveness in human and murine endothelial cells by direct regulation of VEGFR-3 expression. J Clin Invest. 2007;117(11):3369-82.

199.   Lobov IB, Renard RA, Papadopoulos N, Gale NW, Thurston G, Yancopoulos GD, et al. Delta-like ligand 4 (Dll4) is induced by VEGF as a negative regulator of angiogenic sprouting. Proc Natl Acad Sci U S A. 2007;104(9):3219-24.

200. Kangsamaksin T, Tattersall IW, Kitajewski J. Notch functions in developmental and tumour angiogenesis by diverse mechanisms. Biochem Soc Trans. 2014;42(6):1563-8.

201. Bentley K, Franco CA, Philippides A, Blanco R, Dierkes M, Gebala V, et al. The role of differential VE-cadherin dynamics in cell rearrangement during angiogenesis. Nat Cell Biol. 2014;16(4):309-21.

202. Krishnamachary B, Zagzag D, Nagasawa H, Rainey K, Okuyama H, Baek JH, et al. Hypoxia-inducible factor-1-dependent repression of E-cadherin in von Hippel-Lindau tumor suppressor-null renal cell carcinoma mediated by TCF3, ZFHX1A, and ZFHX1B. Cancer Res. 2006;66(5):2725-31.

203. Esteban MA, Tran MG, Harten SK, Hill P, Castellanos MC, Chandra A, et al. Regulation of E-cadherin expression by VHL and hypoxia-inducible factor. Cancer Res. 2006;66(7):3567-75.

204. Manalo DJ, Rowan A, Lavoie T, Natarajan L, Kelly BD, Ye SQ, et al. Transcriptional regulation of vascular endothelial cell responses to hypoxia by HIF-1. Blood. 2005;105(2):659-69.

205. Semenza GL. Hypoxia-inducible factors: mediators of cancer progression and targets for cancer therapy. Trends Pharmacol Sci. 2012;33(4):207-14.

206. Timmerman LA, Grego-Bessa J, Raya A, Bertran E, Perez-Pomares JM, Diez J, et al. Notch promotes epithelial-mesenchymal transition during cardiac development and oncogenic transformation. Genes Dev. 2004;18(1):99-115.

207. Niessen K, Fu Y, Chang L, Hoodless PA, McFadden D, Karsan A. Slug is a direct Notch target required for initiation of cardiac cushion cellularization. J Cell Biol. 2008;182(2):315-25.

208. Hu B, Castillo E, Harewood L, Ostano P, Reymond A, Dummer R, et al. Multifocal epithelial tumors and field cancerization from loss of mesenchymal CSL signaling. Cell. 2012;149(6):1207-20.

209.   Procopio MG, Laszlo C, Al Labban D, Kim DE, Bordignon P, Jo SH, et al. Combined CSL and p53 downregulation promotes cancer-associated fibroblast activation. Nat Cell Biol. 2015;17(9):1193-204.

210.   Klinakis A, Lobry C, Abdel-Wahab O, Oh P, Haeno H, Buonamici S, et al. A novel tumour-suppressor function for the Notch pathway in myeloid leukaemia. Nature. 2011;473(7346):230-3.

211.   Franklin RA, Liao W, Sarkar A, Kim MV, Bivona MR, Liu K, et al. The cellular and molecular origin of tumor-associated macrophages. Science. 2014;344(6186):921-5.

212.   Mao L, Zhao ZL, Yu GT, Wu L, Deng WW, Li YC, et al. gamma-Secretase inhibitor reduces immunosuppressive cells and enhances tumour immunity in head and neck squamous cell carcinoma. Int J Cancer. 2018;142(5):999-1009.

213.   Wang YC, He F, Feng F, Liu XW, Dong GY, Qin HY, et al. Notch signaling determines the M1 versus M2 polarization of macrophages in antitumor immune responses. Cancer Res. 2010;70(12):4840-9.

214.   Liu H, Wang J, Zhang M, Xuan Q, Wang Z, Lian X, et al. Jagged1 promotes aromatase inhibitor resistance by modulating tumor-associated macrophage differentiation in breast cancer patients. Breast Cancer Res Treat. 2017;166(1):95-107.

215.   Chatterjee N, Walker GC. Mechanisms of DNA damage, repair, and mutagenesis. Environ Mol Mutagen. 2017;58(5):235-63.

216.   Reuter S, Gupta SC, Chaturvedi MM, Aggarwal BB. Oxidative stress, inflammation, and cancer: how are they linked? Free Radic Biol Med. 2010;49(11):1603-16.

217.   Perrone S, Lotti F, Geronzi U, Guidoni E, Longini M, Buonocore G. Oxidative Stress in Cancer-Prone Genetic Diseases in Pediatric Age: The Role of Mitochondrial Dysfunction. Oxid Med Cell Longev. 2016;2016:4782426.

218.   Kunkel TA. DNA replication fidelity. J Biol Chem. 2004;279(17):16895-8.

219.   Kunkel TA. Evolving views of DNA replication (in)fidelity. Cold Spring Harb Symp Quant Biol. 2009;74:91-101.

220.   Kunkel TA. Balancing eukaryotic replication asymmetry with replication fidelity. Curr Opin Chem Biol. 2011;15(5):620-6.

221.   Buckland RJ, Watt DL, Chittoor B, Nilsson AK, Kunkel TA, Chabes A. Increased and imbalanced dNTP pools symmetrically promote both leading and lagging strand replication infidelity. PLoS Genet. 2014;10(12):e1004846.

222.   Potenski CJ, Klein HL. How the misincorporation of ribonucleotides into genomic DNA can be both harmful and helpful to cells. Nucleic Acids Res. 2014;42(16):10226-34.

223.   Pommier Y, Barcelo JM, Rao VA, Sordet O, Jobson AG, Thibaut L, et al. Repair of topoisomerase I-mediated DNA damage. Prog Nucleic Acid Res Mol Biol. 2006;81:179-229.

224.   Yonekura S, Nakamura N, Yonei S, Zhang-Akiyama QM. Generation, biological consequences and repair mechanisms of cytosine deamination in DNA. J Radiat Res. 2009;50(1):19-26.

225.   De Bont R, van Larebeke N. Endogenous DNA damage in humans: a review of quantitative data. Mutagenesis. 2004;19(3):169-85.

226.   Goff SP. Death by deamination: a novel host restriction system for HIV-1. Cell. 2003;114(3):281-3.

227.   Blanc V, Davidson NO. APOBEC-1-mediated RNA editing. Wiley Interdiscip Rev Syst Biol Med. 2010;2(5):594-602.

228.   Chandra V, Bortnick A, Murre C. AID targeting: old mysteries and new challenges. Trends Immunol. 2015;36(9):527-35.

229.   Nabel CS, Manning SA, Kohli RM. The curious chemical biology of cytosine: deamination, methylation, and oxidation as modulators of genomic potential. ACS Chem Biol. 2012;7(1):20-30.

230.	Chan K, Resnick MA, Gordenin DA. The choice of nucleotide inserted opposite abasic sites formed within chromosomal DNA reveals the polymerase activities participating in translesion DNA synthesis. DNA Repair (Amst). 2013;12(11):878-89.

231.	Cadet J, Wagner JR. Oxidatively generated base damage to cellular DNA by hydroxyl radical and one-electron oxidants: similarities and differences. Arch Biochem Biophys. 2014;557:47-54.

232.	Giacco F, Brownlee M. Oxidative stress and diabetic complications. Circ Res. 2010;107(9):1058-70.

233.	Liou GY, Storz P. Reactive oxygen species in cancer. Free Radic Res. 2010;44(5):479-96.

234.	Dias V, Junn E, Mouradian MM. The role of oxidative stress in Parkinson's disease. J Parkinsons Dis. 2013;3(4):461-91.

235.	Mohsenzadegan M, Mirshafiey A. The immunopathogenic role of reactive oxygen species in Alzheimer disease. Iran J Allergy Asthma Immunol. 2012;11(3):203-16.

236.	Giloni L, Takeshita M, Johnson F, Iden C, Grollman AP. Bleomycin-induced strand-scission of DNA. Mechanism of deoxyribose cleavage. J Biol Chem. 1981;256(16):8608-15.

237.	Marnett LJ. Oxyradicals and DNA damage. Carcinogenesis. 2000;21(3):361-70.

238.	Broedbaek K, Poulsen HE, Weimann A, Kom GD, Schwedhelm E, Nielsen P, et al. Urinary excretion of biomarkers of oxidatively damaged DNA and RNA in hereditary hemochromatosis. Free Radic Biol Med. 2009;47(8):1230-3.

239.	Mitchell DL, Nairn RS. The biology of the (6-4) photoproduct. Photochem Photobiol. 1989;49(6):805-19.

240.	Davies RJ. Royal Irish Academy Medal Lecture. Ultraviolet radiation damage in DNA. Biochem Soc Trans. 1995;23(2):407-18.

241.   Rastogi RP, Richa, Kumar A, Tyagi MB, Sinha RP. Molecular mechanisms of ultraviolet radiation-induced DNA damage and repair. J Nucleic Acids. 2010;2010:592980.

242.   Douki T, Perdiz D, Grof P, Kuluncsics Z, Moustacchi E, Cadet J, et al. Oxidation of guanine in cellular DNA by solar UV radiation: biological role. Photochem Photobiol. 1999;70(2):184-90.

243.   Peak MJ, Peak JG. DNA-to-protein crosslinks and backbone breaks caused by far- and near-ultraviolet, and visible light radiations in mammalian cells. Basic Life Sci. 1986;38:193-202.

244.   Waters LS, Walker GC. The critical mutagenic translesion DNA polymerase Rev1 is highly expressed during G(2)/M phase rather than S phase. Proc Natl Acad Sci U S A. 2006;103(24):8971-6.

245.   Eppink B, Tafel AA, Hanada K, van Drunen E, Hickson ID, Essers J, et al. The response of mammalian cells to UV-light reveals Rad54-dependent and independent pathways of homologous recombination. DNA Repair (Amst). 2011;10(11):1095-105.

246.   Crutzen PJ, Andreae MO. Biomass burning in the tropics: impact on atmospheric chemistry and biogeochemical cycles. Science. 1990;250(4988):1669-78.

247.   Wyatt MD, Pittman DL. Methylating agents and DNA repair responses: Methylated bases and sources of strand breaks. Chem Res Toxicol. 2006;19(12):1580-94.

248.   Beranek DT. Distribution of methyl and ethyl adducts following alkylation with monofunctional alkylating agents. Mutat Res. 1990;231(1):11-30.

249.   Lawley PD. Effects of some chemical mutagens and carcinogens on nucleic acids. Prog Nucleic Acid Res Mol Biol. 1966;5:89-131.

250.   DeVita VT, Jr., Chu E. A history of cancer chemotherapy. Cancer Res. 2008;68(21):8643-53.

251.   Emadi A, Jones RJ, Brodsky RA. Cyclophosphamide and cancer: golden anniversary. Nat Rev Clin Oncol. 2009;6(11):638-47.

252.   Skipper PL, Kim MY, Sun HL, Wogan GN, Tannenbaum SR. Monocyclic aromatic amines as potential human carcinogens: old is new again. Carcinogenesis. 2010;31(1):50-8.

253.   Hammons GJ, Milton D, Stepps K, Guengerich FP, Tukey RH, Kadlubar FF. Metabolism of carcinogenic heterocyclic and aromatic amines by recombinant human cytochrome P450 enzymes. Carcinogenesis. 1997;18(4):851-4.

254.   Shibutani S, Suzuki N, Tan X, Johnson F, Grollman AP. Influence of flanking sequence context on the mutagenicity of acetylaminofluorene-derived DNA adducts in mammalian cells. Biochemistry. 2001;40(12):3717-22.

255.   Kriek E. Fifty years of research on N-acetyl-2-aminofluorene, one of the most versatile compounds in experimental cancer research. J Cancer Res Clin Oncol. 1992;118(7):481-9.

256.   Mu H, Kropachev K, Wang L, Zhang L, Kolbanovskiy A, Kolbanovskiy M, et al. Nucleotide excision repair of 2-acetylaminofluorene- and 2-aminofluorene-(C8)-guanine adducts: molecular dynamics simulations elucidate how lesion structure and base sequence context impact repair efficiencies. Nucleic Acids Res. 2012;40(19):9675-90.

257.   Yu H. Environmental carcinogenic polycyclic aromatic hydrocarbons: photochemistry and phototoxicity. J Environ Sci Health C Environ Carcinog Ecotoxicol Rev. 2002;20(2):149-83.

258.   Phillips DH. Fifty years of benzo(a)pyrene. Nature. 1983;303(5917):468-72.

259.   Cosman M, de los Santos C, Fiala R, Hingerty BE, Singh SB, Ibanez V, et al. Solution conformation of the major adduct between the carcinogen (+)-anti-benzo[a]pyrene diol epoxide and DNA. Proc Natl Acad Sci U S A. 1992;89(5):1914-8.

260. Jha V, Bian C, Xing G, Ling H. Structure and mechanism of error-free replication past the major benzo[a]pyrene adduct by human DNA polymerase kappa. Nucleic Acids Res. 2016;44(10):4957-67.

261. Bartsch H, Montesano R. Relevance of nitrosamines to human cancer. Carcinogenesis. 1984;5(11):1381-93.

262. Herrmann SS, Granby K, Duedahl-Olesen L. Formation and mitigation of N-nitrosamines in nitrite preserved cooked sausages. Food Chem. 2015;174:516-26.

263. Gafter-Gvili A, Zingerman B, Rozen-Zvi B, Ori Y, Green H, Lubin I, et al. Oxidative stress-induced DNA damage and repair in human peripheral blood mononuclear cells: protective role of hemoglobin. PLoS One. 2013;8(7):e68341.

264. Luoto KR, Kumareswaran R, Bristow RG. Tumor hypoxia as a driving force in genetic instability. Genome Integr. 2013;4(1):5.

265. Kantidze OL, Velichko AK, Luzhin AV, Razin SV. Heat Stress-Induced DNA Damage. Acta Naturae. 2016;8(2):75-8.

266. Chatterjee N, Lin Y, Yotnda P, Wilson JH. Environmental Stress Induces Trinucleotide Repeat Mutagenesis in Human Cells by Alt-Nonhomologous End Joining Repair. J Mol Biol. 2016;428(15):2978-80.

267. Meeker JD, Ehrlich S, Toth TL, Wright DL, Calafat AM, Trisini AT, et al. Semen quality and sperm DNA damage in relation to urinary bisphenol A among men from an infertility clinic. Reprod Toxicol. 2010;30(4):532-9.

268. Hanawalt PC. Historical perspective on the DNA damage response. DNA Repair (Amst). 2015;36:2-7.

269. Ciccia A, Elledge SJ. The DNA damage response: making it safe to play with knives. Mol Cell. 2010;40(2):179-204.

270. Lord CJ, Ashworth A. The DNA damage response and cancer therapy. Nature. 2012;481(7381):287-94.

271. Hsieh P, Yamane K. DNA mismatch repair: molecular mechanism, cancer, and ageing. Mech Ageing Dev. 2008;129(7-8):391-407.

272. Kamileri I, Karakasilioti I, Garinis GA. Nucleotide excision repair: new tricks with old bricks. Trends Genet. 2012;28(11):566-73.

273. Dianov GL, Hubscher U. Mammalian base excision repair: the forgotten archangel. Nucleic Acids Res. 2013;41(6):3483-90.

274. Hartlerode AJ, Scully R. Mechanisms of double-strand break repair in somatic mammalian cells. Biochem J. 2009;423(2):157-68.

275. Moynahan ME, Jasin M. Mitotic homologous recombination maintains genomic stability and suppresses tumorigenesis. Nat Rev Mol Cell Biol. 2010;11(3):196-207.

276. Lieber MR. The mechanism of double-strand DNA break repair by the nonhomologous DNA end-joining pathway. Annu Rev Biochem. 2010;79:181-211.

277. Artandi SE, DePinho RA. Telomeres and telomerase in cancer. Carcinogenesis. 2010;31(1):9-18.

278. Hanahan D, Weinberg RA. The hallmarks of cancer. Cell. 2000;100(1):57-70.

279. Fernandez-Capetillo O, Lee A, Nussenzweig M, Nussenzweig A. H2AX: the histone guardian of the genome. DNA Repair (Amst). 2004;3(8-9):959-67.

280. Lamarche BJ, Orazio NI, Weitzman MD. The MRN complex in double-strand break repair and telomere maintenance. FEBS Lett. 2010;584(17):3682-95.

281. Bakkenist CJ, Kastan MB. DNA damage activates ATM through intermolecular autophosphorylation and dimer dissociation. Nature. 2003;421(6922):499-506.

282. Falck J, Coates J, Jackson SP. Conserved modes of recruitment of ATM, ATR and DNA-PKcs to sites of DNA damage. Nature. 2005;434(7033):605-11.

283.   Matsuoka S, Ballif BA, Smogorzewska A, McDonald ER, 3rd, Hurov KE, Luo J, et al. ATM and ATR substrate analysis reveals extensive protein networks responsive to DNA damage. Science. 2007;316(5828):1160-6.

284.   Cortez D, Wang Y, Qin J, Elledge SJ. Requirement of ATM-dependent phosphorylation of brca1 in the DNA damage response to double-strand breaks. Science. 1999;286(5442):1162-6.

285.   Gatei M, Zhou BB, Hobson K, Scott S, Young D, Khanna KK. Ataxia telangiectasia mutated (ATM) kinase and ATM and Rad3 related kinase mediate phosphorylation of Brca1 at distinct and overlapping sites. In vivo assessment using phospho-specific antibodies. J Biol Chem. 2001;276(20):17276-80.

286.   Desouky O, Ding N, Zhou GJJoRR, Sciences A. Targeted and non-targeted effects of ionizing radiation. 2015;8(2):247-54.

287.   Vignard J, Mirey G, Salles B. Ionizing-radiation induced DNA double-strand breaks: a direct and indirect lighting up. Radiother Oncol. 2013;108(3):362-9.

288.   Henner WD, Grunberg SM, Haseltine WA. Sites and structure of gamma radiation-induced DNA strand breaks. J Biol Chem. 1982;257(19):11750-4.

289.   Obe G, Johannes C, Schulte-Frohlinde D. DNA double-strand breaks induced by sparsely ionizing radiation and endonucleases as critical lesions for cell death, chromosomal aberrations, mutations and oncogenic transformation. Mutagenesis. 1992;7(1):3-12.

290.   Jilani A, Ramotar D, Slack C, Ong C, Yang XM, Scherer SW, et al. Molecular cloning of the human gene, PNKP, encoding a polynucleotide kinase 3'-phosphatase and evidence for its role in repair of DNA strand breaks caused by oxidative damage. J Biol Chem. 1999;274(34):24176-86.

291.   Zhou T, Lee JW, Tatavarthi H, Lupski JR, Valerie K, Povirk LF. Deficiency in 3'-phosphoglycolate processing in human cells with a hereditary mutation in tyrosyl-DNA phosphodiesterase (TDP1). Nucleic Acids Res. 2005;33(1):289-97.

292.   El-Khamisy SF, Hartsuiker E, Caldecott KW. TDP1 facilitates repair of ionizing radiation-induced DNA single-strand breaks. DNA Repair (Amst). 2007;6(10):1485-95.

293.   Iliakis G. The role of DNA double strand breaks in ionizing radiation-induced killing of eukaryotic cells. Bioessays. 1991;13(12):641-8.

294.   Lomax ME, Folkes LK, O'Neill P. Biological consequences of radiation-induced DNA damage: relevance to radiotherapy. Clin Oncol (R Coll Radiol). 2013;25(10):578-85.

295.   Begg AC, Stewart FA, Vens C. Strategies to improve radiotherapy with targeted drugs. Nat Rev Cancer. 2011;11(4):239-53.

296.   Shuryak I. Review of microbial resistance to chronic ionizing radiation exposure under environmental conditions. J Environ Radioact. 2019;196:50-63.

297.   Painter RB, Cleaver JE. Repair replication in HeLa cells after large doses of x-irradiation. Nature. 1967;216(5113):369-70.

298.   Canman CE, Lim DS, Cimprich KA, Taya Y, Tamai K, Sakaguchi K, et al. Activation of the ATM kinase by ionizing radiation and phosphorylation of p53. Science. 1998;281(5383):1677-9.

299.   Falck J, Mailand N, Syljuasen RG, Bartek J, Lukas J. The ATM-Chk2-Cdc25A checkpoint pathway guards against radioresistant DNA synthesis. Nature. 2001;410(6830):842-7.

300.   Taylor AM, Harnden DG, Arlett CF, Harcourt SA, Lehmann AR, Stevens S, et al. Ataxia telangiectasia: a human mutation with abnormal radiation sensitivity. Nature. 1975;258(5534):427-9.

301.   Blunt T, Finnie NJ, Taccioli GE, Smith GC, Demengeot J, Gottlieb TM, et al. Defective DNA-dependent protein kinase activity is linked to V(D)J recombination and DNA repair defects associated with the murine scid mutation. Cell. 1995;80(5):813-23.

302.   McQuestion M. Evidence-based skin care management in radiation therapy: clinical update. Semin Oncol Nurs. 2011;27(2):e1-17.

303.   Fitzgerald TJ, Jodoin MB, Tillman G, Aronowitz J, Pieters R, Balducci S, et al. Radiation therapy toxicity to the skin. Dermatol Clin. 2008;26(1):161-72, ix.

304.   Radvansky LJ, Pace MB, Siddiqui A. Prevention and management of radiation-induced dermatitis, mucositis, and xerostomia. Am J Health Syst Pharm. 2013;70(12):1025-32.

305.   Morgan K. Radiotherapy-induced skin reactions: prevention and cure. Br J Nurs. 2014;23(16):S24, S6-32.

306.   Pignol JP, Olivotto I, Rakovitch E, Gardner S, Sixel K, Beckham W, et al. A multicenter randomized trial of breast intensity-modulated radiation therapy to reduce acute radiation dermatitis. J Clin Oncol. 2008;26(13):2085-92.

307.   Glover D, Harmer V. Radiotherapy-induced skin reactions: assessment and management. Br J Nurs. 2014;23(4):S28, S30-5.

308.   Amber KT, Shiman MI, Badiavas EV. The use of antioxidants in radiotherapy-induced skin toxicity. Integr Cancer Ther. 2014;13(1):38-45.

309.   Kim JH, Kolozsvary AJ, Jenrow KA, Brown SL. Mechanisms of radiation-induced skin injury and implications for future clinical trials. Int J Radiat Biol. 2013;89(5):311-8.

310.   Vano-Galvan S, Fernandez-Lizarbe E, Truchuelo M, Diaz-Ley B, Grillo E, Sanchez V, et al. Dynamic skin changes of acute radiation dermatitis revealed by in vivo reflectance confocal microscopy. J Eur Acad Dermatol Venereol. 2013;27(9):1143-50.

311.   Hu SC, Hou MF, Luo KH, Chuang HY, Wei SY, Chen GS, et al. Changes in biophysical properties of the skin following radiotherapy for breast cancer. J Dermatol. 2014;41(12):1087-94.

312.   Haase O, Rodemann HP. Fibrosis and cytokine mechanisms: relevant in hadron therapy? Radiother Oncol. 2004;73 Suppl 2:S144-7.

313.   Bentzen SM. Preventing or reducing late side effects of radiation therapy: radiobiology meets molecular pathology. Nat Rev Cancer. 2006;6(9):702-13.

314.   Yarnold J, Brotons MC. Pathogenetic mechanisms in radiation fibrosis. Radiother Oncol. 2010;97(1):149-61.

315.   Marconi R, Serafini A, Giovanetti A, Bartoleschi C, Pardini MC, Bossi G, et al. Cytokine Modulation in Breast Cancer Patients Undergoing Radiotherapy: A Revision of the Most Recent Studies. Int J Mol Sci. 2019;20(2).

316.   Saito-Fujita T, Iwakawa M, Nakamura E, Nakawatari M, Fujita H, Moritake T, et al. Attenuated lung fibrosis in interleukin 6 knock-out mice after C-ion irradiation to lung. J Radiat Res. 2011;52(3):270-7.

317.   Malachowska B, Tomasik B, Stawiski K, Kulkarni S, Guha C, Chowdhury D, et al. Circulating microRNAs as Biomarkers of Radiation Exposure: A Systematic Review and Meta-Analysis. Int J Radiat Oncol Biol Phys. 2020;106(2):390-402.

318.   Weigel C, Schmezer P, Plass C, Popanda O. Epigenetics in radiation-induced fibrosis. Oncogene. 2015;34(17):2145-55.

319.   Squillaro T, Galano G, De Rosa R, Peluso G, Galderisi U. Concise Review: The Effect of Low-Dose Ionizing Radiation on Stem Cell Biology: A Contribution to Radiation Risk. Stem Cells. 2018;36(8):1146-53.

320.   Uhlen M, Fagerberg L, Hallstrom BM, Lindskog C, Oksvold P, Mardinoglu A, et al. Proteomics. Tissue-based map of the human proteome. Science. 2015;347(6220):1260419.

321.   Hoadley KA, Yau C, Hinoue T, Wolf DM, Lazar AJ, Drill E, et al. Cell-of-Origin Patterns Dominate the Molecular Classification of 10,000 Tumors from 33 Types of Cancer. Cell. 2018;173(2):291-304 e6.

322. Gao J, Aksoy BA, Dogrusoz U, Dresdner G, Gross B, Sumer SO, et al. Integrative analysis of complex cancer genomics and clinical profiles using the cBioPortal. Sci Signal. 2013;6(269):pl1.

323. Thompson BJ, Buonamici S, Sulis ML, Palomero T, Vilimas T, Basso G, et al. The SCFFBW7 ubiquitin ligase complex as a tumor suppressor in T cell leukemia. J Exp Med. 2007;204(8):1825-35.

324. Bishop AC, Ubersax JA, Petsch DT, Matheos DP, Gray NS, Blethrow J, et al. A chemical switch for inhibitor-sensitive alleles of any protein kinase. Nature. 2000;407(6802):395-401.

325. Salvo N, Barnes E, van Draanen J, Stacey E, Mitera G, Breen D, et al. Prophylaxis and management of acute radiation-induced skin reactions: a systematic review of the literature. Curr Oncol. 2010;17(4):94-112.

326. Kitagawa M. Notch signalling in the nucleus: roles of Mastermind-like (MAML) transcriptional coactivators. J Biochem. 2016;159(3):287-94.

327. Stylianou S, Clarke RB, Brennan K. Aberrant activation of notch signaling in human breast cancer. Cancer Res. 2006;66(3):1517-25.

328. Yuan X, Zhang M, Wu H, Xu H, Han N, Chu Q, et al. Expression of Notch1 Correlates with Breast Cancer Progression and Prognosis. PLoS One. 2015;10(6):e0131689.

329. Manderfield LJ, Aghajanian H, Engleka KA, Lim LY, Liu F, Jain R, et al. Hippo signaling is required for Notch-dependent smooth muscle differentiation of neural crest. Development. 2015;142(17):2962-71.

330. Gao J, Azmi AS, Aboukameel A, Kauffman M, Shacham S, Abou-Samra AB, et al. Nuclear retention of Fbw7 by specific inhibitors of nuclear export leads to Notch1 degradation in pancreatic cancer. Oncotarget. 2014;5(11):3444-54.

331. Rinaldo C, Prodosmo A, Mancini F, Iacovelli S, Sacchi A, Moretti F, et al. MDM2-regulated degradation of HIPK2 prevents p53Ser46 phosphorylation and DNA damage-induced apoptosis. Mol Cell. 2007;25(5):739-50.

332. Calzado MA, de la Vega L, Moller A, Bowtell DD, Schmitz ML. An inducible autoregulatory loop between HIPK2 and Siah2 at the apex of the hypoxic response. Nat Cell Biol. 2009;11(1):85-91.

333. D'Orazi G, Cecchinelli B, Bruno T, Manni I, Higashimoto Y, Saito S, et al. Homeodomain-interacting protein kinase-2 phosphorylates p53 at Ser 46 and mediates apoptosis. Nat Cell Biol. 2002;4(1):11-9.

334. Weiss CS, Ochs MM, Hagenmueller M, Streit MR, Malekar P, Riffel JH, et al. DYRK2 negatively regulates cardiomyocyte growth by mediating repressor function of GSK-3beta on eIF2Bepsilon. PLoS One. 2013;8(9):e70848.

335. Friedmann DR, Wilson JJ, Kovall RA. RAM-induced allostery facilitates assembly of a notch pathway active transcription complex. J Biol Chem. 2008;283(21):14781-91.

336. Del Bianco C, Aster JC, Blacklow SC. Mutational and energetic studies of Notch 1 transcription complexes. J Mol Biol. 2008;376(1):131-40.

337. Zong D, Ouyang R, Li J, Chen Y, Chen P. Notch signaling in lung diseases: focus on Notch1 and Notch3. Ther Adv Respir Dis. 2016;10(5):468-84.

338. Zeng JS, Zhang ZD, Pei L, Bai ZZ, Yang Y, Yang H, et al. CBX4 exhibits oncogenic activities in breast cancer via Notch1 signaling. Int J Biochem Cell Biol. 2018;95:1-8.

339. Stoyanova T, Riedinger M, Lin S, Faltermeier CM, Smith BA, Zhang KX, et al. Activation of Notch1 synergizes with multiple pathways in promoting castration-resistant prostate cancer. Proc Natl Acad Sci U S A. 2016;113(42):E6457-E66.

340. Moreno P, Lara-Chica M, Soler-Torronteras R, Caro T, Medina M, Alvarez A, et al. The Expression of the Ubiquitin Ligase SIAH2 (Seven In Absentia Homolog 2) Is Increased in Human Lung Cancer. PLoS One. 2015;10(11):e0143376.

341. Yogosawa S, Yoshida K. Tumor suppressive role for kinases phosphorylating p53 in DNA damage-induced apoptosis. Cancer Sci. 2018;109(11):3376-82.

342. Grabher C, von Boehmer H, Look AT. Notch 1 activation in the molecular pathogenesis of T-cell acute lymphoblastic leukaemia. Nat Rev Cancer. 2006;6(5):347-59.

343. Liu YP, Yang CJ, Huang MS, Yeh CT, Wu AT, Lee YC, et al. Cisplatin selects for multidrug-resistant CD133+ cells in lung adenocarcinoma by activating Notch signaling. Cancer Res. 2013;73(1):406-16.

344. Adamowicz M, Vermezovic J, d'Adda di Fagagna F. NOTCH1 Inhibits Activation of ATM by Impairing the Formation of an ATM-FOXO3a-KAT5/Tip60 Complex. Cell Rep. 2016;16(8):2068-76.

345. Jundt F, Anagnostopoulos I, Forster R, Mathas S, Stein H, Dorken B. Activated Notch1 signaling promotes tumor cell proliferation and survival in Hodgkin and anaplastic large cell lymphoma. Blood. 2002;99(9):3398-403.

346. Parplys AC, Petermann E, Petersen C, Dikomey E, Borgmann K. DNA damage by X-rays and their impact on replication processes. Radiother Oncol. 2012;102(3):466-71.

347. Giuranno L, Roig EM, Wansleeben C, van den Berg A, Groot AJ, Dubois L, et al. NOTCH inhibition promotes bronchial stem cell renewal and epithelial barrier integrity after irradiation. Stem Cells Transl Med. 2020;9(7):799-812.

348. Waterhouse NJ, Finucane DM, Green DR, Elce JS, Kumar S, Alnemri ES, et al. Calpain activation is upstream of caspases in radiation-induced apoptosis. Cell Death Differ. 1998;5(12):1051-61.

349. Yano H, Hamanaka R, Zhang JJ, Yano M, Hida M, Matsuo N, et al. MicroRNA-26 regulates the expression of CTGF after exposure to ionizing radiation. Radiat Environ Biophys. 2021;60(3):411-9.

350. Levy D, Adamovich Y, Reuven N, Shaul Y. Yap1 phosphorylation by c-Abl is a critical step in selective activation of proapoptotic genes in response to DNA damage. Mol Cell. 2008;29(3):350-61.

351.   Cottini F, Hideshima T, Xu C, Sattler M, Dori M, Agnelli L, et al. Rescue of Hippo coactivator YAP1 triggers DNA damage-induced apoptosis in hematological cancers. Nat Med. 2014;20(6):599-606.

352.   Xiong S, Patrushev N, Forouzandeh F, Hilenski L, Alexander RW. PGC-1alpha Modulates Telomere Function and DNA Damage in Protecting against Aging-Related Chronic Diseases. Cell Rep. 2015;12(9):1391-9.

353.   Lai CQ, Tucker KL, Parnell LD, Adiconis X, Garcia-Bailo B, Griffith J, et al. PPARGC1A variation associated with DNA damage, diabetes, and cardiovascular diseases: the Boston Puerto Rican Health Study. Diabetes. 2008;57(4):809-16.

354.   Cazzalini O, Scovassi AI, Savio M, Stivala LA, Prosperi E. Multiple roles of the cell cycle inhibitor p21(CDKN1A) in the DNA damage response. Mutat Res. 2010;704(1-3):12-20.

Annex

ORIGINAL ARTICLE

Phosphorylation-dependent regulation of the NOTCH1 intracellular domain by dual-specificity tyrosine-regulated kinase 2

Rosario Morrugares[1,2,3] · Alejandro Correa-Sáez[1,2,3] · Rita Moreno[4] · Martín Garrido-Rodríguez[1,2,3,5] · Eduardo Muñoz[1,2,3] · Laureano de la Vega[4] · Marco A. Calzado[1,2,3]

Abstract
NOTCH proteins constitute a receptor family with a widely conserved role in cell cycle, growing and development regulation. NOTCH1, the best characterised member of this family, regulates the expression of key genes in cell growth and angiogenesis, playing an essential role in cancer development. These observations provide a relevant rationale to propose the inhibition of the intracellular domain of NOTCH1 (Notch1-IC) as a strategy for treating various types of cancer. Notch1-IC stability is mainly controlled by post-translational modifications. FBXW7 ubiquitin E3 ligase-mediated degradation is considered one of the most relevant, being the previous phosphorylation at Thr-2512 residue required. In the present study, we describe for the first time a new regulation mechanism of the NOTCH1 signalling pathway mediated by DYRK2. We demonstrate that DYRK2 phosphorylates Notch1-IC in response to chemotherapeutic agents and facilitates its proteasomal degradation by FBXW7 ubiquitin ligase through a Thr-2512 phosphorylation-dependent mechanism. We show that DYRK2 regulation by chemotherapeutic agents has a relevant effect on the viability, motility and invasion capacity of cancer cells expressing NOTCH1. In summary, we reveal a novel mechanism of regulation for NOTCH1 which might help us to better understand its role in cancer biology.

Keywords DYRK2 · NOTCH1 · Degradation · Kinase · Phosphorylation · Cancer

Rosario Morrugares and Alejandro Correa-Sáez contributed equally to this work.

Electronic supplementary material The online version of this article (https://doi.org/10.1007/s00018-019-03309-9) contains supplementary material, which is available to authorized users.

✉ Marco A. Calzado
mcalzado@uco.es

1 Instituto Maimónides de Investigación Biomédica de Córdoba (IMIBIC), Avda. Menéndez Pidal s/n. 14004, Córdoba, Spain

2 Departamento de Biología Celular, Fisiología e Inmunología, Universidad de Córdoba, Córdoba, Spain

3 Hospital Universitario Reina Sofía, Córdoba, Spain

4 Division of Cancer Research, School of Medicine, Jacqui Wood Cancer Centre, James Arrott Drive, Ninewells Hospital and Medical School, University of Dundee, Dundee, Scotland, UK

5 Innohealth Group, Madrid, Spain

Introduction

NOTCH proteins (NOTCH1-4) constitute a receptor family with a widely conserved role in cell cycle, growing, development regulation and cell fate determination [1]. Most of the canonical Notch ligands are transmembrane proteins with an extracellular domain primarily comprised of multiple EGF (Epidermal Growth Factor) repeated similar structures [2]. The best characterised member of this family is NOTCH1, which regulates the expression of key genes in cell growth and angiogenesis, playing an essential role in cancer development. After ligand coupling, NOTCH1 is activated and the receptor is cleaved by a gamma-secretase, leading to the formation of a peptide sequence that corresponds to the intracellular domain of NOTCH1 (Notch1-IC) [3, 4]. In human cells, once Notch1-IC enters the nucleus, and together with the DNA-binding protein CSL (CBF1—Suppressor of Hairless—LAG1) and the co-activator MAML1 (Mastermind-like transcriptional co-activator 1), it stimulates the transcription of target genes related to processes

such as proliferation, angiogenesis, cell survival and migration [5, 6].

Functional studies implicate Notch signalling in essentially all of the hallmarks of cancer, being associated with abnormal expression, high mutation rate and poor survival in several cancers such as lung, breast, gastric or lymphoid cancer [7–11]. This oncogenic function of NOTCH in human cancers is related with its capacity to increase cell growth, centered on the ability to induce the expression of Myc [12, 13] and to enhance PI3K-Akt signalling [14]. Additionally, NOTCH has also been described as a mediator of chemoresistance in various human cancers [15, 16]. These observations have provided a rationale for pharmacologic inhibition of Notch1-IC as a potential strategy for treating various cancers [17].

Another potential way to regulate the NOTCH pathway is modulating the activity or stability of Notch1-IC, which is controlled by protein–protein interactions, endocytosis or post-translational modifications (ubiquitination and phosphorylation) [18, 19]. From among them, NOTCH1 degradation by the ubiquitin E3 ligase FBXW7 is considered to be one of the most relevant [20]. FBXW7 binds directly to Notch1-IC promoting its polyubiquitination and proteasomal degradation, which requires phosphorylation at Thr-2512 residue [21–23]. To date, only homeodomain-interacting protein kinase 2 (HIPK2) and MEKK1 have been described to phosphorylate NOTCH1 at Thr-2512, promoting its subsequent proteasomal degradation [24, 25].

Dual-specificity tyrosine-phosphorylation-regulated kinase 2 (DYRK2) is a Ser/Thr kinase that plays key roles in the regulation of proliferation, cell differentiation and survival [26]. DYRK2 contributes to the regulation of various signalling pathways via the phosphorylation of relevant proteins such as NFAT, p53, c-Jun, c-Myc, eIF2Bε, tau, hPXR, glycogen synthase, CRMP4, 4E-BP1, Snail, katanin and SIAH2 [26–30]. Several studies highlighted the importance of DYRK2 impairing the development and progression of human cancers, such as non-small cell lung cancer, esophageal adenocarcinomas, breast cancer and ovarian serous adenocarcinoma [31–34]. In agreement, DYRK2 knockdown increases cancer cell growth and invasion [29]. Similarly, DYRK2 reduces epithelial–mesenchymal transition (EMT) by degrading SNAIL in ovarian cancer [33]. In response to genotoxic stress, ataxia-telangiectasia mutated (ATM) phosphorylates and stabilises DYRK2, which in turn phosphorylates p53 at Ser46 promoting apoptosis [35, 36].

This study describes for the first time DYRK2 as a new upstream negative regulator of the NOTCH1 signalling pathway. We prove that DYRK2 directly interacts with and phosphorylates Notch1-IC at Thr-2512 facilitating its proteasomal degradation by FBXW7. Moreover, we found that DYRK2 modulation by chemotherapeutic agents has a relevant effect on the viability, motility and invasion capacity

of cancer cells expressing NOTCH1. In summary, we reveal DYRK2 as a novel negative regulator of NOTCH1 levels and activity, which represents a new control mechanism of the expression and function of this transcription factor with potential implications in cancer.

Materials and methods

Cell culture, transfection and reagents

HEK-293T (wt/DYRK2$^{-/-}$/HIPK2$^{-/-}$), HeLa (wt/DYRK2$^{-/-}$/DYRK1A$^{-/-}$), MDA-MB-468 (wt/DYRK2$^{-/-}$), MDA-MB-231 (wt/DYRK2$^{-/-}$), MOR, MCF7, CHO and A549 cells were maintained in Dulbecco's Modified Eagle's Medium (DMEM) supplemented with 10% FBS (Fetal Bovine Serum) and 1% (v/v) penicillin/streptomycin (Sigma-Aldrich, St Louis, MO, USA) at 37 °C in a humidified atmosphere containing 5% CO$_2$. H727 cells were maintained in Roswell Park Memorial Institute (RPMI) medium at the same conditions. Cell lines were obtained from ATCC (LGC Standards, Teddington, Middlesex, UK) and were routinely tested to be free of mycoplasma and cross contamination. Cell lines validation was performed by a multiplex PCR with Geneprint10 System (Promega, Madison, WI, USA). MG-132 was from Enzo Life Science (Lausen, Switzerland). Transient transfections were carried out with Roti-Fect (Carl Roth, Karlsruhe, Germany) and harvested between 36 and 48 h after transfection. DNA amounts in each transfection were kept constant after the addition of empty expression vector. DYRK2 and Notch1-IC plasmids were previously described or generated in this lab by standard cloning techniques [30]. Point mutants were produced by conventional point mutagenesis. HeLa control and DYRK1A$^{-/-}$ cells were a gift from Dr. Susana de la Luna (Centre for Genomic Regulation, Barcelona, Spain). DYRK2-analogue-sensitive expression plasmid (GFP-DYRK2-AS) was previously described [37]. Myc-tagged Notch1-IC and 4xCSL vectors were provided by Dr. Hee-Sae Park (Korea Basic Science Institute, Gwang Ju, South Korea). pLentiCRISPr-V2 was a gift from Dr. Feng Zhang (Addgene plasmid # 52961). Flag-tagged Notch2-IC and Notch4-IC vectors were a gift from Dr. Raphael Kopan (Addgene plasmids # 20184 and # 20186). HA-tagged Notch1-IC plasmid was a gift from Dr. Urban Lendahl (Addgene plasmid # 47618). HA-tagged Notch1-IC WT and mutant plasmids were kindly provided by Dr. Aifantis (NYU Langone Medical Center, New York, USA). Flag-FBXW7-ΔFbox was kindly provided by Dr. Rocio Sancho (Centre for Stem Cells & Regenerative Medicine King's College London, UK). Adriamycin (ADR), harmine, etoposide (ETP) and the rest of the reagents were from Sigma-Aldrich. PP1 analogue II 1NM-PP1 (SC-203214) was obtained from Santa Cruz Biotechnology

(Santa Cruz, California, USA). Scramble control oligonucleotide siRNA non-targeting pool (D-001810) and ON-TARGET plus SMARTpool against DYRK2 (L-004730-00) were purchased from Dharmacon (Waltham, MA, USA). DYRK2 human recombinant protein was purchased from Abcam (Cambridge, UK).

Generation of CRISPR/Cas9-cell lines

The endogenous DYRK2 gene was knocked out by transfecting cells with pLentiCRISPR-v2 (which codes for Cas9 and a puromycin cassette) containing gRNAs against the first exon of the short DYRK2 isoform or a combination of gRNAs against the first and the last exon. For HeLa and MDA-MB-468 DYRK2-KO cells, the gRNA sequence used was GCTTGCCAGTGGTGCCAGAG and for MDA-MB-231 and HEK-293T DYRK2-KO cells, the gRNAs used were N-term sequence GCTTGCCAGTGGTGCCAGAG and C-term sequence GAAGCTGAGCTAGAAGGTGG. Control cells were transfected with the empty pLentiCRIS-PRV2 vector. After transfection, cells were exposed to 2 μg/ml of puromycin for 2 days followed by a medium exchange. Surviving cells were clonally selected (in the case of control cells were used as pool population) by serial dilution, and positive clones were identified by genomic analysis and western blot.

Western blotting and antibodies

Soluble fractions were obtained after lysis of cells in NP-40 buffer [20 mM Tris–HCl (pH 7.5), 150 mM NaCl, 1 mM phenylmethylsulfonyl fluoride, 10 mM NaF, 0.5 mM sodium orthovanadate, leupeptine (10 μg/ml), aprotinin (10 μg/ml), 1% (v/v) NP-40, and 10% (v/v) glycerol]. Proteins were diluted and boiled at 95 °C in SDS buffer, resolved on sodium dodecyl sulphate polyacrylamide gels (SDS-PAGE), transferred to PVDF membranes, blocked with non-fat milk in TTBS buffer and incubated with primary antibodies. The washed membranes were incubated with appropriate secondary antibodies coupled to horseradish peroxidase, which were detected by chemiluminescence using Clarity™ Western ECL Substrate (Bio-rad Hercules, California, USA). Antibodies against the FLAG epitope (clone M2, A2220) and anti-β-actin (A5316) were purchased from Sigma Aldrich; anti-ubiquitin (P4D1, 3936S) from Cell Signaling Technology (Danvers, Massachusetts, USA). Anti-Notch1 (ab25374), anti-Hes1 (ab71559) and anti-Hes5 (ab25374) were obtained from Abcam. Anti-HA (clone 3F10), anti-myc (clone 9E10), anti-GFP (11814460001) (Roche Molecular Biochemical) and anti-phosphoserine (AB1603) (Millipore, Burlington, Massachusetts, USA) were from the indicated suppliers. Anti-DYRK2 (H80; sc-66867) and anti-DYRK1A (RR7; sc-100376) antibodies were obtained from Santa Cruz

Biotechnology. Secondary horseradish peroxidase-coupled antibodies were purchased from Jackson ImmunoResearch Laboratories (Cambridgeshire, UK). Texas Red goat anti-rabbit IgG antibody (T-6391) was from Thermo Fisher Scientific (Waltham, Massachusetts, USA).

Immunoprecipitation

Cells were washed in PBS and lysed in IP buffer [50 mM Hepes (pH 7.5), 50 mM NaCl, 1% (v/v) Triton X-100, 2 mM EDTA, 10 mM sodium fluoride, 0.5 mM sodium orthovanadate, 10 μg/ml aprotinin, 10 μg/ml leupeptin, and 1 mM PMSF]. Cell lysates were pre-cleared with protein A/G Sepharose (Santa Cruz) and immunoprecipitation was performed on a rotating wheel upon the addition of 1 μg of the indicated antibodies and 25 μl of protein A/G Sepharose beads. Immunoprecipitated proteins were then washed for five times in IP buffer and eluted in 2 × SDS sample buffer, followed by western blotting.

Luciferase reporter assays

Cells were collected in PBS and lysed in luciferase assay buffer (25 mM Tris–phosphate pH 7.8, 8 mM MgCl$_2$, 1 mM DTT, 1% Triton X-100 and 7% glycerol) during 15 min at room temperature in a horizontal shaker. Luciferase assay was performed using Luciferase Assay Reagent (Promega) according to the manufacturer's instructions. Luciferase activity was measured using an Autolumat LB 953 (Berthold Technologies GmbH, Bad Wildbad, Germany) and normalised with protein concentration.

Immunofluorescence

Cells were seeded on glass coverslips and 48 h after transfection fixed with 3.7% of pre-warmed paraformaldehyde/PBS for 10 min, permeabilized with 0.1% Triton X-100/PBS for 15 min, blocked with 3% BSA/PBS and incubated overnight with primary antibodies. After being washed with PBS and incubated for 45 min with the secondary antibody, cells were mounted on glass slides with mounting medium-containing DAPI (Vectashield Burlingame, CA, USA). Fluorescence images were captured using an LSM 5 EXCITER (Carl Zeiss MicroImaging GmbH, Oberkochen, Germany) confocal laser scanning microscope using a 40 ×/1.30 oil objective (EC Plan-Neofluar) and ZEN 2008 software (Carl Zeiss MicroImaging GmbH). To determine fluorescent signal, colocalization between different channels the Coloc_2 module was used. The degree of channel colocalization was analysed by considering the following indexes: thresholded Manders' coefficients A and B and Pearson's coefficient. To evaluate the spatial relations between channel intensity, we used the ImageJ tool RGB Profiler to create a profile

of fluorescence intensity values across a line drawn on the image.

mRNA extraction and qPCR

Total RNA was extracted using the High Pure RNA Isolation kit (Roche Diagnostics, Switzerland), reverse transcription performed with the iScript cDNA Synthesis kit (Bio-Rad) and real-time PCR carried out in an iCYCLER detection system (Bio-Rad) with iQTM SYBR Green Supermix (Bio-Rad). Amplification efficiencies were validated and normalised against HPRT, and fold change in gene expression was calculated using the $2^{-\Delta\Delta C_t}$ method. Primer sequences are available upon request.

In vitro phosphorylation

Immunoprecipitated myc-tagged Notch1-IC endogenous protein was incubated with 50 ng of commercial recombinant DYRK2 protein (Millipore, 14-669) in kinase buffer (20 mM Hepes pH 7.5, 10 mM $MgCl_2$, 1 mM DTT) with or without ATP (0.1 µM). After 60 min of incubation at 37 °C, reactions were stopped using 1 M glycine pH 2.5 in agitation for 20 min at room temperature and A/G beads (Santa Cruz Biotecnology) were removed by centrifugation. Finally, readjustment of pH levels of the supernatant was performed employing 1 M Tris–HCl pH 7.5.

Cell viability and flow cytometry analyses

For apoptosis studies, cells were harvested and washed in cold PBS and then resuspended in binding buffer consisting of 10 mM Hepes, 140 mM NaCl and 2.5 mM $CaCl_2$ pH 7.4. Cells were stained with Annexin V, Alexa Fluor 488 conjugate (Molecular Probes by Life Technologies, Carlsbad, CA, USA) and propidium iodide. Cell cycle distribution and apoptosis were determined by BD FACSCanto™ flow cytometer (BD Biosciences, San Jose, CA, USA) using BD FACSDiva™ software. For cytotoxicity assay, cells were seeded in a 96-well plate and after 12 h YOYO-1 (Life Technologies) was added to a final concentration of 0.1 µM. Object counting analysis was performed using the cell imaging system IncuCyte HD (Essen BioScience).

Cell motility assay

Cells were seeded in a 96-well Essen ImageLock plate (Essen BioScience, Ann Arbor, Michigan, USA) 24 h after transfection and grown to confluence. After 12 h, the scratches were made using the 96-pin WoundMaker (Essen BioScience), followed by incubation with 10 ng/ml of mitomycin C. Wound images were taken every 60 min for 24 h and the data analysed by the integrated metric Relative Wound Density part of the live content cell imaging system IncuCyte HD (Essen BioScience).

Cell invasion assay

Invasion assays were performed in Boyden chamber using a 48-well Neuro Probe, Inc. insert system (Gaithersburg, MD, USA). Polyethylene membrane inserts (8.0 µm pore size) were precoated with 200 µg/µl of Matrigel® Matrix (Corning®, Corning, NY, USA) (in coating buffer 0.01 M Tris and 0.7% NaCl). Cells were subcultured in an mw6 plate, and 24 h prior the assay, FBS was removed from the media and ADR was added in the specific conditions. Then, cells were seeded with 2.5×10^4 cells per insert (cells suspended in 50 µl in DMEM, in addition to 25 µl FBS free DMEM in the bottom side of the chamber) and incubated at 37 °C, 5% CO_2 for 12 h. Then, the membrane was washed at least three times for 10 min with PBS. The membranes were then cut out of the inserts by a scalpel, dyed in methyl violet for 30 min and mounted between two thin cover slips. The total number of migrated cells was counted for each group ($n = 4$) with an inverted microscope. Only cells which had completely migrated through the membrane were counted.

Enrichment of His-tagged proteins

Cells were collected in PBS and pellets resuspended in lysis buffer (6 M guanidinium-HCl, 0.1 M Na_2HPO_4/NaH_2PO_4, 0.01 M Tris–HCl [pH 8], 5 mM imidazole and 0.01 M β-mercaptoethanol). Samples were sonicated and cell debris was removed by centrifugation. Supernatants were mixed with 75 µl of equilibrated Ni–NTA resin (Quiagen, Hilden, Germany), followed by incubation for 4 h at room temperature on a rotating wheel. Precipitates were washed once with lysis buffers, once in wash buffer (8 M urea, 0.1 M Na_2HPO_4/NaH_2PO_4, 0.01 M Tris–HCl [pH 6.8], 5 mM imidazole, and 0.01 M β-mercaptoethanol), and twice in wash buffer plus 0.1% Triton X-100. Proteins were eluted in 75 µl of 0.2 M imidazole, 0.15 M Tris–HCl (pH 6.8), 30% glycerol, 0.72 M β-mercaptoethanol and 5% SDS for 20 min at room temperature with gentle agitation and further analysed by immunoblotting.

Data analysis

Protein abundance in tumor tissue was obtained from The Human Protein Atlas database as antibody staining level (not detected, low, medium and high) per patient [38]. Data were accessed via the R hpar package. Gene alteration frequencies were calculated using the TCGA PanCancer dataset that includes 10967 samples across 33 different tumor types [39]. To calculate the alteration frequencies, the number of samples containing a missense/non-sense mutation or a deep
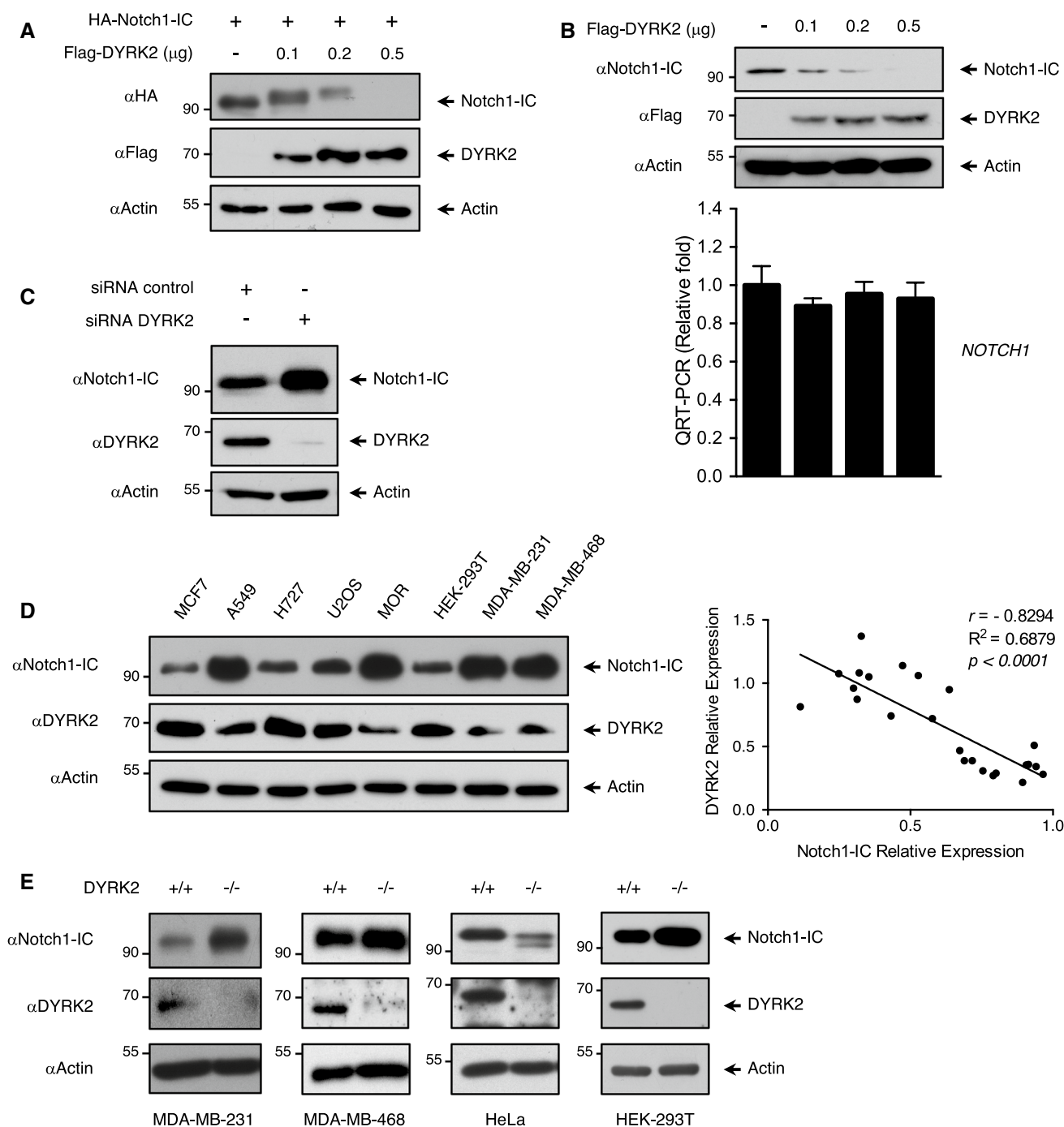
Fig. 1 NOTCH1 protein levels are modulated by DYRK2. **a** HEK-293T cells were transfected (2 × 10^5 cells in a 35-mm dish, increasing amounts of DYRK2) with the indicated plasmids and lysed 48 h after transfection. Protein expression was evaluated by immunoblotting. We show a representative blot of three independent experiments. **b** HEK-293T cells (2 × 10^5 cells in a 35 mm dish) were transfected with the indicated amounts of DYRK2, harvested and lysed. One fraction was used to analyse endogenous Notch1-IC protein levels, while another aliquot was used to analyse Notch1-IC mRNA levels by quantitative PCR. Data are mean ± SD of $n = 3$. We show a representative blot of three independent experiments. **c** HEK-293T cells were transfected with DYRK2 or scrambled (control) siRNAs, lysed

after 4 days of culture and Notch1-IC or DYRK2 analysed by western blot. We show a representative blot of three independent experiments. **d** Notch1-IC and DYRK2 endogenous protein levels were analysed in the indicated cell lines by immunoblotting. We show a representative blot of three independent experiments (left panel). Notch1-IC and DYRK2 signals from three independent experiments were quantified, normalised to actin protein levels and correlation was analysed (right panel). **e** Endogenous protein levels of DYRK2 and Notch1-IC were evaluated in MDA-MB-231, MDA-MB-468, HeLa and HEK-293T both WT and DYRK2$^{-/-}$ by immunoblot. We show a representative blot of three independent experiments
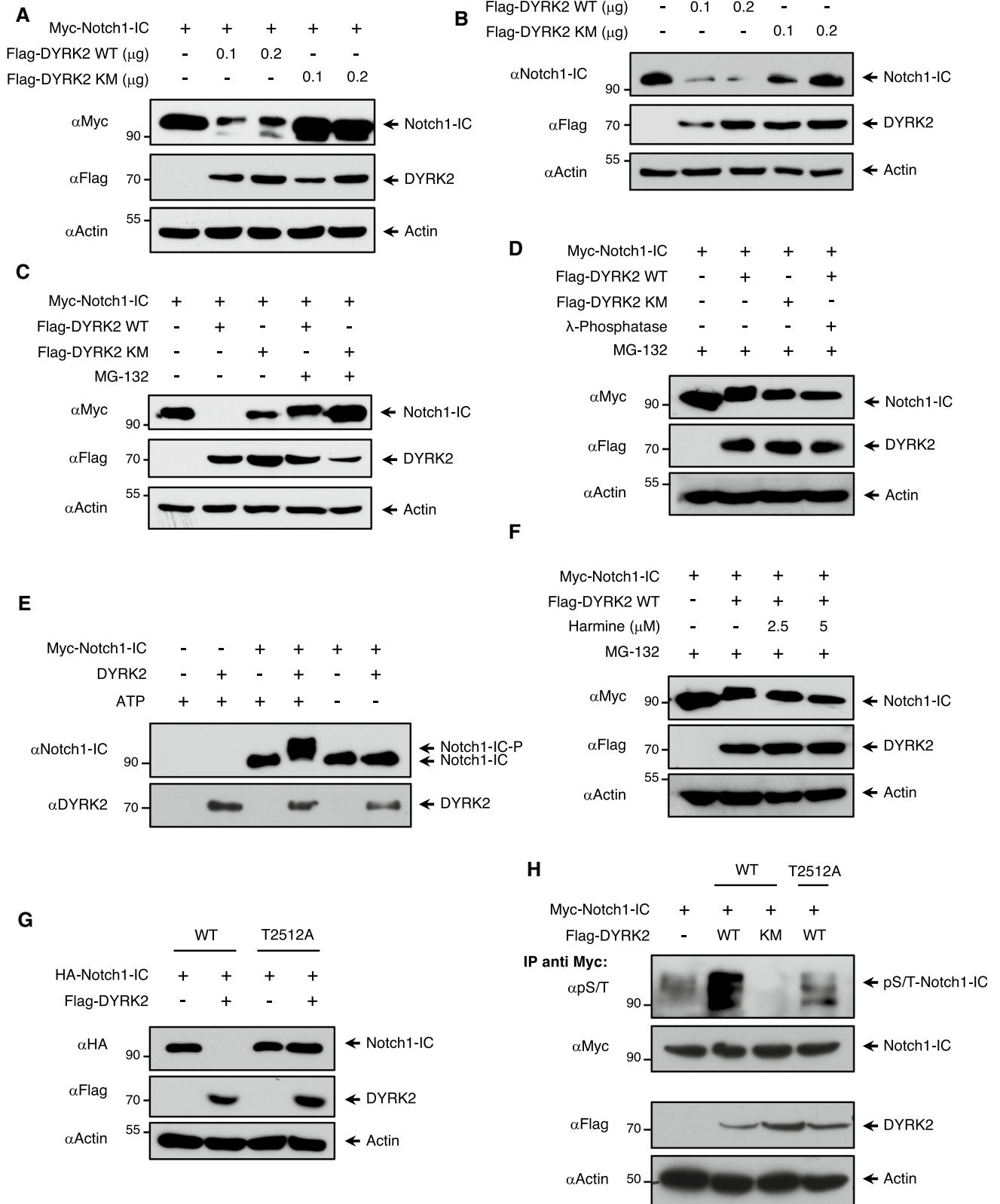
A

Myc-Notch1-IC	+	+	+	+	+
Flag-DYRK2 WT (μg)	-	0.1	0.2	-	-
Flag-DYRK2 KM (μg)	-	-	-	0.1	0.2

αMyc   ← Notch1-IC
90

αFlag   ← DYRK2
70

αActin   ← Actin
55

B

Flag-DYRK2 WT (μg)	-	0.1	0.2	-	-
Flag-DYRK2 KM (μg)	-	-	-	0.1	0.2

αNotch1-IC   ← Notch1-IC
90

αFlag   ← DYRK2
70

αActin   ← Actin
55

C

Myc-Notch1-IC	+	+	+	+	+
Flag-DYRK2 WT	-	+	-	+	-
Flag-DYRK2 KM	-	-	+	-	+
MG-132	-	-	-	+	+

αMyc   ← Notch1-IC
90

αFlag   ← DYRK2
70

αActin   ← Actin
55

D

Myc-Notch1-IC	+	+	+	+
Flag-DYRK2 WT	-	+	-	+
Flag-DYRK2 KM	-	-	+	-
λ-Phosphatase	-	-	-	+
MG-132	+	+	+	+

αMyc   ← Notch1-IC
90

αFlag   ← DYRK2
70

αActin   ← Actin
55

E

Myc-Notch1-IC	-	-	+	+	+	+
DYRK2	-	+	-	+	-	+
ATP	+	+	+	+	-	-

αNotch1-IC   ← Notch1-IC-P
90   ← Notch1-IC

αDYRK2   ← DYRK2
70

F

Myc-Notch1-IC	+	+	+	+
Flag-DYRK2 WT	-	+	+	+
Harmine (μM)	-	-	2.5	5
MG-132	+	+	+	+

αMyc   ← Notch1-IC
90

αFlag   ← DYRK2
70

αActin   ← Actin
55

G

		WT		T2512A	
HA-Notch1-IC		+	+	+	+
Flag-DYRK2		-	+	-	+

αHA   ← Notch1-IC
90

αFlag   ← DYRK2
70

αActin   ← Actin
55

H

			WT		T2512A
Myc-Notch1-IC		+	+	+	+
Flag-DYRK2		-	WT	KM	WT

IP anti Myc:

αpS/T   ← pS/T-Notch1-IC
90

αMyc   ← Notch1-IC
90

αFlag   ← DYRK2
70

αActin   ← Actin
50

◄**Fig. 2** DYRK2 phosphorylates Notch1-IC. **a** HEK-293T cells were transfected to express Myc-Notch1-IC and increasing amounts of Flag-DYRK2 wild type (WT) or kinase mutant (KM). Cell lysates were analysed by immunoblotting with the indicated antibodies. We show a representative blot of four independent experiments. **b** HEK-293T cells were transfected to express DYRK2 WT or KM. Twenty-four hours post-transfection, cells were lysed and protein expression was analysed by immunoblot with the indicated antibodies. We show a representative blot of three independent experiments. **c** HEK-239T cells were co-transfected with the indicated plasmids and then treated or not for 12 h with the proteasome inhibitor MG-132 (10 μM). Cell lysates were analysed by immunoblotting with anti-Myc and Flag antibodies. We show a representative blot of three independent experiments. **d** HEK-293T cells were transfected with the indicated plasmids and treated with MG-132 for 12 h and were lysed in phosphatase inhibitor-free buffer in the absence or presence of λ-phosphatase. Electrophoretic mobility was determined by immunoblotting. We show a representative blot of four independent experiments. **e** Immunoprecipitated Notch1-IC endogenous protein from HEK-293T cells was incubated with DYRK2 recombinant protein in the presence or absence of ATP (0.1 μM). Electrophoretic mobility was determined by immunoblotting with the indicated antibodies. We show a representative blot of four independent experiments. **f** HEK-239T cells were co-transfected with the indicated plasmids and after 36 h treated with MG-132 in the presence or not of harmine for 12 h before lysis. Protein expression was analysed by immunoblot with the indicated antibodies. We show a representative blot of three independent experiments. **g** Cells were transfected to express HA-Notch1-IC WT or HA-Notch1-IC T2512A (threonine 2512 mutated to alanine) in the presence or not of Flag-DYRK2 WT. Cells were further cultivated and lysed and protein expression was analysed by immunoblot with the indicated antibodies. We show a representative blot of three independent experiments. **h** HEK-293T cells were transfected to express Myc-Notch1-IC WT or Myc-Notch1-IC T2512A in the presence or not of Flag-DYRK2-WT or KM and, after 36 h, treated with MG-132 for 8 h and lysed. A fraction was subjected to immunoprecipitation (IP) using anti-Myc antibody. After elution phosphorylation was revealed with an anti-phospho-serine/threonine antibody, while exogenous Notch1-IC protein levels were visualised with an anti-Myc antibody by western blotting (top panel). The remaining extract fraction was tested for the occurrence of the indicated proteins (lower panel). We show a representative blot of three independent experiments

deletion for a given gene was divided by the total number of samples in a given cancer type. Data were accessed via the cBioPortal web service using the R cgdsr package [40]. Images were evaluated and quantified using the Image J (http://rsbweb.nih.gov/ij/). Data are expressed as mean ± SD. Differences were analysed by Student's t test. $P < 0.05$ was considered significant. Statistical analysis was performed using GraphPad Prism® version 6.01 (GraphPad, San Diego, CA, USA).

Results

Notch1-IC protein levels are modulated by DYRK2

To identify new potential DYRK2 interaction partners, we performed an immunoprecipitation assay followed by mass spectrometry (Fig. S1a and Supplementary Materials and methods). As NOTCH1 and other members of the family showed positive results, we decided to focus on this protein in detail. We first co-expressed Notch1-IC alone or with increasing amounts of DYRK2 in HEK-293T cells. Expression of DYRK2 resulted in a dose-dependent decrease in Notch1-IC protein levels, which was accompanied by the appearance of slower migrating bands (Fig. 1a). The activity of the rest of the members of human DYRK subfamily protein kinases (DYRK1A, DYRK1B, DYRK2, DYRK3, and DYRK4) was also analysed. As shown in Supplementary Figure S1b, DYRK1A and DYRK1B overexpression showed a similar effect as compared to DYRK2, which was not observed with DYRK3 and 4. Similarly, DYRK2 overexpression resulted in a decrease of the rest of NOTCH human family members (NOTCH2, NOTCH3 and NOTCH4) (Fig. S1c).

Next, we decided to analyse the impact of DYRK2 expression on the levels of endogenous Notch1-IC. Transfection of increasing amounts of DYRK2 led to a dose-dependent decrease of endogenous Notch1-IC protein levels without affecting its mRNA expression (Fig. 1b). Similar results were obtained with DYRK1B (Fig. S1d). It has been previously described that DYRK1A phosphorylates NOTCH1 [41]. In this sense, the specificity of the antibodies and plasmids used for DYRK2 detection was analysed (Fig. S1e). In addition, DYRK2 effect on endogenous Notch1-IC protein levels was reanalysed in DYRK1A knockout cells obtaining similar results (Fig. S1f). Then we analysed the effect of knocking down DYRK2 using a specific siRNA. In agreement with our previous results, DYRK2 depletion increased Notch1-IC levels (Fig. 1c) as well as its half-life (Fig. S1g), further proving that Notch1-IC basal levels were regulated by DYRK2.

Our results suggested that DYRK2 might negatively regulate NOTCH1 protein levels, and thus we hypothesised that the endogenous levels of DYRK2 and NOTCH1 might show a correlation. To test our hypothesis, we analysed the levels of these two proteins in eight different cell lines, and as shown in Fig. 1d, a negative correlation was observed. Next, to further confirm the ability of this kinase to regulate Notch1-IC, DYRK2 knockout cell lines were generated by CRISPR/Cas9 gene-editing tools and Notch1-IC protein levels were evaluated. As shown in Fig. 1e, specific stable DYRK2 knockout resulted in increased levels of Notch1-IC in three of the four cell lines tested. In the case of HeLa, DYRK2 knockout led to the appearance of faster migrating bands, which might reflect unphosphorylated NOTCH1. Collectively, these results demonstrate that DYRK2 negatively regulates Notch1-IC levels.
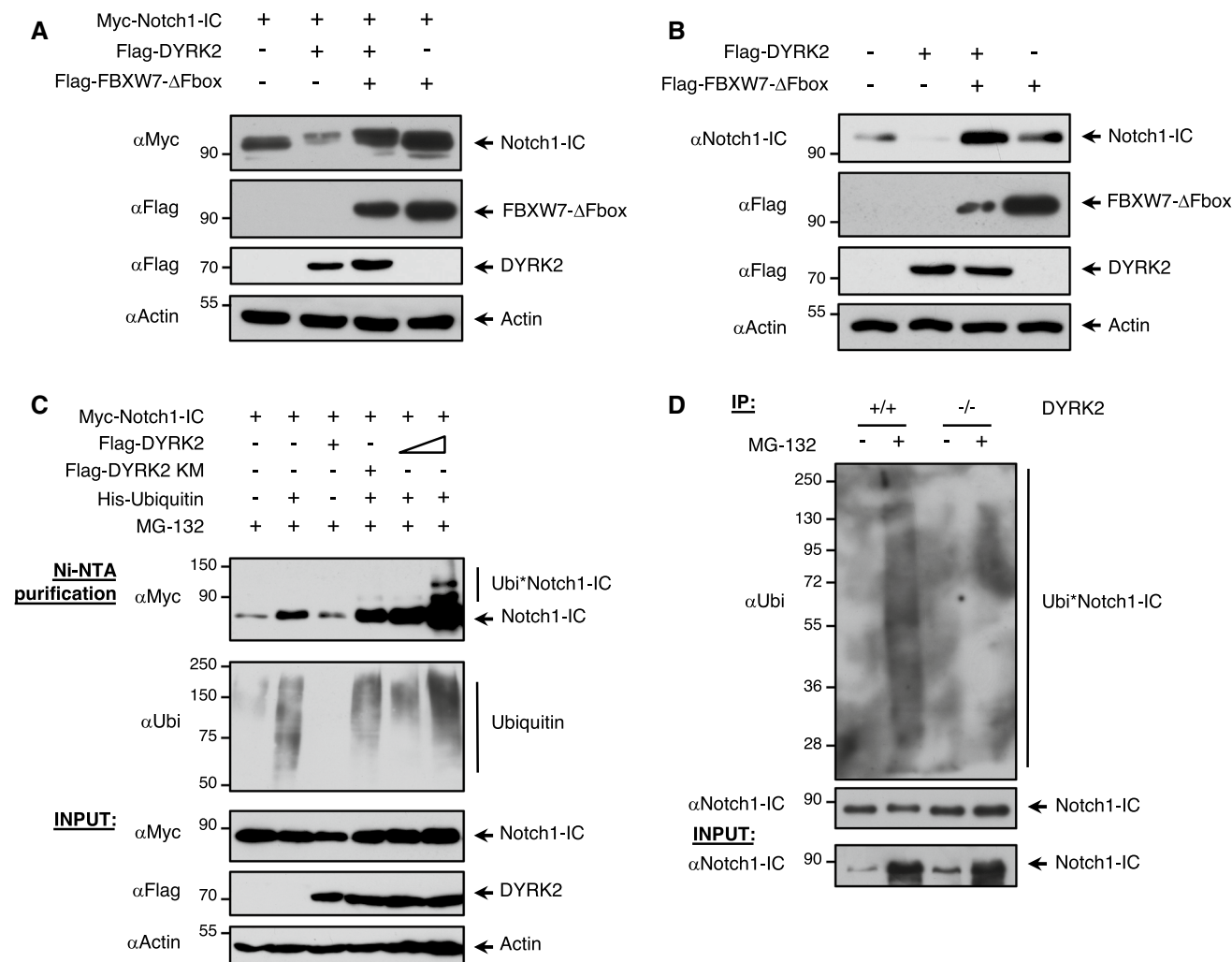
Fig. 3 DYRK2 regulates Notch1-IC protein levels via Fbxw7-mediated proteasomal degradation. **a** HEK-293T cells were co-transfected to express Notch1-IC together with DYRK2, and the levels were evaluated in response to FBXW7 dominant negative (FBXW7-ΔFbox) lacking the F-box domain that recruits ubiquitination machinery. We show a representative blot of three independent experiments. **b** HEK-293T cells were transfected with Flag-DYRK2 in the presence or absence of a dominant-negative form of FBXW7. Endogenous Notch1-IC protein levels were evaluated by western blotting. We show a representative blot of three independent experiments. **c** HEK-293T cells were transfected with expression plasmids encoding Flag-tagged DYRK2, Myc-tagged Notch1-IC and His-tagged ubiquitin.

After 36 h, cells were incubated in the presence of MG-132 (10 µM) during 12 h and lysed under denaturing conditions. His-tagged ubiquitin was purified with Ni–NTA agarose columns and ubiquitinated Notch1-IC was analysed by western blotting. A fraction was tested for the occurrence of the indicated proteins (INPUT). We show a representative blot of three independent experiments. **d** Wild-type and DYRK2$^{-/-}$ MDA-MB-231 cells were stimulated or not with MG-132 during 9 h, lysed and subjected to immunoprecipitation using anti-Notch1-IC antibody. A small fraction of the lysate was tested for the occurrence of Notch1-IC (INPUT). The precipitates were subjected to western blot analysis with anti-Notch1-IC or anti-Ubi antibodies. We show a representative blot of three independent experiments

DYRK2 phosphorylates Notch1-IC in vivo and in vitro

Based on the capacity of DYRK2 to induce the appearance of slower migrating bands compatible with phospho-forms of Notch1-IC, next we analysed whether DYRK2 kinase activity was necessary for its effect on Notch1-IC levels. We co-expressed Notch1-IC with either increasing amounts of DYRK2 or a kinase point mutant version (DYRK2 KM). As shown in Fig. 2a, DYRK2 overexpression led to a reduction of Notch1-IC levels concomitant with the appearance

of upshifted bands. By contrast, Notch1-IC levels were not altered in the presence of the DYRK2 KM. Similar results were obtained at the endogenous level (Fig. 2b). To test whether that reduction in protein levels was mediated by protein degradation, we decided to examine this effect in the presence or absence of the proteasome inhibitor MG-132. As shown in Fig. 2c, the addition of MG-132 considerably prevented DYRK2-mediated Notch1-IC degradation and stabilised band mobility. To confirm that the upshifted Notch1-IC bands were phosphorylated forms, we incubated

cell extracts with λ-phosphatase in the presence of MG-132. As shown in Fig. 2d, λ-phosphatase treatment transformed a slower electrophoretic band mobility into a faster migrating movement, similar to those obtained in response to DYRK2 KM expression. To evaluate the ability of DYRK2 to directly phosphorylate Notch1-IC, we performed an in vitro kinase assay (Fig. 2e). The presence of recombinant DYRK2 showed the occurrence of upper Notch1-IC bands, which appeared only in the presence of ATP. Moreover, the relevance of the DYRK2 kinase activity for Notch1-IC was highlighted by experiments with chemical inhibitors. As shown in Figure S2a, treatment with the pan-specific DYRK inhibitor harmine inhibited the negative effect of DYRK2 on Notch1-IC levels, and also caused a clear increase in the motility of the Notch1-IC bands in the presence of MG-132 (Fig. 2f). Similar results were obtained with curcumin, another DYRK2 inhibitor [42] (Fig. S2b). Altogether, these experiments demonstrate that DYRK2 directly phosphorylates Notch1-IC.

To identify the Notch1-IC sites phosphorylated by DYRK2, we analysed different relevant residues mutated to alanine involved in Notch1-IC regulation previously described [22]. Co-expression of the mutants with DYRK2 and subsequent analysis of their electrophoretic behaviour showed that mutation of Thr-2512 significantly reduced DYRK2-mediated Notch1-IC degradation (Fig. S2c). Similar results were obtained when we compared the co-expression of DYRK2 with Notch1-IC WT vs T2512A (Fig. 2g), indicating that phosphorylation of Thr-2512 is necessary for the effect of DYRK2 on Notch1-IC stability. To further prove that DYRK2 phosphorylates Notch1-IC in cells, NOTCH1 WT and T2512A phospho-deficient mutant constructs were transfected together with DYRK2 WT or DYRK2 KM, immunoprecipitated, and their phosphorylation status was analysed with a phospho-serine/threonine antibody (as there is no specific phospho-T2512 NOTCH1 antibody available) (Fig. 2h). Mutation of Thr-2512 to alanine clearly reduced the phosphorylation of Notch1-IC mediated by DYRK2 (by comparing lanes 2 and 4). However, DYRK2 was still able to induce some phosphorylation in the T2512A Notch1-IC mutant, indicating that it might not be the only site phosphorylated by DYRK2 in cells. Collectively, these results clearly demonstrate that DYRK2-mediated phosphorylation of Notch1-IC at threonine 2512 is crucial for its degradation.

DYRK2 regulates proteasomal degradation of Notch1-IC

As shown in Fig. 2c, treatment with the proteasome inhibitor MG-132 restored the level of Notch1-IC upon DYRK2 expression (lanes 2 and 4). These results indicated that DYRK2 decreased the stability of Notch1-IC through a ubiquitin/proteasome-dependent process. Based on the

previous reports showing that Thr-2512 phosphorylation facilitated Notch1-IC proteasomal degradation through FBXW7 [21], we decided to evaluate if this ubiquitin ligase was implicated in the degradation of Notch1-IC mediated by DYRK2. To analyse the role of FBXW7 in this process, we first co-expressed DYRK2 and Notch1-IC in the presence or absence of a dominant-negative form of FBXW7 lacking the F-box (FBXW7ΔFbox). As shown in Fig. 3a, FBXW7ΔFbox expression recovered the level of Notch1-IC decreased by DYRK2, preserving the reduction of the band mobility. Similar results were obtained at the endogenous level (Fig. 3b). These results showed that FBXW7 is important for the degradation of NOTCH1 mediated by DYRK2.

We next examined the effect of DYRK2 on Notch1-IC ubiquitination. We co-expressed Myc-Notch1-IC and His-Ubiquitin with or without different concentrations of DYRK2 and DYRK2 KM in the presence of MG-132 and analysed the ubiquitination status of Notch1-IC. As shown in Fig. 3c, Notch1-IC polyubiquitination became more evident in the presence of increasing concentrations of DYRK2. Furthermore, we examined the effect of DYRK2 depletion on the basal level of Notch1-IC polyubiquitination, comparing control and DYRK2$^{-/-}$ cells in the presence or absence of MG-132. As shown in Fig. 3d, ubiquitination levels of Notch1-IC were significantly lower in cells lacking DYRK2. Collectively, these data show that DYRK2 promotes basal Notch1-IC polyubiquitination and proteasomal degradation via FBXW7.

DYRK2 interacts and colocalizes with Notch1-IC

Next, we analysed the ability of DYRK2 to interact with Notch1-IC. We first co-expressed Myc-Notch1-IC alone or in the presence of Flag-DYRK2 and performed coimmunoprecipitation assays. As shown in Fig. 4a, DYRK2 coimmunoprecipitated efficiently with Notch1-IC. Then, we analysed the subcellular localization of both proteins and the effect of DNA damage. Confocal microscopy showed that GFP-DYRK2 and endogenous Notch1-IC mainly colocalize in the nucleus, with a high degree of nuclear localization of DYRK2 in cells stimulated with ETP (Pearson's coefficient = 0.65 and Manders' coefficients of $A = 0.789$; $B = 0.773$) (Fig. 4b and c).

To map the interaction sites of Notch1-IC with DYRK2, first we performed an in vitro interaction peptide array experiment. A peptide library consisting of overlapping fragments representing the entire Notch1-IC or DYRK2 proteins was incubated with GST-DYRK2 or GST-Notch1-IC, respectively, using GST as a control. Detection of bound material by antibodies showed six potential binding regions of Notch1-IC with DYRK2. Likewise, DYRK2 showed two potential binding regions with Notch1-IC,
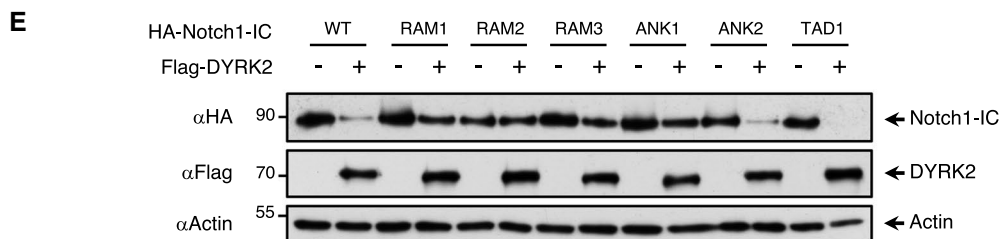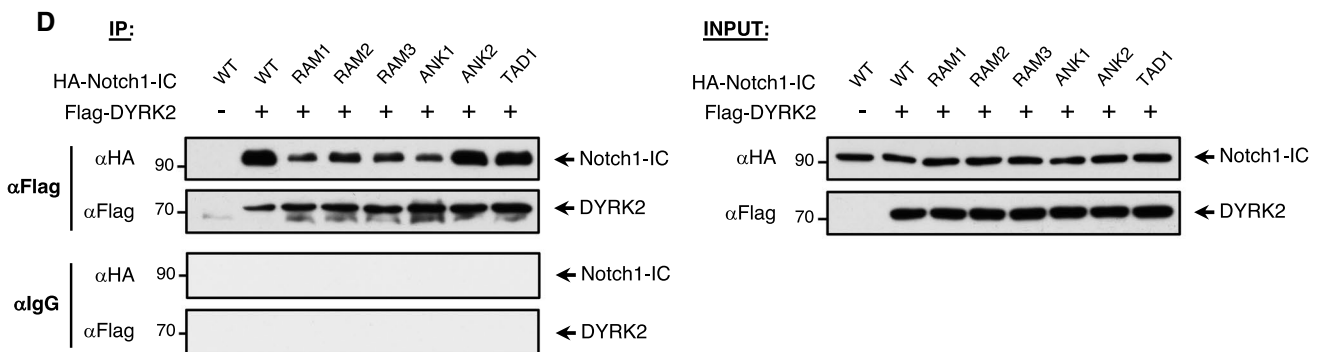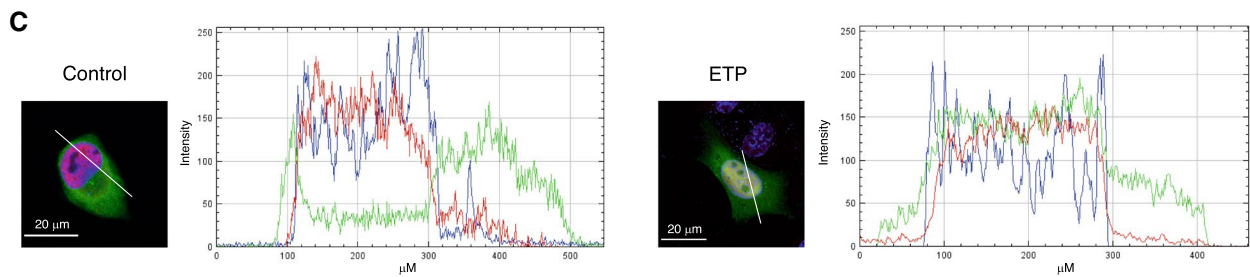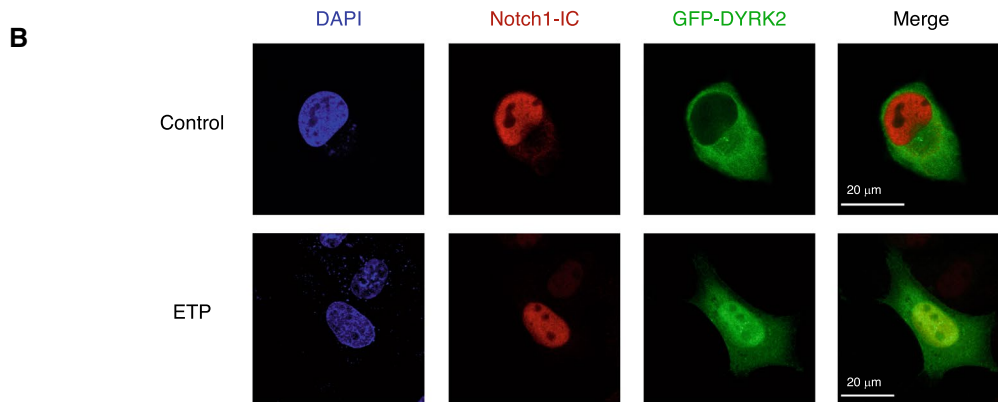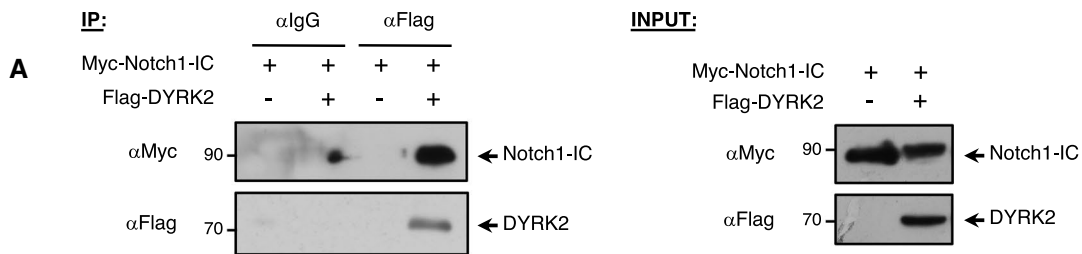
◄Fig. 4 Notch1-IC interacts and colocalizes with DYRK2. **a** HEK-293T cells were transfected with expression plasmids Myc-tagged Notch1-IC and Flag-DYRK2 as indicated and after 36 h the proteasome inhibitor MG-132 was added for another 12 h to avoid Notch1 degradation. Cells were lysed and subjected to immunoprecipitation (IP) using anti-Flag antibody. After elution, Myc-Notch1-IC protein was detected by western blotting. A small fraction (5%) of the lysate was tested for the occurrence of the indicated proteins by immunoblot (INPUT). The positions and molecular weights (in kDa) are indicated. We show a representative blot of three independent experiments. **b** CHO cells were transfected with GFP-DYRK2 and analysed for the subcellular localization of DYRK2 and endogenous Notch1-IC proteins by confocal microscopy stimulated or not during 6 h with ETP (10 μM). Nuclear DNA was stained with DAPI. We show a representative picture where overlapping localization in merged pictures is shown in yellow. **c** Fluorescence intensity profiles through the white line shown indicate GFP-DYRK2 and Notch1-IC cellular localization in both control and DNA damage conditions. Pearson's coefficient (0.65) and thresholded Manders' coefficients *A* and *B* ($A = 0.789$; $B = 0.773$) were calculated for both situations. **d** HEK-293T cells were transfected with Flag-DYRK2 and HA-Notch1-IC plasmids (WT and mutant versions) as indicated, and after 36 h the proteasome inhibitor MG-132 (10 μM) was added for another 12 h. Cells were lysed, subjected to immunoprecipitation (IP) using anti-Flag antibody and the different proteins detected by western blotting (left panel). A small fraction (5%) of the lysate was tested by immunoblot for the occurrence of the indicated proteins (INPUT, right panel). We show a representative blot of three independent experiments. **e** HEK-293T cells were co-transfected with HA-Notch1-IC or the indicated mutants either alone or along with DYRK2. After 36 h, cells were lysed and the stability of Notch1-IC was revealed by immunoblotting. We show a representative blot of three independent experiments

which correspond to the C-terminal region of the protein (Fig. S4a and S4b). Next, to validate the functional relevance of the regions present in Notch1-IC, all were mutated and tested for their interaction with DYRK2 (Notch1-IC mutant constructs. Fig. S4c). As shown in Fig. 4d, the individual mutation of the regions in the RAM domain and one adjacent in the ANK (ankyrin) domain caused a marked reduction in the ability to coimmunoprecipitated efficiently with DYRK2. Furthermore, the ability of DYRK2 to negatively regulate Notch1-IC protein levels was strongly reduced (Fig. 4e and S4d). All these results clearly prove the direct interaction between Notch1-IC and DYRK2, and suggest the existence of more than one region responsible for binding in both proteins, highlighting the possible relevant role of the RAM domain present in Notch1-IC.

Genotoxic stress induces Notch1-IC degradation mediated by DYRK2

Next, we decided to evaluate the physiological relevance of the observed effect of DYRK2 on Notch1-IC levels. Among the stimuli able to regulate the activity of this kinase, the

response to DNA damage upon exposure to genotoxic stress [30, 35, 36] stands out. Therefore, we tested the ability of DNA damage to regulate NOTCH1 signalling via DYRK2. HEK-293T cells were stimulated with increasing concentrations of DNA-damaging agent adriamycin (ADR) and protein levels of both Notch1-IC and DYRK2 were evaluated by western blot. As depicted in Fig. 5a, upregulation of DYRK2 in response to ADR was inversely correlated with Notch1-IC protein levels. Similar results were obtained in MDA-MB-231 cells (Fig. S5a), DYRK1A knockout cells (Fig. S5b) and with other genotoxic agents such as etoposide and cisplatin in different cell lines (Fig. S5c and S5d). Next, we evaluated the consequences of genotoxic stress on Notch1-IC transcriptional activity. In agreement with our previous results, ADR treatment impaired Notch1-IC transcriptional activity (Fig. 5b). Similar results were obtained with HIPK2 knockout cells (Fig. S5e) and after DYRK2 overexpression (Fig. S5f). We then investigated whether modulation of DYRK2 levels affected the transcriptional activity of Notch1-IC. As shown in Fig. 5c, ectopic expression of DYRK2 reduced Notch1-IC transcriptional activity. Moreover, Hes5 and Hes1 induction by Notch1-IC at both mRNA and protein levels was reduced by DYRK2 overexpression. Similarly, to demonstrate the role of DYRK2 kinase activity on the control of Notch1-IC transcriptional activity, we used an analogue-sensitive DYRK2 form (DYRK2-AS), which presents a mutation in the gatekeeper residue and is selectively sensitive to PP1 inhibitors [43]. As shown in Figure S5g, the specific inhibition of DYRK2 activity by PP1 analogue II stimulation reduced drastically the effect of DYRK2 on Notch1-IC protein levels with clear effects on Hes5 at both mRNA and protein levels. Taken together, these results further suggest that DYRK2 modulates Notch1-IC regulation in response to genotoxic stress.

To demonstrate the role of DYRK2 on the regulation of Notch1-IC in response to DNA damage, we assessed the effect of DYRK2 knockdown with siRNA. As shown in Fig. 5d, DYRK2 depletion avoided adriamycin-mediated reduction of Notch1-IC (lanes 2 and 5). In the same sense, Hes5 and Hes1 expression (RNA and protein) reduced by ADR treatment was restored by harmine and DYRK2 knockdown (lanes 2, 3 and 5) in MDA-MB-231 cells. Similar results were obtained in HEK-293T cells (Fig. S5h). Finally, we compared the effect of Notch1-IC ectopic expression in knockout cells lacking DYRK2. As shown in Figure S5i, Notch1-IC-induced expression of luciferase reporter gene was higher in DYRK2 knockout cells than in control cells. Altogether these data suggest that DYRK2 has a relevant role on Notch1-IC protein levels and activity in response to DNA damage.
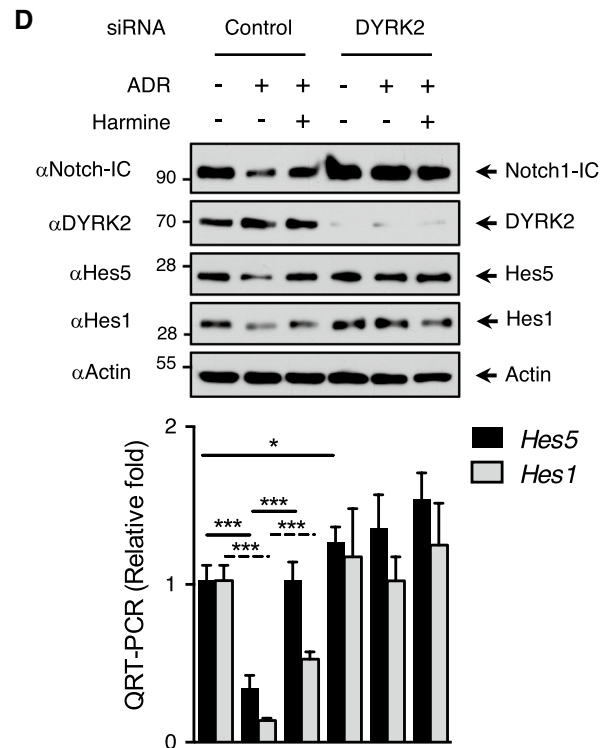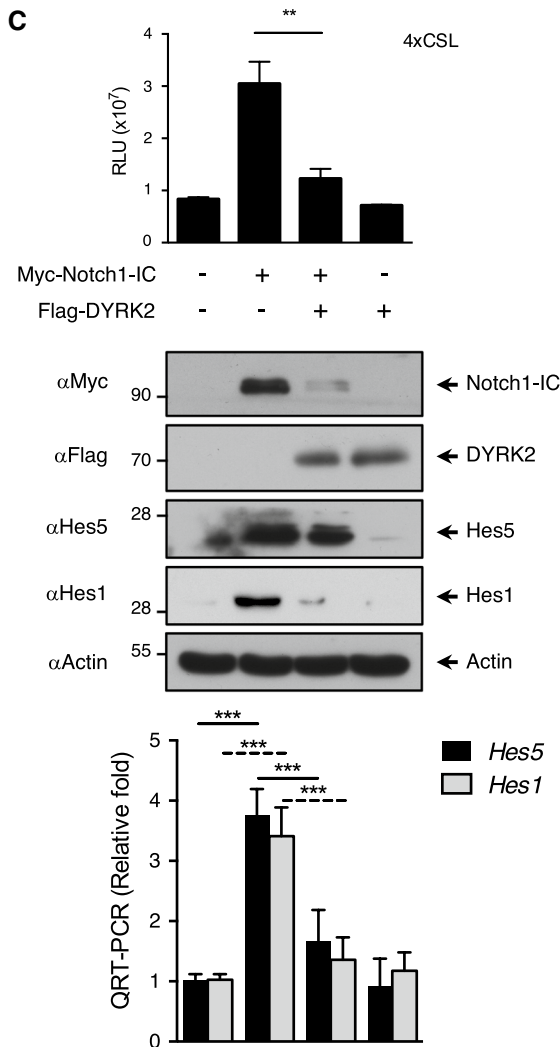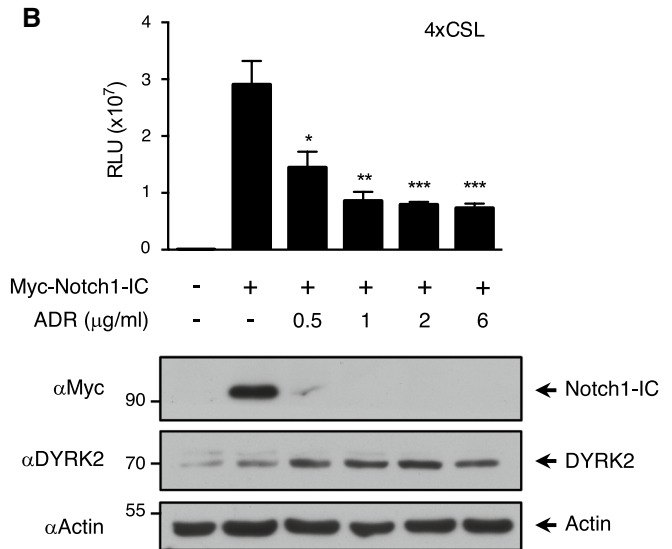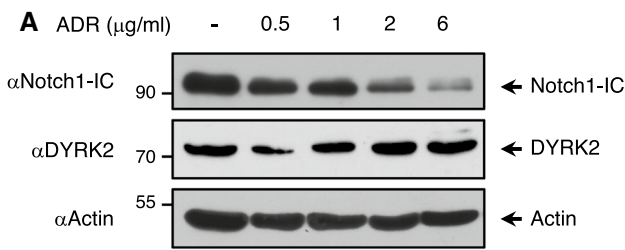
DYRK2 modulation modifies Notch1-IC physiological effects

Finally, in order to investigate the clinical significance of our findings, we first analysed data from the public database The Human Protein Atlas to determine the protein abundance of

DYRK2 and NOTCH1 in tumour tissues. As we previously observed in different cell lines, a considerable number of tissues present in a high number of patients showed low levels of DYRK2 expression and a high NOTCH1 abundance, from which the differences observed in ovarian, cervical, colorectal or pancreatic cancer stand out (Fig. 6a).

◄**Fig. 5** Genotoxic stress affects Notch1-IC signalling via DYRK2. **a** HEK-293T cells were stimulated with increasing concentrations of ADR for 12 h, lysed and endogenous levels of Notch1-IC and DYRK2 measured by immunoblotting. We show a representative blot of four independent experiments. **b** HEK-293T cells were transfected with the indicated plasmids and the 4xCSL-luciferase reporter and 24 h later stimulated with the indicated doses of ADR for another 12 h. Cells were lysed and one aliquot was used for the luciferase reporter assay (upper panel), while another fraction was used to analyse the levels of the indicated protein by immunoblot. We show a representative blot of three independent experiments. Data are mean ± SD of $n = 3$ experiments. *$P < 0.05$, **$P < 0.01$, ***$P < 0.001$. **c** HEK-293T cells were transfected with the indicated plasmids. One aliquot was used for the luciferase reporter assay and immunoblot (upper panel), while another was used to analyse *Hes5* and *Hes1* mRNA levels by qPCR (lower panel). We show a representative blot of three independent experiments. Data are mean ± SD of n = 3 experiments. ***$P < 0.001$. **d** MDA-MB-231 cells were transfected with DYRK2 or scrambled (control) siRNAs and, after 3 days of culture, stimulated or not with ADR (2 μg/ml) for 12 h in the presence or absence of harmine (5 μM). One fraction was used to analyse the levels of the indicated protein by immunoblot (upper panel), while another was used to analyse Hes5 and Hes1 mRNA levels by qPCR (lower panel). We show a representative blot of three independent experiments. Data are mean ± SD of $n = 3$ experiments. *$P < 0.05$, ***$P < 0.001$

Similarly, the analysis of the frequency of loss-of-function mutations on DYRK2 and/or NOTCH1 in tumours showed that mutations on DYRK2 and NOTCH1 occur very rarely together, suggesting that both proteins might be in the same pathway (Fig. 6b). Next, we examined the effect of DYRK2 modulation on cell viability and apoptosis in response to ADR. We observed that knocking down DYRK2 in MDA-MB-231 cells increased cell viability in response to ADR (Fig. 6c). However, the opposite effect was observed with cells overexpressing DYRK2, showing a strong reduction on cell survival in response to ADR. In the same context, the percentage of apoptotic cells upon exposure to ADR was increased by DYRK2 overexpression, and a significant reduction was observed in the presence of harmine in MDA-MB-231 (Fig. 6d) and MDA-MB-468 cells (Fig. S6a). Similarly, DYRK2 overexpression affected the expression of genes involved in cell viability such as *BCL2* (Fig. S6b). Additionally, DYRK2 is necessary for adriamycin-induced suppression of cell invasion (Fig. 6e). Finally, cell motility experiments in MDA-MB-231 (Fig. 6f) and MDA-MB-468 cells (Fig. S6c) showed that, although in the presence of DYRK2 the protein levels of Notch1-IC affected cancer cell migration significantly, Notch1-IC overexpression considerably increased cell migration of DYRK2-KO cells, suggesting that DYRK2 restrains Notch1-mediated cancer cell migration. Associated with these results, changes in the expression of genes related with mobility and invasion, such as *FGF*, *TFG-β, TNF* or *OCT-4*, were observed (Fig. S6d).

Altogether, these results indicate a new role of DYRK2 in cancer cell migration/invasion through the regulation of Notch1-IC levels.

Discussion

In the present work, we describe DYRK2 as a new kinase that regulates NOTCH1 pathway via phosphorylation, controlling its protein levels and activity in response to DNA damage. Different reports have shown how some kinases have the ability to regulate Notch1-IC by phosphorylation, thus facilitating its subsequent ubiquitination. Phosphorylation of the PEST domain is a substrate for recognition by FBXW7, which binds directly to Notch1-IC promoting its polyubiquitination and proteasomal degradation recruiting the components of an SCF ubiquitin ligase complex degradation [18, 20, 21]. Although different kinases such as cyclin C and various CDKs (CDK3, CDK8 and CDK19) [44] have been described able to regulate Notch1-IC by phosphorylation of the PEST domain, requirement of previous Thr-2512 phosphorylation for FBXW7 interaction has been described in bibliography [22, 23]. To date, to our knowledge, only MEKK1 and HIPK2 have been described to be able to phosphorylate Thr-2512 and promote proteasomal degradation of Notch1-IC by this pathway [18, 25]. Our findings show that DYRK2 is also able to directly phosphorylate Notch1-IC at Thr-2512 in the PEST domain and facilitate its proteasomal degradation.

Our results related to the interaction between Notch1-IC and DYRK2 suggest the possible relevant role of the RAM domain present in Notch1-IC. Previous studies suggested that the primary function of the RAM region is to recruit Notch1-IC to CSL [45, 46], which, together with MAML1, stimulate the transcription of target genes. In this sense, further studies should be done to clarify whether the interaction with DYRK2 in response to some stimuli could presumably inhibit Notch1-IC downstream signalling through interaction with this domain.

It is also important to mention the evolutive proximity between DYRK2 and HIPK2. Both kinases belong to the CMGC group and are evolutionarily very close [26]. They are both ubiquitinated by MDM2 [36, 47] and SIAH2 ubiquitin ligases, and present both common and specific substrates for each of them [30, 48]. Similarly, although both respond to certain common stimuli, they may also be present in some pathways exclusively. In the specific case of cellular response to DNA damage stimulus, both kinases are able to phosphorylate p53 at Ser46 to irreversibly induce p53-dependent apoptosis [35, 49]. Our findings indicate that Notch1-IC regulation seems to be also common for both
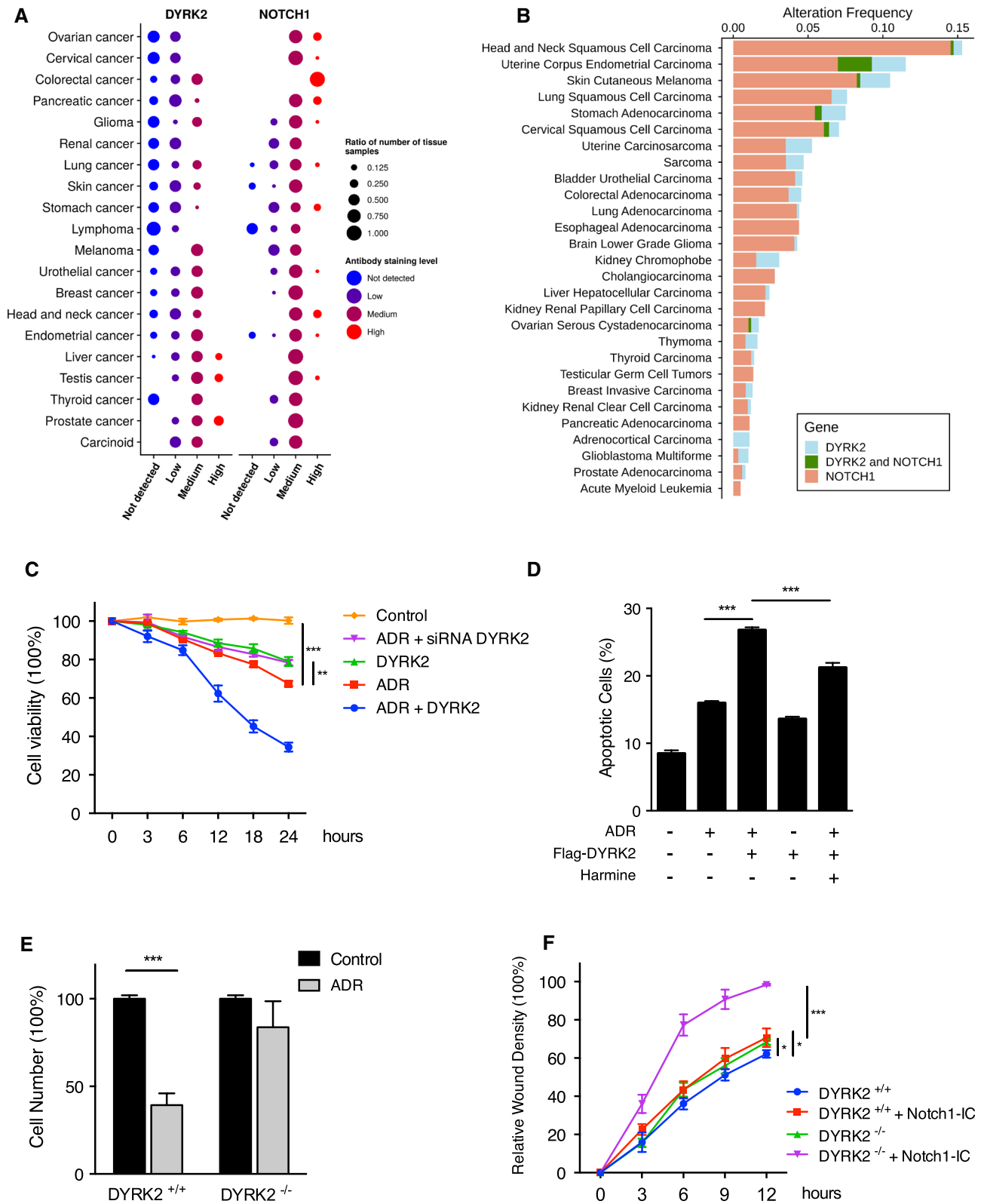
◄**Fig. 6** DYRK2 inhibition increases Notch1-IC tumorigenesis effect in breast cancer. **a** DYRK2 and NOTCH1 protein abundance in tumour tissues obtained from The Human Protein Atlas. Column and circle colour show the antibody stain level observed in tumour tissues. The point size indicates the number of patients showing particular expression to the total patients. The tumour tissues were sorted based on the abundance score differences between proteins. To calculate this, every staining level was assigned to a number (Not detected: 1, Low: 2, Medium: 3 and High: 4) and multiplied by the number of patients for each tissue and protein. Then, the absolute mean differences were calculated for every tumour tissue. **b** DYRK2 and NOTCH1 mutation frequency separately or together (missense, non-sense or deep deletions) for every tumour type included in the TCGA PanCancer dataset. **c** MDA-MB-231 cells were transfected with DYRK2 or scrambled (control) siRNAs or Flag-DYRK2 as indicated, and after 48 h of culture stimulated or not with ADR (2 μg/ml). Cell viability was determined using YOYO-1 fluorescence. Data are mean ± SD of n = 3 experiments. **P < 0.01, ***P < 0.001. **d** MDA-MB-231 cells were transfected or not with Flag-DYRK2 and after 36 h of culture stimulated or not with ADR (2 μg/ml) for 12 h in the presence or absence of harmine (5 μM) and used for apoptosis analysis by Annexin V/PI staining. Cell viability was measured by flow cytometry. Data are mean ± SD of n = 3 experiments. **P < 0.01, ***P < 0.001. **e** MDA-MB-231 WT and DYRK2 $^{-/-}$ cells were stimulated or not with ADR (2 μg/ml) for 12 h and used for matrigel motility assays. Data are mean ± SD of n = 3 experiments. ***P < 0.001. **f** MDA-MB-231 WT and DYRK2 $^{-/-}$ cells were transfected or not with Flag-Notch1-IC and after 36 h used for cell motility assays. Data are mean ± SD of n = 3 experiments. *P < 0.05, ***P < 0.001

kinases, being the action mechanism of DYRK2 described in this study HIPK2 independent (Figure S5e and data not shown). The concerted regulation in response to DNA damage of Notch1-IC executed by DYRK2 and also HIPK2 may represent a fail-safe mechanism to ensure a corrected reduction of Notch1-IC levels in this context. However, further studies should be done to elucidate the connection between these two pathways. Similarly, analysing the response of Notch1-IC to other stimuli able to regulate the activity or expression of DYRK2, such as hypoxia [30], serum starvation [50], β-adrenergic stimulation [51], LPS [52] or heat shock [37], would be of interest.

In the context of chemotherapy resistance, one of the most important problems in cancer treatment, understanding the molecular mechanisms implicated in the DNA damage response (DDR) pathway is crucial. In this sense, it has been reported that overexpression of Notch1-IC in lung and liver cancer cells increases resistance to cisplatin [53, 54]. Similarly, NOTCH1 plays a direct negative regulatory role on DDR following ionising radiation treatment by interacting with ATM and disrupting its activation [55]. On the other hand, Li et al. [56], recently described that cisplatin induces expression of Notch1-IC in a dose-dependent manner in cervical cancer cells. In fact, in some specific types of tumours such as skin cancer, small cell lung cancer or hepatocellular carcinoma, contradictory data indicate that NOTCH1 signalling could be playing anti-proliferative rather than oncogenic roles [57]. In this study, we provide new insights into the consequences of exposure to DNA damage on the NOTCH1 signalling pathway, since different chemotherapeutic agents (adriamycin, etoposide or cisplatin) promote Notch1-IC inhibition mediated by DYRK2 in different cell lines.

Previous studies have broadly shown that perturbation of the NOTCH1 signalling pathway is linked to the pathogenesis of important lung diseases, in particular, lung cancer and lung lesions [58, 59]. However, it has also been proved to play a key role in breast cancer [60, 61] and prostate cancer [62]. Additionally, Notch1-IC aberrant overexpression correlates with leukaemia [63] and breast cancer [9, 64]. Although DYRK2 distinct role in cancer development has been broadly proved, there is controversy concerning its pro- or anti-tumour potentials. However, various studies have shown that DYRK2 is down-regulated in various cancer tissues such as lung, breast, prostate and colon, associated with poor patient prognosis [32, 50, 65–69]. The data showing the correlation in the levels of both proteins in tumour tissue (Fig. 6a) agree with our in vitro data and suggest that the degradation of Notch1-IC by DYRK2 might also be relevant in cancer patients. Additionally, our results prove that DYRK2 Thr-2512 direct phosphorylation is an important milestone in Notch1-IC regulation. These results might clarify previous analyses focused on the relevance of Thr-2515 mutation in some cancers such as human T cell acute lymphoblastic leukaemia [70].

In summary, our results show the ability of DYRK2 to regulate Notch1-IC stability affecting its transcriptional activity. In response to DNA damage, DYRK2 phosphorylated Notch1-IC and facilitated its proteasomal degradation by FBXW7 (Fig. 7). We propose that this new regulatory mechanism induced by chemotherapeutic agents has an influence on cancer cells behaviour. Further studies are needed to understand the potential implications for those tumours with over-expressed Notch1-IC.
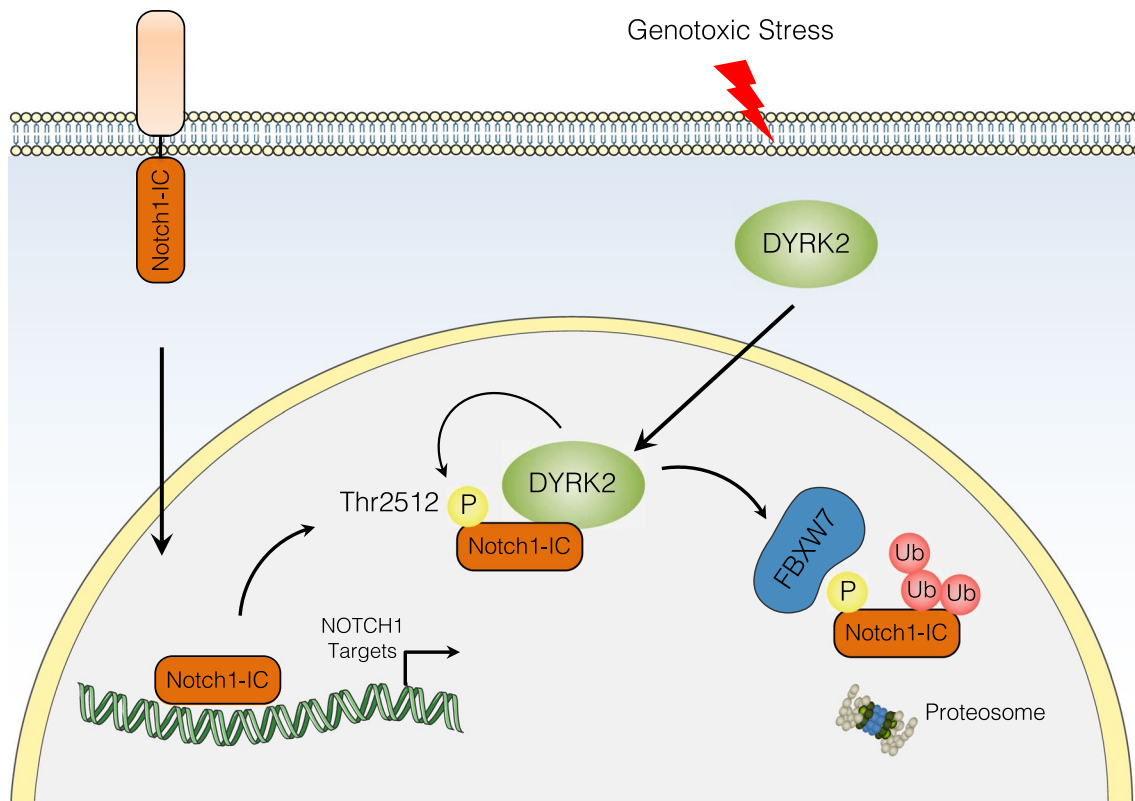
Fig. 7 Schematic model for the ability of DYRK2 to regulate Notch1-IC. Under genotoxic stress, DYRK2 is able to regulate Notch1-IC by FBXW7-dependent proteasome degradation by phosphorylating residue Thr-2512

Compliance with ethical standards

Conflict of interest The authors declare that they have no conflict of interest.

References

1. Borggrefe T, Oswald F (2009) The Notch signaling pathway: transcriptional regulation at Notch target genes. Cell Mol Life Sci 66(10):1631–1646. https://doi.org/10.1007/s00018-009-8668-7
2. Bray SJ (2016) Notch signalling in context. Nat Rev Mol Cell Biol 17(11):722–735. https://doi.org/10.1038/nrm.2016.94
3. Chillakuri CR, Sheppard D, Lea SM, Handford PA (2012) Notch receptor-ligand binding and activation: insights from molecular studies. Semin Cell Dev Biol 23(4):421–428. https://doi.org/10.1016/j.semcdb.2012.01.009
4. Kovall RA, Gebelein B, Sprinzak D, Kopan R (2017) The canonical notch signaling pathway: structural and biochemical insights into shape, sugar, and force. Dev Cell 41(3):228–241. https://doi.org/10.1016/j.devcel.2017.04.001
5. Kopan R, Ilagan MX (2009) The canonical Notch signaling pathway: unfolding the activation mechanism. Cell 137(2):216–233. https://doi.org/10.1016/j.cell.2009.03.045
6. Kitagawa M (2016) Notch signalling in the nucleus: roles of Mastermind-like (MAML) transcriptional coactivators. J Biochem 159(3):287–294. https://doi.org/10.1093/jb/mvv123
7. Koch U, Radtke F (2007) Notch and cancer: a double-edged sword. Cell Mol Life Sci 64(21):2746–2762. https://doi.org/10.1007/s00018-007-7164-1
8. Ranganathan P, Weaver KL, Capobianco AJ (2011) Notch signalling in solid tumours: a little bit of everything but not all the time. Nat Rev Cancer 11(5):338–351. https://doi.org/10.1038/nrc3035

9. Stylianou S, Clarke RB, Brennan K (2006) Aberrant activation of notch signaling in human breast cancer. Can Res 66(3):1517–1525. https://doi.org/10.1158/0008-5472.can-05-3054

10. Luo DH, Zhou Q, Hu SK, Xia YQ, Xu CC, Lin TS, Pan YT, Wu JS, Jin R (2014) Differential expression of Notch1 intracellular domain and p21 proteins, and their clinical significance in gastric cancer. Oncol Lett 7(2):471–478. https://doi.org/10.3892/ol.2013.1751

11. Aster JC, Pear WS, Blacklow SC (2017) The varied roles of notch in cancer. Annu Rev Pathol 12:245–275. https://doi.org/10.1146/annurev-pathol-052016-100127

12. Palomero T, Lim WK, Odom DT, Sulis ML, Real PJ, Margolin A, Barnes KC, O'Neil J, Neuberg D, Weng AP, Aster JC, Sigaux F, Soulier J, Look AT, Young RA, Califano A, Ferrando AA (2006) NOTCH1 directly regulates c-MYC and activates a feed-forward-loop transcriptional network promoting leukemic cell growth. Proc Natl Acad Sci USA 103(48):18261–18266. https://doi.org/10.1073/pnas.0606108103

13. Dang CV, Le A, Gao P (2009) MYC-induced cancer cell energy metabolism and therapeutic opportunities. Clin Cancer Res 15(21):6479–6483. https://doi.org/10.1158/1078-0432.CCR-09-0889

14. Palomero T, Sulis ML, Cortina M, Real PJ, Barnes K, Ciofani M, Caparros E, Buteau J, Brown K, Perkins SL, Bhagat G, Agarwal AM, Basso G, Castillo M, Nagase S, Cordon-Cardo C, Parsons R, Zuniga-Pflucker JC, Dominguez M, Ferrando AA (2007) Mutational loss of PTEN induces resistance to NOTCH1 inhibition in T-cell leukemia. Nat Med 13(10):1203–1210. https://doi.org/10.1038/nm1636

15. Deftos ML, He YW, Ojala EW, Bevan MJ (1998) Correlating notch signaling with thymocyte maturation. Immunity 9(6):777–786

16. Piovan E, Yu J, Tosello V, Herranz D, Ambesi-Impiombato A, Da Silva AC, Sanchez-Martin M, Perez-Garcia A, Rigo I, Castillo M, Indraccolo S, Cross JR, de Stanchina E, Paietta E, Racevskis J, Rowe JM, Tallman MS, Basso G, Meijerink JP, Cordon-Cardo C, Califano A, Ferrando AA (2013) Direct reversal of glucocorticoid resistance by AKT inhibition in acute lymphoblastic leukemia. Cancer Cell 24(6):766–776. https://doi.org/10.1016/j.ccr.2013.10.022

17. Yuan X, Wu H, Xu H, Xiong H, Chu Q, Yu S, Wu GS, Wu K (2015) Notch signaling: an emerging therapeutic target for cancer treatment. Cancer Lett 369(1):20–27. https://doi.org/10.1016/j.canlet.2015.07.048

18. Ann EJ, Kim MY, Yoon JH, Ahn JS, Jo EH, Lee HJ, Lee HW, Kang HG, Choi DW, Chun KH, Lee JS, Choi CY, Ferrando AA, Lee K, Park HS (2016) Tumor suppressor HIPK2 regulates malignant growth via phosphorylation of Notch1. Can Res 76(16):4728–4740. https://doi.org/10.1158/0008-5472.can-15-3310

19. Manderfield LJ, Aghajanian H, Engleka KA, Lim LY, Liu F, Jain R, Li L, Olson EN, Epstein JA (2015) Hippo signaling is required for Notch-dependent smooth muscle differentiation of neural crest. Development 142(17):2962–2971. https://doi.org/10.1242/dev.125807

20. Gao J, Azmi AS, Aboukameel A, Kauffman M, Shacham S, Abou-Samra AB, Mohammad RM (2014) Nuclear retention of Fbw7 by specific inhibitors of nuclear export leads to Notch1 degradation in pancreatic cancer. Oncotarget 5(11):3444–3454. https://doi.org/10.18632/oncotarget.1813

21. O'Neil J, Grim J, Strack P, Rao S, Tibbitts D, Winter C, Hardwick J, Welcker M, Meijerink JP, Pieters R, Draetta G, Sears R, Clurman BE, Look AT (2007) FBW7 mutations in leukemic cells mediate NOTCH pathway activation and resistance to gamma-secretase inhibitors. J Exp Med 204(8):1813–1824. https://doi.org/10.1084/jem.20070876

22. Thompson BJ, Buonamici S, Sulis ML, Palomero T, Vilimas T, Basso G, Ferrando A, Aifantis I (2007) The SCFFBW7 ubiquitin ligase complex as a tumor suppressor in T cell leukemia. J Exp Med 204(8):1825–1835. https://doi.org/10.1084/jem.20070872

23. Demarest RM, Ratti F, Capobianco AJ (2008) It's T-ALL about Notch. Oncogene 27(38):5082–5091. https://doi.org/10.1038/onc.2008.222

24. Lee HJ, Kim MY, Park HS (2015) Phosphorylation-dependent regulation of Notch1 signaling: the fulcrum of Notch1 signaling. BMB Rep 48(8):431–437

25. Ahn JS, Ann EJ, Kim MY, Yoon JH, Lee HJ, Jo EH, Lee K, Lee JS, Park HS (2016) Autophagy negatively regulates tumor cell proliferation through phosphorylation dependent degradation of the Notch1 intracellular domain. Oncotarget 7(48):79047–79063. https://doi.org/10.18632/oncotarget.12986

26. Aranda S, Laguna A, de la Luna S (2011) DYRK family of protein kinases: evolutionary relationships, biochemical properties, and functional roles. FASEB J 25(2):449–462. https://doi.org/10.1096/fj.10-165837

27. Nihira NT, Yoshida K (2015) Engagement of DYRK2 in proper control for cell division. Cell Cycle 14(6):802–807. https://doi.org/10.1080/15384101.2015.1007751

28. Ong SS, Goktug AN, Elias A, Wu J, Saunders D, Chen T (2014) Stability of the human pregnane X receptor is regulated by E3 ligase UBR5 and serine/threonine kinase DYRK2. Biochem J 459(1):193–203. https://doi.org/10.1042/BJ20130558

29. Taira N, Mimoto R, Kurata M, Yamaguchi T, Kitagawa M, Miki Y, Yoshida K (2012) DYRK2 priming phosphorylation of c-Jun and c-Myc modulates cell cycle progression in human cancer cells. J Clin Invest 122(3):859–872. https://doi.org/10.1172/JCI60818

30. Perez M, Garcia-Limones C, Zapico I, Marina A, Schmitz ML, Munoz E, Calzado MA (2012) Mutual regulation between SIAH2 and DYRK2 controls hypoxic and genotoxic signaling pathways. J Mol Cell Biol 4(5):316–330. https://doi.org/10.1093/jmcb/mjs047

31. Miller CT, Aggarwal S, Lin TK, Dagenais SL, Contreras JI, Orringer MB, Glover TW, Beer DG, Lin L (2003) Amplification and overexpression of the dual-specificity tyrosine-(Y)-phosphorylation regulated kinase 2 (DYRK2) gene in esophageal and lung adenocarcinomas. Can Res 63(14):4136–4143

32. Enomoto Y, Yamashita S, Yoshinaga Y, Fukami Y, Miyahara S, Nabeshima K, Iwasaki A (2014) Downregulation of DYRK2 can be a predictor of recurrence in early stage breast cancer. Tumour Biol 35(11):11021–11025. https://doi.org/10.1007/s13277-014-2413-z

33. Yamaguchi N, Mimoto R, Yanaihara N, Imawari Y, Hirooka S, Okamoto A, Yoshida K (2015) DYRK2 regulates epithelial-mesenchymal-transition and chemosensitivity through Snail degradation in ovarian serous adenocarcinoma. Tumour Biol 36(8):5913–5923. https://doi.org/10.1007/s13277-015-3264-y

34. Yamashita S, Chujo M, Tokuishi K, Anami K, Miyawaki M, Yamamoto S, Kawahara K (2009) Expression of dual-specificity tyrosine-(Y)-phosphorylation-regulated kinase 2 (DYRK2) can be a favorable prognostic marker in pulmonary adenocarcinoma. J Thorac Cardiovasc Surg 138(6):1303–1308. https://doi.org/10.1016/j.jtcvs.2009.08.003

35. Taira N, Nihira K, Yamaguchi T, Miki Y, Yoshida K (2007) DYRK2 is targeted to the nucleus and controls p53 via Ser46 phosphorylation in the apoptotic response to DNA damage. Mol Cell 25(5):725–738. https://doi.org/10.1016/j.molcel.2007.02.007

36. Taira N, Yamamoto H, Yamaguchi T, Miki Y, Yoshida K (2010) ATM augments nuclear stabilization of DYRK2 by inhibiting MDM2 in the apoptotic response to DNA damage. J Biol Chem 285(7):4909–4919. https://doi.org/10.1074/jbc.M109.042341

37. Moreno R, Banerjee S, Jackson AW, Quinn J, Baillie G, Dixon JE, Dinkova-Kostova AT, Edwards J, de la Vega L (2019) DYRK2 activates heat shock factor 1 promoting resistance to proteotoxic stress in triplenegative breast cancer. bioRxiv. https://doi.org/10.1101/633560

38. Uhlen M, Fagerberg L, Hallstrom BM, Lindskog C, Oksvold P, Mardinoglu A, Sivertsson A, Kampf C, Sjostedt E, Asplund A, Olsson I, Edlund K, Lundberg E, Navani S, Szigyarto CA, Odeberg J, Djureinovic D, Takanen JO, Hober S, Alm T, Edqvist PH, Berling H, Tegel H, Mulder J, Rockberg J, Nilsson P, Schwenk JM, Hamsten M, von Feilitzen K, Forsberg M, Persson L, Johansson F, Zwahlen M, von Heijne G, Nielsen J, Ponten F (2015) Proteomics. Tissue-based map of the human proteome. Science 347(6220):1260419. https://doi.org/10.1126/science.1260419

39. Hoadley KA, Yau C, Hinoue T, Wolf DM, Lazar AJ, Drill E, Shen R, Taylor AM, Cherniack AD, Thorsson V, Akbani R, Bowlby R, Wong CK, Wiznerowicz M, Sanchez-Vega F, Robertson AG, Schneider BG, Lawrence MS, Noushmehr H, Malta TM, Cancer Genome Atlas N, Stuart JM, Benz CC, Laird PW (2018) Cell-of-origin patterns dominate the molecular classification of 10,000 tumors from 33 types of cancer. Cell 173(2):291–304. https://doi.org/10.1016/j.cell.2018.03.022

40. Gao J, Aksoy BA, Dogrusoz U, Dresdner G, Gross B, Sumer SO, Sun Y, Jacobsen A, Sinha R, Larsson E, Cerami E, Sander C, Schultz N (2013) Integrative analysis of complex cancer genomics and clinical profiles using the cBioPortal. Sci Signal 6(269):pl1. https://doi.org/10.1126/scisignal.2004088

41. Fernandez-Martinez J, Vela EM, Tora-Ponsioen M, Ocana OH, Nieto MA, Galceran J (2009) Attenuation of Notch signalling by the Down-syndrome-associated kinase DYRK1A. J Cell Sci 122(Pt 10):1574–1583. https://doi.org/10.1242/jcs.044354

42. Banerjee S, Ji C, Mayfield JE, Goel A, Xiao J, Dixon JE, Guo X (2018) Ancient drug curcumin impedes 26S proteasome activity by direct inhibition of dual-specificity tyrosine-regulated kinase 2. Proc Natl Acad Sci USA 115(32):8155–8160. https://doi.org/10.1073/pnas.1806797115

43. Bishop AC, Ubersax JA, Petsch DT, Matheos DP, Gray NS, Blethrow J, Shimizu E, Tsien JZ, Schultz PG, Rose MD, Wood JL, Morgan DO, Shokat KM (2000) A chemical switch for inhibitor-sensitive alleles of any protein kinase. Nature 407(6802):395–401. https://doi.org/10.1038/35030148

44. Li N, Fassl A, Chick J, Inuzuka H, Li X, Mansour MR, Liu L, Wang H, King B, Shaik S, Gutierrez A, Ordureau A, Otto T, Kreslavsky T, Baitsch L, Bury L, Meyer CA, Ke N, Mulry KA, Kluk MJ, Roy M, Kim S, Zhang X, Geng Y, Zagozdzon A, Jenkinson S, Gale RE, Linch DC, Zhao JJ, Mullighan CG, Harper JW, Aster JC, Aifantis I, von Boehmer H, Gygi SP, Wei W, Look AT, Sicinski P (2014) Cyclin C is a haploinsufficient tumour suppressor. Nat Cell Biol 16(11):1080–1091. https://doi.org/10.1038/ncb3046

45. Friedmann DR, Wilson JJ, Kovall RA (2008) RAM-induced allostery facilitates assembly of a notch pathway active transcription complex. J Biol Chem 283(21):14781–14791. https://doi.org/10.1074/jbc.M709501200

46. Del Bianco C, Aster JC, Blacklow SC (2008) Mutational and energetic studies of Notch 1 transcription complexes. J Mol Biol 376(1):131–140. https://doi.org/10.1016/j.jmb.2007.11.061

47. Rinaldo C, Prodosmo A, Mancini F, Iacovelli S, Sacchi A, Moretti F, Soddu S (2007) MDM2-regulated degradation of HIPK2 prevents p53Ser46 phosphorylation and DNA damage-induced apoptosis. Mol Cell 25(5):739–750. https://doi.org/10.1016/j.molcel.2007.02.008

48. Calzado MA, de la Vega L, Moller A, Bowtell DD, Schmitz ML (2009) An inducible autoregulatory loop between HIPK2 and Siah2 at the apex of the hypoxic response. Nat Cell Biol 11(1):85–91. https://doi.org/10.1038/ncb1816

49. D'Orazi G, Cecchinelli B, Bruno T, Manni I, Higashimoto Y, Saito S, Gostissa M, Coen S, Marchetti A, Del Sal G, Piaggio G, Fanciulli M, Appella E, Soddu S (2002) Homeodomain-interacting protein kinase-2 phosphorylates p53 at Ser 46 and mediates apoptosis. Nat Cell Biol 4(1):11–19. https://doi.org/10.1038/ncb714

50. Zhang X, Xu P, Ni W, Fan H, Xu J, Chen Y, Huang W, Lu S, Liang L, Liu J, Chen B, Shi W (2016) Downregulated DYRK2 expression is associated with poor prognosis and Oxaliplatin resistance in hepatocellular carcinoma. Pathol Res Pract 212(3):162–170. https://doi.org/10.1016/j.prp.2016.01.002

51. Weiss CS, Ochs MM, Hagenmueller M, Streit MR, Malekar P, Riffel JH, Buss SJ, Weiss KH, Sadoshima J, Katus HA, Hardt SE (2013) DYRK2 negatively regulates cardiomyocyte growth by mediating repressor function of GSK-3beta on eIF2Bepsilon. PLoS One 8(9):e70848. https://doi.org/10.1371/journal.pone.0070848

52. Sun Y, Ge X, Li M, Xu L, Shen Y (2017) Dyrk2 involved in regulating LPS-induced neuronal apoptosis. Int J Biol Macromol 104(Pt A):979–986. https://doi.org/10.1016/j.ijbiomac.2017.06.087

53. Liu YP, Yang CJ, Huang MS, Yeh CT, Wu AT, Lee YC, Lai TC, Lee CH, Hsiao YW, Lu J, Shen CN, Lu PJ, Hsiao M (2013) Cisplatin selects for multidrug-resistant CD133+cells in lung adenocarcinoma by activating Notch signaling. Can Res 73(1):406–416. https://doi.org/10.1158/0008-5472.CAN-12-1733

54. Huang SH, Xiong M, Chen XP, Xiao ZY, Zhao YF, Huang ZY (2008) PJ34, an inhibitor of PARP-1, suppresses cell growth and enhances the suppressive effects of cisplatin in liver cancer cells. Oncol Rep 20(3):567–572

55. Adamowicz M, Vermezovic J, d'Adda di Fagagna F (2016) NOTCH1 inhibits activation of ATM by impairing the formation of an ATM-FOXO3a-KAT5/Tip60 complex. Cell Rep 16(8):2068–2076. https://doi.org/10.1016/j.celrep.2016.07.038

56. Li S, Ren B, Shi Y, Gao H, Wang J, Xin Y, Huang B, Liao S, Yang Y, Xu Z, Li Y, Zeng Q (2019) Notch1 inhibition enhances DNA damage induced by cisplatin in cervical cancer. Exp Cell Res 376(1):27–38. https://doi.org/10.1016/j.yexcr.2019.01.014

57. Jundt F, Anagnostopoulos I, Forster R, Mathas S, Stein H, Dorken B (2002) Activated Notch1 signaling promotes tumor cell proliferation and survival in Hodgkin and anaplastic large cell lymphoma. Blood 99(9):3398–3403

58. Zong D, Ouyang R, Li J, Chen Y, Chen P (2016) Notch signaling in lung diseases: focus on Notch1 and Notch3. Ther Adv Respir Dis 10(5):468–484. https://doi.org/10.1177/1753465816654873

59. Guo L, Zhang T, Xiong Y, Yang Y (2015) Roles of NOTCH1 as a therapeutic target and a biomarker for lung cancer: controversies and perspectives. Dis Markers 2015:520590. https://doi.org/10.1155/2015/520590

60. Zeng JS, Zhang ZD, Pei L, Bai ZZ, Yang Y, Yang H, Tian QH (2018) CBX4 exhibits oncogenic activities in breast cancer via Notch1 signaling. Int J Biochem Cell Biol 95:1–8. https://doi.org/10.1016/j.biocel.2017.12.006

61. Yuan X, Zhang M, Wu H, Xu H, Han N, Chu Q, Yu S, Chen Y, Wu K (2015) Expression of Notch1 correlates with breast cancer progression and prognosis. PLoS One 10(6):e0131689–e0131689. https://doi.org/10.1371/journal.pone.0131689

62. Stoyanova T, Riedinger M, Lin S, Faltermeier CM, Smith BA, Zhang KX, Going CC, Goldstein AS, Lee JK, Drake JM, Rice MA, Hsu EC, Nowroozizadeh B, Castor B, Orellana SY, Blum SM, Cheng D, Pienta KJ, Reiter RE, Pitteri SJ, Huang J, Witte ON (2016) Activation of Notch1 synergizes with multiple pathways in promoting castration-resistant prostate cancer. Proc Natl Acad Sci USA 113(42):E6457–e6466. https://doi.org/10.1073/pnas.1614529113

63. Weng AP, Ferrando AA, Lee W, Morris JP, Silverman LB, Sanchez-Irizarry C, Blacklow SC, Look AT, Aster JC (2004) Activating mutations of NOTCH1 in human T cell acute lymphoblastic leukemia. Science 306(5694):269–271. https://doi.org/10.1126/science.1102160

64. Ma D, Dong X, Zang S, Ma R, Zhao P, Guo D, Dai J, Chen F, Ye J, Ji C (2011) Aberrant expression and clinical correlation of Notch signaling molecules in breast cancer of Chinese population. Asia-Pac J Clin Oncol 7(4):385–391. https://doi.org/10.1111/j.1743-7563.2011.01433.x

65. Mimoto R, Nihira NT, Hirooka S, Takeyama H, Yoshida K (2017) Diminished DYRK2 sensitizes hormone receptor-positive breast cancer to everolimus by the escape from degrading mTOR. Cancer Lett 384:27–38. https://doi.org/10.1016/j.canlet.2016.10.015

66. Moreno P, Lara-Chica M, Soler-Torronteras R, Caro T, Medina M, Álvarez A, Salvatierra Á, Muñoz E, Calzado MA (2015) The expression of the ubiquitin ligase SIAH2 (seven in absentia homolog 2) is increased in human lung cancer. PLoS One 10(11):e0143376–e0143376. https://doi.org/10.1371/journal.pone.0143376

67. Yogosawa S, Yoshida K (2018) Tumor suppressive role for kinases phosphorylating p53 in DNA damage-induced apoptosis. Cancer Sci 109(11):3376–3382. https://doi.org/10.1111/cas.13792

68. Imawari Y, Mimoto R, Hirooka S, Morikawa T, Takeyama H, Yoshida K (2018) Downregulation of dual-specificity tyrosine-regulated kinase 2 promotes tumor cell proliferation and invasion by enhancing cyclin-dependent kinase 14 expression in breast cancer. Cancer Sci 109(2):363–372. https://doi.org/10.1111/cas.13459

69. Yan H, Hu K, Wu W, Li Y, Tian H, Chu Z, Koeffler HP, Yin D (2016) Low expression of DYRK2 (dual specificity tyrosine phosphorylation regulated kinase 2) correlates with poor prognosis in colorectal cancer. PLoS One 11(8):e0159954. https://doi.org/10.1371/journal.pone.0159954

70. Grabher C, von Boehmer H, Look AT (2006) Notch 1 activation in the molecular pathogenesis of T-cell acute lymphoblastic leukaemia. Nat Rev Cancer 6(5):347–359. https://doi.org/10.1038/nrc1880